A&A 451, 157–175 (2006)
DOI: 10.1051/0004-6361:20053396

Astronomy & Astrophysics

The nature of ultraviolet spectra of AG Pegasi and other symbiotic stars: locations, origins, and excitation mechanisms of emission lines⋆

M. Eriksson[1,2], S. Johansson[2], and G. M. Wahlgren[2]

[1] University College of Kalmar, 391 82 Kalmar, Sweden
[2] Atomic Astrophysics, Lund Observatory, Lund University, Box 43, 221 00 Lund, Sweden

Received 10 May 2005 / Accepted 4 December 2005

ABSTRACT

A detailed study of ultraviolet spectra of the symbiotic star AG Peg has been undertaken to derive the atomic excitation mechanisms and origin of formation for the lines common in symbiotic systems. More than 600 emission lines are observed in spectra from *IUE*, *HST* and *FUSE* of which 585 are identified. Population mechanisms and origin of formation are given for a majority of those lines. Based on the understanding of the AG Peg spectra *IUE* data of 19 additional symbiotic stars are investigated and differences and similarities of their spectra are discussed. Fe II fluorescence lines pumped by strong emission lines between 1000 and 2000 Å are observed in 13 of these systems. Some of the symbiotic systems belonging to the subclass symbiotic novae have more than 100 Fe II fluorescence lines in the ultraviolet wavelength region. Forbidden lines are detected for 13 of the stars, mostly from highly-ionized spectra such as Ar V, Ne V and Mg V. Further, [Mg VI] and [Mg VII] lines are observed in a symbiotic star (AG Dra) for the first time. Five of the symbiotic stars have broad white-dwarf wind profiles ($FWHM > 400$ km s^{-1}) for a few lines in their spectra. The stars with no such broad lines can be divided into two similarly sized groups, one where all lines have *FWHM* less than 70 km s^{-1} and the other where one, a few or all of the broad ($FWHM > 400$ km s^{-1}) lines of AG Peg have an enhanced broad wing (110–140 km s^{-1}).

Key words. atomic processes – line: formation – stars: binaries: symbiotic – ultraviolet: stars

1. Introduction

From numerous recordings with the *IUE* satellite during 1978 to 1995 symbiotic stars are today known to be interacting binaries consisting of a white dwarf and a red giant with orbital periods of typically a few years. Symbiotic stars have composite spectra, an M-star continuum dominating at red and infrared wavelengths, a nebula continuum at ultraviolet and optical wavelengths, a rising continuum toward the far ultraviolet from the presence of a hot component and numerous strong emission lines throughout the spectrum indicating large plasma regions within the systems.

AG Peg is a symbiotic system consisting of a white dwarf and a red giant orbiting each other with a period of 812.3 ± 6.3 days (Kenyon et al. 1993). The luminosity of the white dwarf decreased by a factor of ∼4 during 1984–1997 (Kenyon et al. 2001). This decline can be understood as a decrease of its radius by a factor of ∼2 under constant temperature (Altamore & Cassatella 1997; Mürset & Nussbaumer 1994) or as an increase in the temperature of the white dwarf Schmutz 1996, which would imply a even larger decrease of its radius.

Between the two stars there is a region where the fast wind ($v = \sim 900$ km s^{-1}) (Nussbaumer et al. 1995) from the white dwarf collides with the slow wind ($v = \sim 60$ km s^{-1}) (Eriksson et al. 2004) from the red giant (Mürset et al. 1995). More recent and detailed ideas are discussed with respect to the wind structure concerning shock fronts from the wind collision region (Contini 2003) and the possibility of bipolar outflow (Yoo et al. 2002).

AG Peg belongs to a small subclass of symbiotic stars called symbiotic novae that have undergone nova events when the luminosity has increased by three to four magnitudes. Ultraviolet region line lists are available for two symbiotic novae, RR Tel (Penston et al. 1983) and V1016 Cyg (Nussbaumer & Schild 1981). Both of these systems have spectra dominated by allowed transitions from one to three times ionized elements, but also forbidden lines from more highly ionized elements have an impact on the spectrum. V1016 Cyg erupted in 1964 and RR Tel in 1944, while AG Peg erupted at least 150 years ago. An interesting open question is whether the decline of the UV flux in AG Peg during the 1980s is a natural evolutionary stage of symbiotic novae and whether, subsequently, RR Tel and V1016 Cyg will undergo a similar spectrum evolution in the future. A time analysis of the AG Peg spectrum can therefore give insights into what happens at the end of nova eruptions in symbiotic stars.

⋆ Full Table 13 and Tables 14–16 are only available in electronic form at `http://www.edpsciences.org`

During the last 25 years the emission lines in AG Peg have been used for various diagnostics to measure parameters such as electron density (Keyes & Plavec 1980; Penston & Allen 1985) and temperature (Kenyon & Webbink 1984; Altamore & Cassatella 1997). By careful analysis of the spectra it is possible to categorize the emission lines in terms of population processes and line profiles. It is important to understand the origins of the emission lines as well as the processes that populate the corresponding upper levels when using them in any analysis. Here we explain the appearance of most of the emission lines formed at UV wavelengths in AG Peg. The main goal is to obtain an enhanced understanding of the emission lines, which would be helpful for anyone who wants to use emission lines as a diagnostic tool for symbiotic stars or related novae-like environments. Furthermore, the spectral investigation gives insight into how the UV spectum has evolved during the period 1978–1995.

Symbiotic stars are categorized in terms of stellar (S) and dusty (D) types based on their appearence at IR wavelengths (Allen 1982). The S-types have typical orbital periods of a few years and the cooler component consists of a solar-mass star on the red giant branch, while the D-types have orbital periods mostly in excess of 20 years and the cool component in those systems is typically a Mira. The small subset of D′ type symbiotic stars has a cool star of spectral type G or K rather than M (Belczynski et al. 2000). The hot components are dominantly white dwarfs in both the S and D type systems. However, a few exceptions have the hot component as an accreation disk around a main sequence star (Kenyon & Garcia 1986).

Beyond the shared basic properties defining the group, the characteristics of symbiotic stars differ significantly. Besides the nova-like outbursts exhibited by the symbiotic novae, other phenomena observed in symbiotic stars are white-dwarf winds (Nussbaumer et al. 1995), recurrent-novae eruptions (Belczynski & Mikalojewska 1998), jets (Burgarella et al. 1992) and wind collision regions (Mürset et al. 1997).

By applying the understanding of the AG Peg spectrum at UV wavelengths to a set of 19 symbiotic stars we aim to detect differences and similarities among them. A detailed study of the lines showing broad white-dwarf wind lines in AG Peg is done to see how common such winds are in symbiotic systems. Fe II lines caused by photo-exitation by accidental resonance (PAR) are investigated to see whether this phenomenon is unique to a few symbiotic stars (Eriksson et al. 2003; Hartman & Johansson 2000) or more common among such systems. Also, forbidden lines of highly-ionized ions are analyzed to compare the ionization degree of low-density regions in symbiotic stars.

Table 1. Spectra used for AG Peg.

Instrument	Coverage (Å)	Spectum identification
IUE (LWR)	1900–3350	02591, 06389, 07504
		09672, 09310, 10579
IUE (LWP)	1900–3350	09698, 16684, 19235
		21635, 24149, 24285
		25565, 25995, 28122
		30936
IUE (SWP)	1150–1980	02326, 02334, 06335
		06809, 08760, 10454
		13957, 15651, 29862
		29863, 37420, 37477
		40149, 43006, 43007
		46149, 47715, 50707
		54749, 55055
HST (GHRS)	1222–1258	z27e0206t
	1354–1389	z27e0207n
	1383–1418	z27e0208t
	1468–1503	z27e0209t
	1532–1567	z27e020at
	1623–1657	z27e020bn
	1696–1737	z27e020dt
FUSE (LWRS)	920–1190	Q1110101
FUSE (MDRS)	920–1190	Q1110103

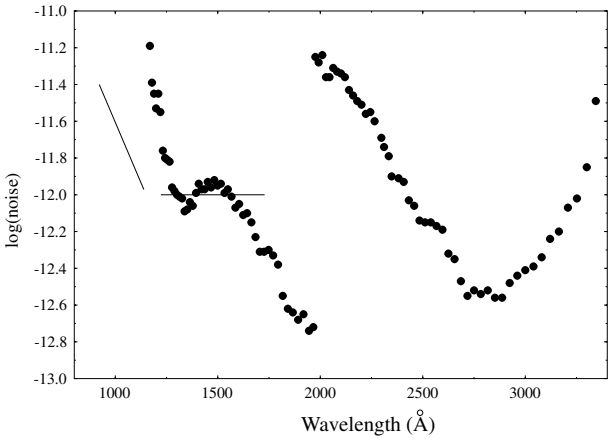

Fig. 1. The dots represent the noise level for each of the different orders in the longest exposed *IUE* spectra, LWP25995 and SWP47715. The lines represent the noise level in the *HST* and *FUSE* spectra used in this work. The *y*-axis gives the value of the logarithm of the noise level measured in erg cm^{-2} s^{-1} Å^{-1}. The noise level is defined as twice the standard deviation of the pixel intensity from the mean intensity, measured in wavelength regions not affected by spectral lines.

2. Data

The present study utilizes ultraviolet spectral data obtained from three different satellite observatories, spanning over nearly 25 years. The data were extracted from the Multimission Archive at STScI (MAST) in reduced format and are listed in Table 1. The extensive temporal coverage (1978–1995) of the *International Ultraviolet Explorer IUE* data for AG Peg allows us to follow spectrum developments during these years. The same data were exploited by Eriksson et al. (2004) to study wind affected line profiles for this star. Figure 1 prestents the noise levels for each spectral order for the longest exposures of the *IUE* high resolution observations. The figure thus provides a guide to the weakest detectable features and possible explanation for the relative strength of observed features. The resolution of *IUE* spectra depends on several parameters, such as the

dispersion angle, the reduction routine used and the wavelength being considered. No instrumental profile is deconvolved from the *FWHM* given in tables in this paper. Imhoff 1984 measured widths of platinum lines, with the *FWHM* being between 16 and 30 km s^{-1}. Therefore, the widths of lines narrower than 40 km s^{-1} in our tables should be treated with caution.

The data recorded by the Goddard High Resolution Spectrograph (GHRS) onboard the *Hubble Space Telescope* (*HST*) during 1994 overlap in wavelength with the *IUE* data but were recorded at a later epoch and for only limited wavelength intervals. The greater sensitivity of the GHRS detectors makes it possible to measure intensities to a greater accuracy than can be done from the *IUE* spectra.

Two spectra of AG Peg have been recorded by the *Far Ultraviolet Spectroscopic Explorer* (*FUSE*) satellite, one in July 2001 and one in June 2003. The inclusion of *FUSE* spectra in our analysis increases the wavelength range for the detection of emission lines. However, since those spectra were obtained several years after the *IUE* and *HST* data we must be careful when incorporating these data sets into the analysis. The spectrum of AG Peg underwent obvious changes during the lifetime of the *IUE* (Eriksson et al. 2004) and we might expect that its development would continue in the sense that certain spectral lines would increase or decrease in intensity and width. Without contemporaneous observations in other wavelength regions, emission line intensities from the *FUSE* data cannot be rigorously correlated with the line intensities at longer wavelengths.

For the symbiotic stars other than AG Peg presented in this analysis only *IUE* data are used. Since some of the Fe II lines as well as some of the forbidden lines are quite weak, one SWP and one LWP spectrum, observed with large aperture and with long exposure time, were selected for each system. The emission lines associated with the white-dwarf wind in AG Peg were easily saturated in the *IUE* spectrum, which is why an extra SWP spectrum was retrieved from the MAST archive for some of the symbiotic systems. Table 2 lists the data used for the selected objects.

Table 2. *IUE* spectra used for the selected symbiotic stars.

Object	LWP/LWR[a]	SWP[a]	SWP[b]
Z And	LWP06225	26177	26938
EG And	LWP25855	56021	46879
R Aqr	LWP21998	31102	40265
T CrB	LWP01536	28490	
BF Cyg	LWP15253	35843	58386
CH Cyg	LWP08631	28011	
CI Cyg	LWR10427	18602	50760
AG Dra	LWP24400	15656	55373
RW Hya	LWR10227	13601	
SY Mus	LWR10829	14236	16383
AX Per	LWP19332	21443	06807
RX Pup	LWR10831	31285	16597
HM Sge	LWP12921	40081	
RR Tel	LWR16187	20246	18371
KX Tra	LWP17871	38742	
PU Vul	LWP26780	37190	49265
V1016 Cyg	LWP04961	29830	24657
V1329 Cyg	LWP13121	24663	05615
HBV475	LWP08277	30853	

[a] Spectrum with long exposure times used to detect weak Fe II fluorescence lines and forbidden lines.
[b] Spectrum with short exposure times used when allowed lines are saturated in longer exposed spectra.

3. Excitation and origin of AG Peg emission lines

The spectral lines can be divided into different categories depending upon their widths and profiles. However, lines that look similar in one spectrum can show a different appearance in later spectra. This means that the time history of a spectral line is also important. Some narrow lines are selectively populated by radiative line excitation and they are classified as fluorescence lines, whereas others originate from excited levels populated by collisions or recombination. We have categorized the spectral lines by their overall appearance in the following way:

1. Broad emission lines (*FWHM* > 500 km s^{-1}) in spectra until 1981 that later evolve into narrower (*FWHM* < 80 km s^{-1}) emission lines.
2. Emission lines caused by fluorescence.
3. Narrow emission lines from levels excited by collisions.
4. Narrow emission lines from levels populated by recombination.
5. Narrow emission lines from levels with an uncertain population mechanism.
6. Interstellar absorption lines
7. Stellar absorption lines.

The lines showing a broad structure originate from ions of higher ionization stages, and they are partially or completely formed in the wind of the white dwarf before 1980 (Eriksson et al. 2004). During 1980–1985 the broad contribution from the white-dwarf wind to these lines vanished as a result of the reduced bolometric luminosity (a factor of 2–3) of the white dwarf. Narrow "nebular" lines replaced these broad wind lines in later spectra. Unfortunately, no *IUE* spectra of AG Peg were recorded during the years 1982 to 1985, when most of the line profiles must have undergone a rapid change. The narrow lines are most probably formed at further distance from the white dwarf, like in the extended parts of the red giant, such as its wind or upper atmosphere, or in the surrounding nebula. These lines involve mostly permitted lines and intercombination lines, but there are also a few forbidden lines originating from metastable states with lifetimes on the order of seconds. Most of the absorption lines are believed to be formed in the outer parts of the surrounding nebula (Penston & Allen 1985). In Table 3 we present for each element the number of identified lines observed in the UV spectrum of AG Peg.

3.1. Broad wind lines

In *IUE* spectra recorded before 1986 there are 22 emission lines with a *FWHM* larger than 600 km s^{-1} (Table 4). These lines originate from abundant elements in higher ionization stages than for the narrow lines, and they are presumably

Table 3. The distribution of emission lines for AG Peg, according to population processes.

Spec.	Process[a]				Tot	Spec.	Process[a]				Tot
	fl.	rec.	col.	unk			fl.	rec.	col.	unk	
H I		1			1	[Ne V]			3		3
He I		8			8	Mg II			2	7	9
He II		14			14	Mg IV		7			7
C II			5	3	8	[Mg V]			3		3
C III		8		3	11	Al II]			1		1
C III]			2		2	Al III			2		2
C IV			2		2	Si I				5	5
N I	1			4	5	Si II			3	5	8
N I]			4		4	Si II]			2		2
N III		5		4	9	Si III				4	4
N III]			5		5	Si III]			1		1
N IV		1			1	Si IV			2	5	7
N IV]			2		2	P II			3	1	4
N V			2		2	P II]			1		1
O I			2		2	P III			2		2
O I]				2	2	P IV				1	1
O III	16	6			22	P IV]			1		1
O III]	1	1	3	2	7	S I	1		5		6
[O III]			1		1	S I]			1		1
O IV		3		2	5	S II]			1		1
O IV]		5			5	S IV]			5		5
O V		3		1	4	S V				1	1
O V]				1	1	S V]				1	1
O VI			2		2	[Ar V]			1		1
Ne III		8			8	Fe II*	226	3	85	32	346
Ne III]		2			2	Fe III	3			11	14
[Ne III]			1		1	Fe V		4			4
[Ne IV]			4		4	[Fe VI]			2		2
Ne V]			2		2	Co II*	5			6	11

* Spin-forbidden transitions are also included.

[a] fl = fluorescence; rec = recombination; col = collision; unk = unknown.

formed in the hot white-dwarf wind. An analysis of some of these lines has yielded that the terminal velocity of the white-dwarf wind is ∼900 km s^{-1} (Vogel & Nussbaumer 1994). A few of the lines are ground-state transitions (resonance lines) and show P Cygni structure while others are LS-allowed transitions having an excited lower level. In a few cases the transitions are spin-forbidden (intercombination lines). After 1986, when the broad wind lines were replaced by narrow emission (Fig. 2), it is notable that the six lines with highest peak intensity in the *IUE* spectra (He II λ1640, C IV $\lambda\lambda$1548, 1550, N IV] λ1486, N V $\lambda\lambda$1238, 1242) had broad line profiles in earlier spectra.

He^+ has a low ionization energy compared to the other emitting ions detected in the white-dwarf wind, which is why the He II lines can be considered as recombination lines. The He II lines with wavelengths in the range of *IUE* are Balmer α, Balmer β, and the whole Paschen series except Paα. He II Balmer β is close in wavelength to H Lyα and therefore totally absorbed. The He II lines detected in *IUE* spectra of AG Peg are He II Balmer α and 13 consecutive Pashen lines starting with Paβ and reaching upper levels with quantum numbers n = 5−17. Only the second to the sixth lines can be detected from the noise before 1986 when the lines were broad.

For a few of the white-dwarf lines (C IV $\lambda\lambda$1548, 1558, N IV]1486, Si IV λ1402, Si IV λ1393) the development into narrow "nebular" lines had already started in 1978, and the structure in the line profile, as shown in Fig. 3, is caused by the narrow line superimposed on the broad line. That the contribution of narrow emission lines occurred earlier for the ions of lower ionisation potential gives an idea into why the emission lines changed origin. As the white dwarf emerged at the end of the nova-like outburst the wind became less dense and more transparent for UV photons. The line intensities from the white-dwarf wind would then decrease at the same time that the material in the extended part of the red-giant atmosphere facing the white dwarf would be subjected to more of the white-dwarf UV radiation. The heated part of the red giant atmosphere became hotter and more ionised, resulting in the strong, narrow-emission lines. In recent *FUSE* observations of AG Peg it is clear that the O VI resonance doublet still has contributions from the white-dwarf wind (Fig. 8). Since the ionisation energy of O VI is 114 eV its presence would be expected with a temperature increase in the white-dwarf wind, contrary to what

Table 4. The broad emission lines in AG Peg spectra.

		Before 1986		After 1986	
Line	IP[a]	*FWHM*[b]	Int[c]	*FWHM*[b]	Int[c]
He II λ3203	24.6	800	394[A]	40	550[B]
He II λ2733		770	235[A]	61	326[B]
He II λ2511		790	215[A]	40	243[B]
He II λ2385		800	207[A]	48	300[C]
He II λ2307		740	143[A]	40	235[C]
He II λ1640		770	7370[D]	66	22 040[E]
C IV λ1550	47.9	tcp	tcp	45	24 420[E]
C IV λ1548		tcp	tcp	37	44 470[E]
N IV λ1718	47.5	680	1443[D]	<145	214[F]
N IV] λ1486		tcp	tcp	32	14 200[E]
N V λ1242	77.5	800	4168[D]	56	12 570[E]
N V λ1238		430	3529[D]	70	19 560[E]
O V λ2781	77.4	820	54[A]	38	29[C]
O V λ1371		860	424[G]	<83	473[F]
Ne III λ2678	41.0	480	128[A]	37	28[C]
Si IV λ1402	33.5	tcp	tcp	36	2439[E]
Si IV λ1393		tcp	tcp	37	3796[E]
S V λ1502	45.1	820	358[G]		
S V] λ1199		770	480[G]	40	1066[C]
unid λ1266		550	858[G]		
unid λ1260		700	1556[G]		
unid λ1253		790	1469[G]		

[a] The ionization potential in eV of the next lower ion. [b] Given in km s^{-1}. [c] Peak intensity in units of 10^{-14} erg cm^{-2} s^{-1} Å^{-1}. The indices on the measured intensities stand for: [A] As measured in LWR05596, [B] LWP28122, [C] LWP25995, [D] SWP02326, [E] SWP55055, [F] SWP47715, [G] SWP02334. tcp = Two component profile as the spectral line has a narrow emission component superimposed on the broad white dwarf wind profile.

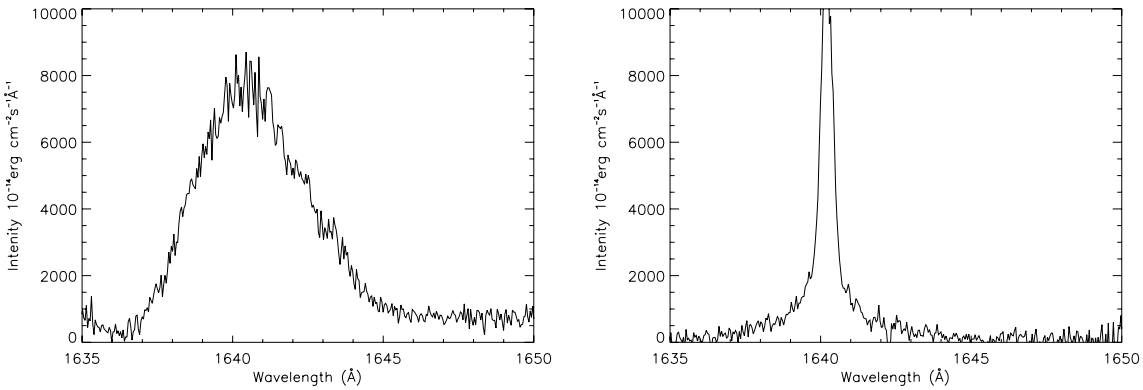

Fig. 2. The development of He II Balmer α. The spectrum to the left (SWP02326) was recorded in 1978 and the spectrum to the right (SWP40148) was recorded in 1990. The large change in profile width is related to the change in origin for He II emission between those dates. In 1978 most of the He II emission originated from the white-dwarf wind while in 1990 the emission instead came from the heated part of the extended red-giant atmosphere.

is given by Zanstra determinations (Altamore & Cassatella 1997).

The O III Bowen lines were also broader than the nebular lines in early *IUE* spectra. Like the white-dwarf lines discussed earlier the O III Bowen lines also evolved into narrower lines during the 1980s. The reason that they are not included in Table 4 is that they have less than half of the *FWHM* of the other broad line profiles and are formed in a different way (fluorescence). The Bowen lines are discussed in Sect. 3.3.

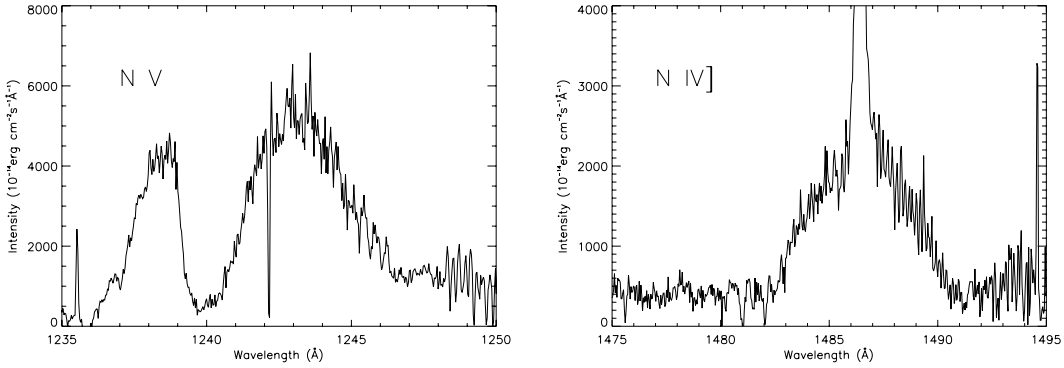

Fig. 3. The *IUE* spectrum (SWP02334) of AG Peg, recorded in 1978, illustrates the difference in the profiles between lines from ions of ionisation energy near 40 eV and those of higher ionisation energy (around 70 eV). The N IV] λ1486 had a contribution from a "nebular line" already in 1978 while all flux in the N V resonance doublet came from the white-dwarf wind.

3.2. The "nebular" lines

A majority of the emission lines observed in *IUE* spectra of AG Peg have a *FWHM* between 10 and 50 km s^{-1} and have had the same line profile although changed in intensity between 1978 and 1995. There is a wide range in ionisation energy for the narrow lines, from singly-ionised elements to more highly-ionised species such as Mg V, S IV and Fe V. Most of the emission lines correspond to LS-allowed transitions or intercombination lines but there are also a few parity-forbidden lines such as [Mg V] λ2928.

3.2.1. Narrow fluorescence lines

The process of photo-excitation by accidental resonance (PAR) can account for as many as 218 of the 585 identified lines in *IUE* spectra of AG Peg. The Fe II levels y^{4}H$_{11/2}$ and w^{2}D$_{3/2}$ are known to be pumped by C IV λ1548 in at least eight symbiotic systems (Johansson 1983; Eriksson et al. 2001). The levels (^{5}D)5p ^{6}F$_{9/2}$ and (^{3}F)4p ^{4}G$_{9/2}$ are known to be pumped by H Lyα in the symbiotic star RR Tel (Johansson & Jordan 1984; Hartman & Johansson 2000) and they are involved in laser action in gas condensations of η Car (Johansson & Letokhov 2004). In an analysis of AG Peg (Eriksson et al. 2003) 29 Fe II levels were shown to be populated by the PAR mechanism, and in the present work 11 newly identified pumped channels lead to a total of 40 presumably pumped Fe II levels, of which 22 are confirmed by three or more fluorescence lines (Table 5).

Most of the spectral lines that pump (selectively excite) Fe II are formed in the white-dwarf wind. Since the profiles of those lines change as their origin evolves from being dominated by the white-dwarf wind to the heated part of the red-giant atmosphere (or wind) the emission from the pumped Fe II levels also changes after 1986. Fe II channels that are separated by more than 40 km s^{-1} from their pumping line cannot be pumped by the narrow emission lines and therefore those lines disappeared after 1986 (Fig. 4). However, the Fe II fluorescence lines excited in channels that are close in wavelength to their pumping lines can be pumped by the narrow "nebular" emission lines and they do appear in the spectrum throughout the lifetime of *IUE*. There are four lines from highly- ionised elements (Si III] λ1892, O III] $\lambda\lambda$1660, 1666 and O IV] λ1401), which are not white-dwarf wind lines but still responsible for PAR processes in Fe II. These lines have in common that they are narrower than the other pumping lines, even compared to the *FWHM* after 1986, and that they, along with the corresponding fluorescence lines, did not change during the years 1978–1995.

In AG Peg H Lyα activates numerous Fe II channels resulting in fluorescence lines from both primary and secondary decays of the pumped levels. Lines from the (^{5}D)5s levels

Table 5. Pumped Fe II channels confirmed by 3 or more fluorescence lines.

Pumping Line	Fe II channel	$\delta\lambda^a$ (Å)	No.^{b}
Si III] λ1892.03	$a^4P_{3/2}$–$x^4F_{5/2}$	0.15	6
Si III] λ1892.03	$a^4D_{7/2}$–$z^4G_{9/2}$	0.05	14
N IV λ1718.55	$a^6D_{3/2}$–$z^4G_{5/2}$	–0.45	6
O III] λ1666.15	$a^6D_{7/2}$–$y^4P_{5/2}$	0.03	4
O III] λ1660.81	$a^4F_{9/2}$–$z^2G_{9/2}$	0.03	5
He II λ1640.07	$a^4F_{3/2}$–$y^4G_{5/2}$	0.08	4
C IV λ1548.19	$a^4F_{9/2}$–$y^4H_{11/2}$	0.01	13
C IV λ1548.19	$a^4F_{7/2}$–$y^2D_{5/2}$	0.51	7
C IV λ1548.19	$a^4P_{1/2}$–$w^2D_{3/2}$	0.22	13
N IV] λ1486.50	$a^4G_{5/2}$–$u^4F_{3/2}$	–0.03	7
O IV] λ1401.16	$a^6D_{5/2}$–(^{3}D)4p $^4P_{3/2}$	–0.12	4
N V λ1242.78	$a^4F_{5/2}$–$v^2G_{7/2}$	–0.04	3
N V λ1238.80	$a^4P_{5/2}$–(^{4}P)4s4p $^4P_{5/2}$	–0.22	5
H I λ1215.67	$a^4D_{5/2}$–(b^3P)4p $^4S_{3/2}$	0.31	4
H I λ1215.67	$a^4D_{5/2}$–(^{5}D)5p $^4D_{5/2}$	0.18	6
H I λ1215.67	$a^4D_{1/2}$–(^{5}D)5p $^4D_{3/2}$	0.85	5
He II λ1084.94	$a^6D_{9/2}$–$x^4H_{7/2}$	0.96	4
He II λ1084.94	$a^6D_{9/2}$–$x^4H_{9/2}$	0.64	3
He II λ1084.94	$a^6D_{9/2}$–$x^4H_{11/2}$	0.05	3
He II λ1084.94	$a^6D_{9/2}$–$u^2G_{9/2}$	–0.01	3
He II λ1025.27	$a^4D_{1/2}$–(^{4}F)4s4p $^6F_{3/2}$	–0.17	5
He II λ933.45	$a^4F_{5/2}$–(^{3}H)5p $^4G_{7/2}$	–0.07	6

[a] λ_{lab}(pumped Fe II channel) – λ_{lab}(pumping line).
[b] Number of observed Fe II fluorescence lines from the pumped level.

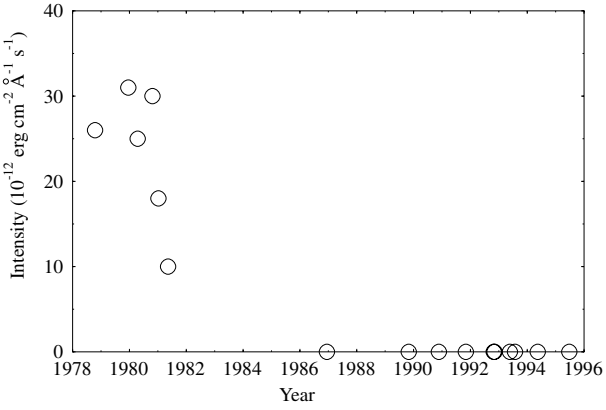

Fig. 4. The total intensity of all Fe II lines from the upper level $y^2D_{5/2}$, which is pumped by the C IV λ1548.187 line through the channel $a^4F_{7/2}$–$y^2D_{5/2}$ at 1548.697 Å. When the broad foot of the C IV resonance lines vanished the activity in this channel stopped.

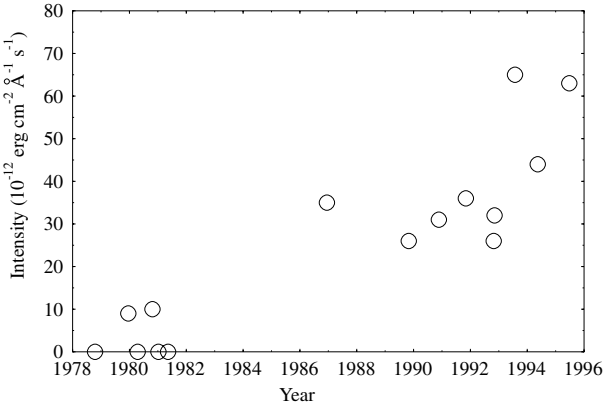

Fig. 5. The strength of the λ2508.34 Fe II line representing the channel $a^4D_{7/2}$–(b^3F) 4p $^4G_{9/2}$ pumped by H Lyα. As the temperature increased the H II region around the white dwarf became larger, which allowed more H Lyα to reach the Fe II regions.

(i.e. the e^{6}D and e^{4}D terms) are seen in the AG Peg spectrum. Those lines are also seen in RR Tel, where they are explained as secondary decay from H Lyα pumped (^{5}D)5p levels (Hartman & Johansson 2000), and we conclude that the same explanation is valid for AG Peg. A consequence of the density decrease in the white-dwarf wind is that it becomes less dominant (less extended in the binary system) as well as less opaque so that the H II region can grow and more H Lyα radiation can reach the Fe$^+$ ions. This leads to an increase of the intensity of the H Lyα pumped Fe II fluorescence lines (Fig. 5). It is interesting to note that the velocity shift is the same for the Fe II fluorescence lines but differs from the velocity shift of the lines from collisionally excited Fe II levels.

We observe lines from Fe II levels that are not selectively photo-excited by strong lines. The population of these levels can in general be explained by collisional or recombination excitation (see later sections). However, we also observe emission lines from 21 Fe II levels of medium excitation energy ($EP \approx$ 7–8 eV), for which neither of the excitation mechanisms mentioned above is plausible. Absorption lines of Fe II at short wavelengths are observed, and they give an explanation

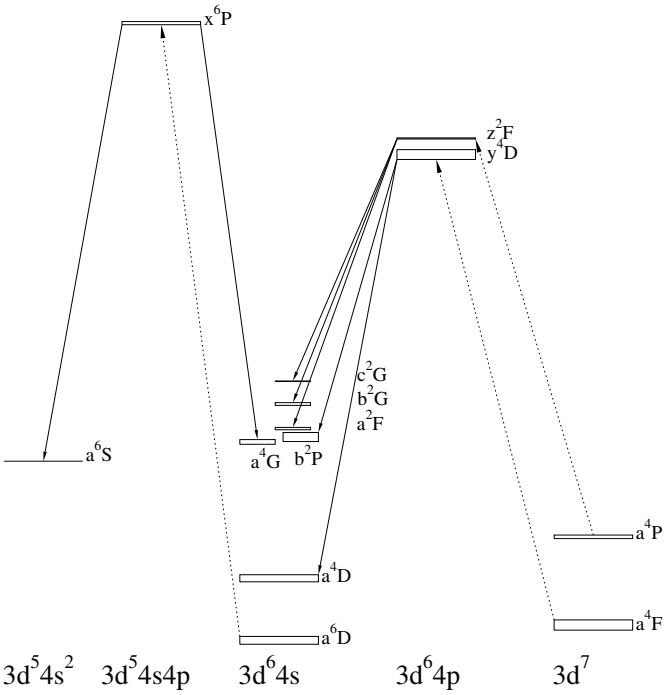

Fig. 6. Grotrian diagram of Fe II showing the levels involved in continuum fluorescence. The dotted lines are the pumped channels while the solid lines represent decay channels observed in AG Peg.

Table 6. Pumped channels in ions other than Fe II.

Pumping line	Pumped element	Pumped transition	λ^a (Å)
O IV] λ1401.16	S I	3p^4 ^{3}P$_2$–(^{4}S)5s ^{3}S$_1$	1401.51
N V λ1242.78	N I	2p^3 ^{2}D$_{5/2}$–(^{1}D)3s ^{2}D$_{5/2}$	1243.18
N V λ1242.78	Co II	4s a^{5}F$_3$–4s4p y^5P$_3$	1242.49
H I λ1215.67	Co II	3d^8 a^{3}P$_2$–(^{4}F)5p ^{5}D$_3$	1213.26
H I λ1215.67	Fe III	3d^6 ^{5}D$_4$–(^{6}S)4p ^{7}P$_3$	1214.57
H I λ1215.67	Fe III	3d^6 ^{5}D$_4$–(^{6}S)4p ^{7}P$_4$	1213.45
continuum^b	Co II	3d^8 ^{3}F$_4$–4p v^3D$_3$	1187.42

^{a} Wavelength of the pumped channel.
^{b} Absorption at 1187 Å is observed, which explains the presence of emission from the Co II v^3D$_3$ level.

to the population of seven of those 21 levels (Fig. 6). These are levels belonging to the LS terms y^4D, z^2F and x^6P (except for $y^4D_{1/2}$ and $x^6P_{3/2}$), and they are photo-excited by continuum radiation from the white dwarf through the channels a^4F–y^4D, a^4P–z^2F and a^6D–x^6P. Only the strongest transitions between these terms are observed as absorption lines in AG Peg, probably due to the low continuum level.

The strong emission line λ1411.94 in AG Peg is identified as the 2p^3 ^{2}P$_{3/2}$–2p^{2}3s ^{2}D$_{5/2}$ transition of N I but no emission is detected from the 2p^{2}3s ^{2}D$_{3/2}$ level. We suggest that the level 2p^{2}3s ^{2}D$_{5/2}$ is selectively populated by being pumped by N V λ1242 in the absorption channel 2p^3 ^{2}D$_{5/2}$–2p^{2}3s ^{2}D$_{5/2}$. A similar case is λ1409.34, which is identified as a transition from the S I level (^{4}S)5s ^{3}S$_1$ having a high excitation energy (8.85 eV). We suggest the S I level is pumped by O IV] λ1401. Furthermore, two pumped channels in Co II and two in Fe III have been detected in the *IUE* spectrum of AG Peg (Table 8).

Table 7. Parity forbidden lines observed in AG Peg.

Spectrum	Ionization (eV)	$\lambda_{\rm lab}$ (vac). (Å)	Shift[a] (km s^{-1})	Width (km s^{-1})	Transition	A_{ij} (s^{-1})	Note[b]
[Fe VI]	75.01	1957.28	bl	bl	$3d^3\ ^2G_{7/2}$–$3d^3\ ^2D1_{5/2}$	0.91	↑
		1944.30	17	20	$3d^3\ ^2G_{7/2}$–$3d^3\ ^2D1_{3/2}$	12	↑
[Mg V]	109.25	2928.0	bl	bl	$2p^4\ ^3P_1$–$2p^4\ ^1D_2$	0.55	↑
		2783.50	bl	bl	$2p^4\ ^3P_2$–$2p^4\ ^1D_2$	1.90	↑
		1324.45	45	20	$2p^4\ ^3P_1$–$2p^4\ ^1S_0$	23	↑
[Ne V]	97.08	2975.66	152	51	$2p^2\ ^1D_2$–$2p^2\ ^1S_0$	2.60	↑
		1575.18	124	84	$2p^2\ ^3P_1$–$2p^2\ ^1S_0$	4.20	↑
[Ar V]	59.81	2692.02	41	40	$3p^2\ ^3P_1$–$3p^2\ ^1S_0$	6.80	↑
[Ne IV]	63.46	2425.23	–6	18	$2p^3\ ^4S_{3/2}$–$2p^3\ ^2D_{5/2}$	0.00018	↔
		2422.60	–7	17	$2p^3\ ^4S_{3/2}$–$2p^3\ ^2D_{3/2}$	0.0053	↔
		1601.67	bl	bl	$2p^3\ ^4S_{3/2}$–$2p^3\ ^2P_{1/2}$	0.53	↔
		1601.50	bl	bl	$2p^3\ ^4S_{3/2}$–$2p^3\ ^2P_{3/2}$	1.33	↔
[Ne III]	40.96	1814.63	21	40	$2p^4\ ^3P_1$–$2p^4\ ^1S_0$	2.20	↔
[O III]	35.12	2321.66	49	25	$2p^2\ ^3P_1$–$2p^2\ ^1S_0$	0.22	↓

[a] $\frac{\lambda_{\rm lab}-\lambda_{\rm obs}}{\lambda_{\rm lab}} \cdot 3 \times 10^5$; [b] ↓ = Only observed before 1986, ↔ = observed throughout 1978 to 1995, ↑ = only observed after 1986, bl = blend.

3.2.2. Parity forbidden lines

Radiative transitions between levels of the same parity must be formed by magnetic dipole (M1) or electric quadrupole (E2) interaction, which means many orders of magnitude smaller transition probabilities than electric dipole (E1) transitions including a parity change. Observations of M1 and E2 radiation from an astrophysical plasma require that the density of the plasma is low enough so the radiative lifetime of the metastable state is smaller than the time scale for deexcitation by collisional quenching. Hence, the lines from the parity forbidden transitions originate from low density regions, such as from a nebula surrounding the system. In the *IUE* spectra of AG Peg, 14 parity-forbidden emission lines have been identified, originating from highly-ionised elements such as Ne V and Fe VI (Table 7). The ionisation energies are very high for the ions emitting M1 and E2 radiation, which implies that all parity-forbidden radiation originates from a thin plasma, heated and ionized by the UV radiation from the white dwarf. There is a difference among the forbidden lines in *IUE* spectra before and after 1986. Before 1986 only six of the 14 observed parity-forbidden lines were present, and they originated from the ions O^{2+}, Ne^{2+} and Ne^{3+}. No forbidden lines from higher ionisation stages were observed. After 1986 the forbidden emission from O^{2+} ([O III] λ2321.66) vanished and the emission from Ne^{2+} ([Ne III] λ1814.63) became weaker, while eight new emission lines from Ar^{4+}, Ne^{4+}, Mg^{4+} and Fe^{5+} appeared in the *IUE* spectrum.

3.2.3. Population by recombination or collisions

Emission lines from a particular ion can originate from different regions in the symbiotic system. Still, after discarding the emission lines that originated from the white-dwarf wind before 1986 as well as all fluorescence lines and parity-forbidden lines, the remaining emission lines from a specific ion have about the same velocity shifts. The widths of these remaining emission lines did not change during 1978–1995, but the relative shift between different ions was variable. In Table 3 all ions observed in AG Peg are listed with the number of corresponding emission lines that are formed by collision or recombination, excluding the white-dwarf wind emission lines. We will now give suggestions for how and where some of those lines are formed.

A) The helium 2s $^3S_1$–np^3P_2 series

Four emission lines from the He I 2s $^3S_1$–np $^3P_2$ series (n = 5–8) are identified in the RR Tel spectrum Penston et al. 1983. In the *IUE* spectra of AG Peg recorded before 1986 there are no traces of He I emission. The broad He II emission lines from the white-dwarf wind before 1986 are presumably formed by recombination. Because of the high temperature and strong UV flux in the white-dwarf wind there is no neutral helium there. However, after 1986 seven He I emission lines of the series 2s $^3S_1$–np $^3P_2$ ($5 \le n \le 11$) are present in the spectrum as "nebular" lines with a mean *FWHM* of 35 km s^{-1}. The explanation of the He I emission is probably linked to the change of the He II lines from broad wind profiles to "narrow" lines having an average *FWHM* of 49 km s^{-1} (see Sect. 3.1). Kenyon et al. (1993) suggest that the presence of He I is caused by heating of the red-giant atmosphere by radiation from He^+ ions in a region around the white dwarf. If He II in the white-dwarf wind is responsible for He I emission from the red-giant atmosphere, then the absence of He I lines before 1986 is a problem. Another suggestion is that when the white-dwarf wind became less dense during the transition period it was not able to produce broad He II emission enough to be observed by *IUE*, but at the same time more continuum radiation

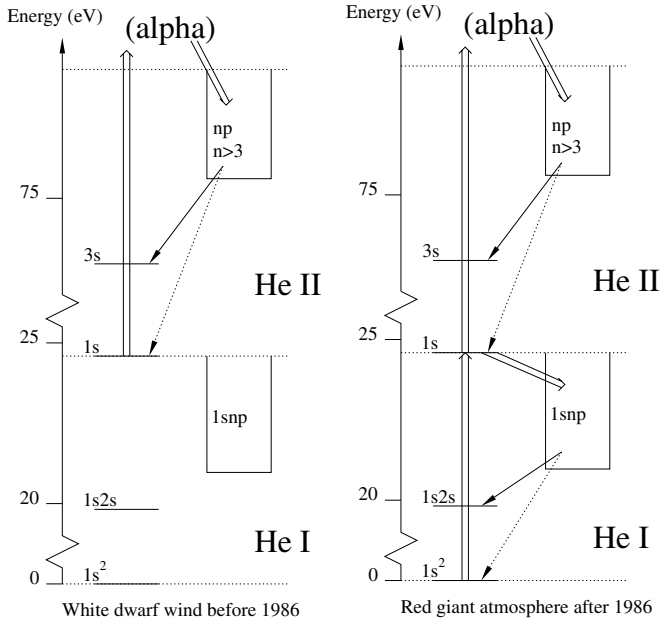

Fig. 7. Suggestion of the origin of broad He emission (*left*) and narrow He emission (*right*) before and after 1986 (see text).

from the white dwarf reached the red-giant atmosphere, ionising helium to both He^+ and He^{2+} (Fig. 7). This implies that after 1986 both the He I and He II emission lines are formed in the red-giant atmosphere facing the white dwarf.

B) The *ns* ^{2}S–*np* ^{2}P transitions in alkali-like spectra

It is only possible to detect the 2s ^{2}S–2p ^{2}P doublet transition for three species, C IV, N V, and O VI, within the wavelength regions covered by *IUE* and *FUSE*. Atomic lithium and the ions Be^+ and B^{2+} are too rare to be observed and for the three-electron systems heavier than oxygen the 2s–2p transition lies shortward of 900 Å. Two of the three observable doublets, C IV $\lambda\lambda$1548.19, 1550.77 and N V $\lambda\lambda$1238.80, 1242.78 are observed as broad (~800 km s^{-1}) emission lines that evolve into narrow emission (~40 km s^{-1}) during the 1980s as discussed in Sect. 3.1. The O VI λ1031.92, 1037.614 resonance doublet is outside the range of *IUE*, but is observed with *FUSE* (Fig. 8). Since *FUSE* was launched in 1999 there have been no data on the O VI resonance doublet in AG Peg prior to the dramatic change of profile of the N V and C IV resonance doublets. However, at the base of the O VI resonance lines there are wings (*FWHM* ~ 800 km s^{-1}, based on Gaussian fit of the line wings in the Q1110101 spectra) indicating that the O VI doublet evolved in the same way as the C IV and N V doublets. The peak intensity of the nebular components appears to have increased from 2001 (Q1110101) to the 2003 *FUSE* observation (Q1110103) while the intensity of the broad underlying wind-profile decreased slightly. This could mean that the same transfer of origin of the C IV resonance doublet at the end of 1970s to the beginning of the 1980s and the N V resonance doublet during the 1980s and beginning of 1990s (Eriksson et al. 2004) is now taking place for the O VI resonance doublet.

For the iso-electronic sequence of spectra involving 11 electrons the 3s ^{2}S–3p ^{2}P doublets are reachable with *IUE* for three different elements (Mg II $\lambda\lambda$2796.35, 2803.53, Al III $\lambda\lambda$1854.72, 1862.79 and Si IV $\lambda\lambda$1393.76, 1402.77), and one with *FUSE* (P V $\lambda\lambda$1117.98, 1128.01). The P V resonance doublet is not detected in the *FUSE* data probably because of a low abundance of phosphorus in the red-giant atmosphere. Energetically it would be possible since the O VI resonance doublet is observed, and the ionisation potential of O V (113.9 eV) is higher than for P IV (51.4 eV). The Si IV resonance lines evolved in the same manner as the C IV and N V resonance lines and are discussed in Sect. 3.1. The Mg II resonance doublet (Fig. 8) is known to be common in the chromospheres of red-giant stars (Kondo et al. 1976) and is probably emitted all around the red giant atmosphere. Both the Mg II and Al III resonance doublets consist of narrow emission lines throughout 1978 to 1995 and have probably never been formed in the white-dwarf wind because of the low ionisation temperature required.

C) The *ns*^{2} ^{1}S–*nsnp* ^{3}P transitions in alkaline-earth-like spectra

The spin-forbidden *ns*^{2} ^{1}S–*nsnp* ^{3}P transition includes two possible intercombination lines: $^1S_0$–$^3P_1$, which is often strong in emission in hot nebular spectra, and $^1S_0$–$^3P_2$. Since $\Delta J = 2$ for the latter line, it can only occur via a magnetic quadrupole transition, which has a very small transition probability. Similar to the observational restrictions for the 2s ^{2}S–2p ^{2}P transitions discussed in the previous subsection, the 2s^2 ^{1}S–2p ^{3}P transitions can only be observed for C III], N IV] and O V]. The C III] λ1908.73 ($^1S_0$–$^3P_1$) emission line is observed as strong ($I \sim 3.5 \times 10^{-11}$ erg cm^{-2} s^{-1} Å^{-1}) and narrow (*FWHM* ~ 35 km s^{-1}) in all of the *IUE* observations. This is probably due to the ionization energy of C III, which is too low for C^{2+} ions to survive in the white-dwarf wind, but the ionisation potential of C II is not too high for C^{2+} to be produced in the heated part of the red-giant atmosphere. At the detection limit in the longest exposed spectra at 1906.67 Å there is a weak feature ($I \sim 30 \times 10^{-13}$ erg cm^{-2} s^{-1} Å^{-1}), which can possibly be identified as the E2 ($^1S_0$–$^3P_2$) transition of C III] blended with Mg IV.

The N IV] λ1486.50 ($^1S_0$–$^3P_1$) emission line is a broad wind line before 1986 and is observed as a narrow emission line after 1986 as discussed in Sect. 3.1. Interestingly, the [N IV] M2 transition at 1483.32 Å is present throughout the *IUE* observations but has a *FWHM* around 150 km s^{-1}, which is very different from the *FWHM* of N IV] λ1486.50 both before and after 1986. Since O V has a higher ionisation energy than N IV one would also expect the O V] λ1218.34 emission line to have evolved from a broad wind profile to a narrow nebular line. However, its relative closeness to H Lyα at 1215.67 Å causes absorption by the neutral hydrogen in the surrounding nebula and the O V] λ1218.34 line is absent before 1986. When the temperature of the white dwarf increased the H II region expanded further out into the surrounding nebula, making it more

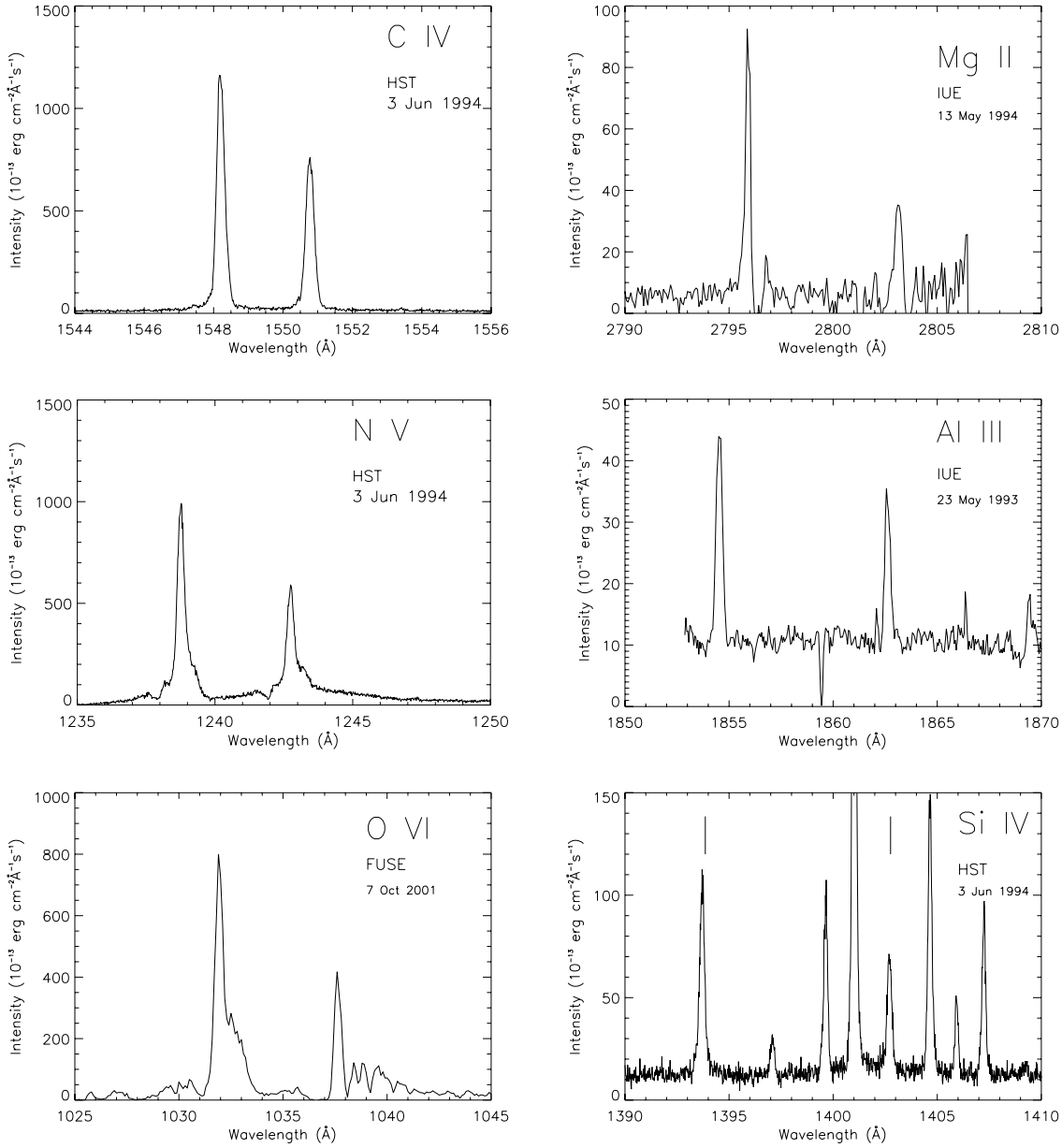

Fig. 8. The ns ^{2}S–np ^{2}P doublets observed in AG Peg. The figures represent the profile of the resonance doublets after the transition period in the middle of the 1980s. The resonance doublets corresponding to $n = 3$ (Si IV, Al III, Mg II) and C IV almost completely consist of narrow components, while the N V and O VI resonance doublets still have detectable contributions from the broad white-dwarf wind profile.

transparent for the O V] λ1218.34 emission, which after 1986 is observed as a strong emission line.

In the Mg I iso-electronic sequence of 12-electron ions the transition $3s^2\ ^1S_0$–$3s3p\ ^3P_1$ is observed in four elements (Al II], Si III], P IV] and S V]). The S V] λ1199.04 feature evolved from a broad wind profile to a narrow nebular line during the 1980s, while Al II] λ2669.95, Si III] λ1892.03, and P IV] λ1467.43 are observed as narrow ($FWHM \sim 30$ km s^{-1}) throughout the time interval 1978 to 1995. The intensity ratio I($^1S_0$–$^3P_1$)/I($^1S_0$–$^3P_2$) has been used in C III and N IV as a diagnostic tool to obtain electron densities in AG Peg Nussbaumer & Schild 1979, Nussbaumer & Schild 1981. The same transitions can be used for O V, Al II, Si III, P IV and S V to derive complementary information about the plasma. Understanding the origin of the ^{1}S–^{3}P lines is therefore of great importance.

D) The excited $(sp)^k$ $2 < k < 8$ configurations

The more ionised an element is the more sensitive the average energy of a configuration is to the principal quantum number, n. Excited states in highly-ionized spectra, for which all electrons have the same n as the ground configuration, are therefore at relatively low excitation energies. As an example the LS term

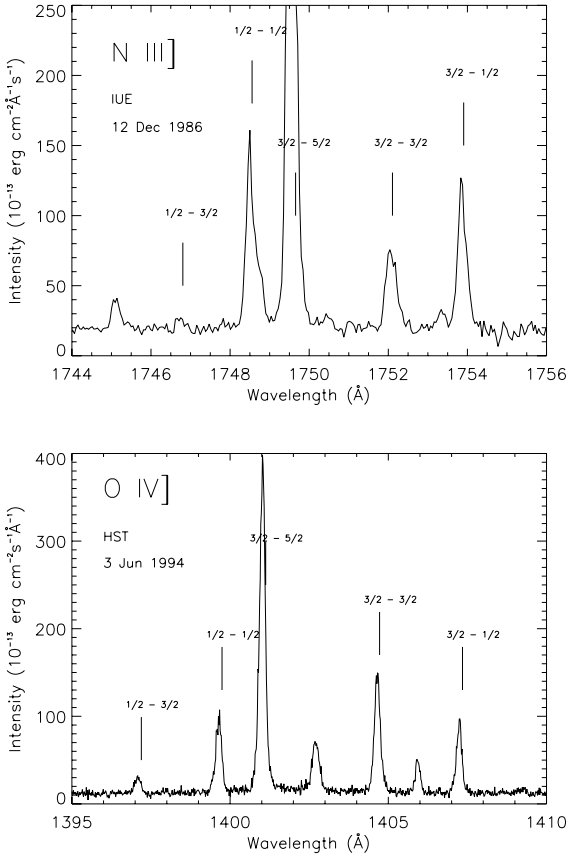

Fig. 9. The intercombination multiplet $2s^2 2p\ ^2P–2s2p^2\ ^4P$ in N III] and O IV] spectra. The fine-structure component 3/2–5/2 is over-exposed in the N III] plot. The region of the N III] multiplet has not been observed by *HST* (GHRS) at high resolution. The dynamic range of *IUE* was not sufficient to record spectra where the weakest N III] components are observable at the same time that N III] 3/2–5/2 is not over-exposed.

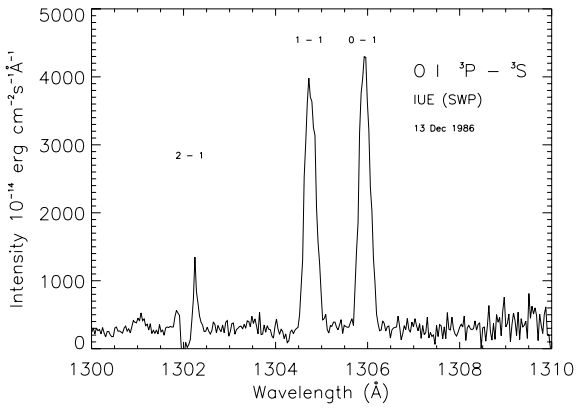

Fig. 10. The O I multiplet $2p^4\ ^3P–2p^3(^4S)3s\ ^3S$. The component $^3P_2–^3S_1$ to the ground level is in absorption while the other two fine-structure components are in emission.

$2s2p^2\ ^4P$ of C II is at ~5.3 eV, while the LS term $2s2p3p\ ^4P$ is at an energy of (~23.1 eV), i.e. more than a factor of four higher. Because of the low energy required for exciting the $(sp)^k$ configurations they can be populated through collisions. Allowed emission lines from $(sp)^k$, $2 < k < 8$, dominate the contribution from C II, N III, O IV, Si II, P II, P III, S II and S IV and they are also present in C III, N IV and O V. An intercombination transition, $ns^2np\ ^2P–nsnp^2\ ^4P$, is specially strong in N III, O IV and S IV (Fig. 9), and is also present in the Si II spectrum. The metastable $nsnp^2\ ^4P$ is the lowest excited term in systems with five and 13 electrons and it can therefore only decay to the ground state, which explains why the corresponding multiplets are so strong. Those multiplets can be used for electron density diagnostics (Nussbaumer & Storey 1982; Nussbaumer & Storey 1979).

E) Emission lines from neutral atoms heavier than helium

Emission lines from NI, OI and SI are observed in the ultraviolet spectrum of AG Peg. Most of the emission lines from neutral elements are from allowed transitions to levels within the ground configuration, except for the ground state (Fig. 9). That the emitting gas is optically thick for transitions to the ground state indicates that the region of neutral elements is of relatively high density and low temperature (<3000 K). All of the four observed oxygen lines and five of the six observed sulphur lines correspond to transitions from $np^3(^4S)n$'s ^5S or ^3S to the ground term $np^4\ ^3P$. That the $^3P–^5S$ intercombination lines of S I λ1900.29 and O I $\lambda\lambda$1355.60, 1358.51 are observed is interesting since their transition probabilities are $\sim 10^4$ times smaller than for the $^3P–^3S$ transitions. This limits the electron density of the emitting region, presumably the outermost part of the surrounding nebula or the part of the red giant obscured from the white-dwarf emission.

F) Recombination to third, fourth and fifth ionization states

The population of some levels, from which emission is observed in AG Peg, cannot be understood by collisions or any pumping mechanisms. These include levels with very high excitation energy having no known decay channels that coincide with strong UV emission lines of other elements, and exotic configurations (doubly-excited and/or involving f-electrons) rarely populated in astrophysical plasmas. If an ion is emitting lines from doubly-excited levels or levels close to the ionization energy, recombination is the most plausible explanation. Based on this reasoning we suggest recombination as the excitation mechanism for some lines. The previous discussion of the strong $2s\ ^2S–2p\ ^2P$ transitions reveals a large abundance of C IV, N V and O VI in a hot region of AG Peg, implying that recombination to C III, N IV and O V is reasonable. Both C III and O V lines have been observed from levels rarely populated by collisions and are most certainly populated by recombination (such as $4f\ ^3F_4$ in C III and $5f\ ^3F_4$ in O V). Although the N V $\lambda\lambda$1238.80, 1242.78 doublet is almost as strong as the C IV resonance doublet none of the observed N IV lines originate from levels that require recombination excitation. However, the N IV] λ1486.50 emission line is one of the strongest lines in

Table 8. The relative line strengths of the Fe II multiplet a^6D–z^6D.

Transition	λ_{vac}(lab) (Å)	gA^a	I^b
9/2–9/2	2600.17	2.39	0[c]
9/2–7/2	2586.65	0.37	0[c]
7/2–9/2	2626.45	0.75	1.23
7/2–7/2	2612.65	1.00	1.00
7/2–5/2	2599.15	0.32	0.39
5/2–7/2	2632.11	0.87	bl
5/2–5/2	2618.40	0.30	0.92
5/2–3/2	2607.87	0.45	0.61
3/2–5/2	2631.83	0.70	bl
3/2–3/2	2621.19	0.02	0.72
3/2–1/2	2614.61	0.37	0.47
1/2–3/2	2629.08	0.43	0.53
1/2–1/2	2622.45	0.12	0.52

[a] The gA values from Schnabel et al. (2004) are scaled in such a way that gA for the $a^6D_{7/2}$–$z^6D_{7/2}$ transition is equal to 1.00.
[b] The observed intensity relative to $I(a^6D_{7/2}–z^6D_{7/2}) = 1.00$.
[c] Both transitions to the ground level $a^6D_{9/2}$ are observed in absorption.

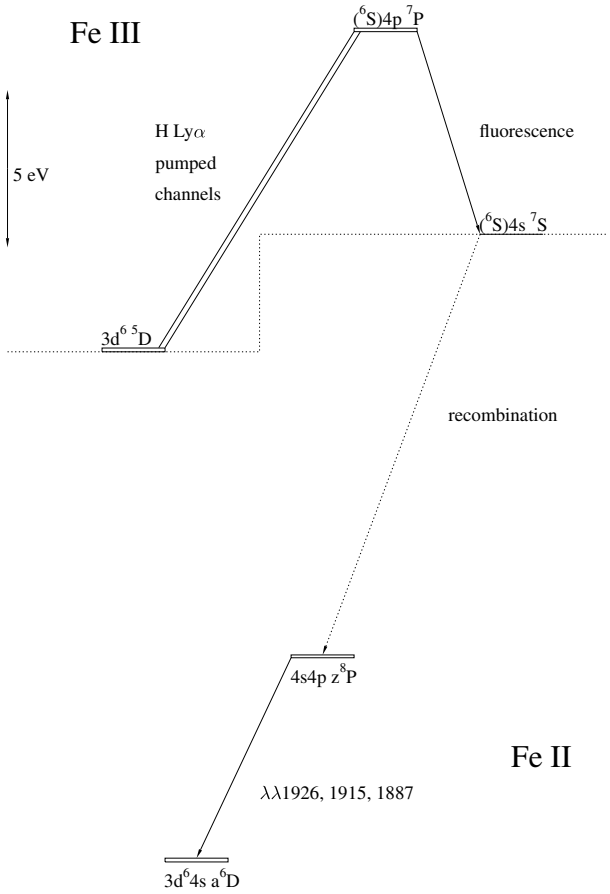

Fig. 11. Figure demonstrating our idea of the excitation mechanism in Fe III and Fe II responsible for the observed octet transitions in Fe II. The presumed recombination channels are presented as dotted lines, the pumped channel as a double lines and the decay channels as solid lines. Only the levels involved in the process are plotted in this Grotrian diagram.

the *IUE* wavelength range, indicating high presence of N^{3+} ions and the N III spectrum shows a few lines, such as N III λ1387.38, with upper level 4d $^2D_{3/2}$ presumably populated by recombination. Also, recombination lines of the third spectra, C III, N III and O III, were present throughout 1978–1995 and are formed in the extended red-giant atmosphere at a distance from the white dwarf sufficient to provide a temperature that gives a mixture of two and three times ionised elements.

The O V recombination lines first appeared after 1986. Before 1986, O^{5+} ions probably only existed in the white-dwarf wind, but after the transition period in the middle of 1980s O^{5+} ions were produced in the red-giant atmosphere by photo-ionisation, which explains the appearance of O V recombination lines. Four emission lines between 1669–1699 Å are identified as Mg IV lines corresponding to the multiplet (^{3}P)3s ^{4}P–(^{3}P)3p ^{4}D. These lines are the only observed Mg IV lines in the spectra of AG Peg, and the (^{3}P)3p ^{4}D term has an excitation energy of ∼75 eV. The population of these levels is likely to be due to recombination of Mg V 2p^4 ^{3}P in less dense parts of the surrounding nebula since only parity forbidden lines from Mg V are observed.

G) The Fe II (^{5}D)4p levels

The lowest excited odd-parity levels in Fe II belong to the subconfiguration (^{5}D)4p, which is built on the lowest parent term ^{5}D of Fe III. This subconfiguration contains six LS terms (^{4}P, ^{4}D ^{4}F, ^{6}P, ^{6}D and ^{6}F) and accounts for 25 fine-structure levels. Transitions from (^{5}D)4p are observed in the ultraviolet region to levels within the terms (^{5}D)4s ^{6}D, (^{5}D)4s ^{4}D, 3d^7 ^{4}F and 3d^7 a^{4}P forming strong Fe II multiplets. Since transitions from all the 25 levels are observed, collisional excitation is the most likely population process. However, the decay of the (^{5}D)5s levels, populated by the cascading decay of the H Lyα pumped (^{5}D)5p levels (see Sect. 3.2.1), causes deviations in the thermal population of (^{5}D)4p. Thus, the observed line strengths within the (^{5}D)4s–(^{5}D)4p and 3d^7–(^{5}D)4p multiplets are different from what is expected from their gA-values, as measured by Schnabel et al. (2004) (Table 8). Also of importance is that the transition to the ground level (^{5}D)4s $^6D_{9/2}$ is in absorption, which indicates that the optical depths also will influence the relative line strengths.

H) The octet levels in Fe II

Three emission lines ($\lambda\lambda$1926.07, 1915.62 and 1887.83) have been identified as originating from the z^8P term in Fe II, which has no spin-allowed decay channels. These three lines require an explanation since the Fe II octet transitions are very rare in stellar spectra. In fact, they have only been observed in the spectrum of the sun Johansson 1977.

If Fe III is to recombine to any octet level of Fe II by electron capture the metastable septet level (^{6}S)4s $^7S_3$ of Fe III has to be populated. The PAR mechanism in Fe III results in population of the (^{6}S)4p ^{7}P levels. Furthermore, by the observed Fe III fluorescence lines at 1955.27, 1914.06 and

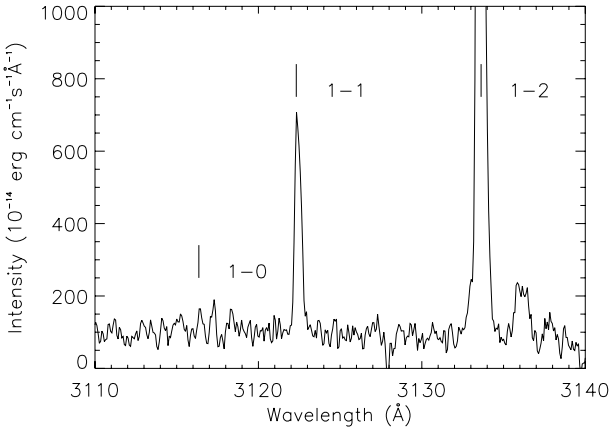

Fig. 12. The three O III 2p3p ^{3}S–2p3d ^{3}P transitions in spectrum lwp25995. Whit the dynamical range of *IUE* it is not sufficient to observe the $^3S_1$–$^3P_0$ transition without having the $^3S_1$–$^3P_2$ transition saturated because of the large difference of intensity.

1895.46 Å corresponding to (^{6}S)4s ^{7}S–(^{6}S)4p ^{7}P transitions the metastable Fe III (^{6}S)4s $^7S_3$ level is known to be populated. In Fig. 11 our suggestion of the process leading to the Fe II octet transitions is shown.

3.3. The O III Bowen lines

The first known PAR process was the pumping of O III through the channel 2p^2 $^3P_2$–2p3d $^3P_2$ at 303.80 Å by He II Lyα at 303.78 Å Bowen 1934, 1935. In the spectra of AG Peg emission lines corresponding to 2p3p ^{3}S–2p3d ^{3}P and 2p3p ^{3}D–2p3d ^{3}P transitions are observed, which concludes that the Bowen mechanism is active in the system. The possibility of allowed primary decays from 2p3d ^{3}P to 2p3p ^{3}P, which form emission lines around 3430 Å, is outside the *IUE* range. However, all six possible emission lines corresponding to the secondary decays 2p3s ^{3}P–2p3p ^{3}P are observed and hence, the 2p3p ^{3}P–2p3d ^{3}P is certainly active. Also, two emission lines, O III λ3341.73, 3300.34 are observed as secondary decays from 2p3s ^{3}P–2p3p ^{3}S transitions.

It is not only the $^3P_2$ level that is populated by PAR in AG Peg, the two other fine structure levels, $^3P_1$ and $^3P_0$, are also populated through channels within 2p^2 ^{3}P–2p3d ^{3}P between 303.41 Å and 303.80 Å (Eriksson et al. 2005). From the three emission lines corresponding to 2p3p ^{3}S–2p3d ^{3}P (Fig. 12) the relative population rate of the fine structure levels in 2p3d ^{3}P can be estimated. The theoretical relative LS intensities for the transitions ($^3S_1$–$^3P_2$:$^3S_1$–$^3P_1$:$^3S_1$–$^3P_0$) are 100:60:20 and the observed relative intensities, which can not be measured exactly because of saturation of the strongest line, are 100:$<$20:$<$3. The population rate of $^3P_1$ and $^3P_0$ is less than for $^3P_2$ by a factor of at least 3 and 7, respectively.

When the observed Balmer α and Pashen lines of He II became narrower by a factor of ∼20 during the middle of the 1980s the He II Lyα pumped O III lines also changed in appearance. In spectra recorded in 1981 and earlier the *FWHM* of the Bowen lines was ∼120 km s^{-1}, which was a factor of ∼6 smaller than that of the white-dwarf wind lines but more than a factor of 3 broader than the emission lines from the nebula and the red-giant atmosphere. The *FWHM* of the O III Bowen lines then decreased and was ∼45 km s^{-1} in the early 1990s. The widths of the emission lines associated with the white-dwarf wind in early *IUE* spectra decreased more rapidly during the 1980s, and the Bowen lines were actually among the broadest UV emission lines in spectra of AG Peg in the early 1990s. After 1986 the net flux of the O III Bowen lines increased by ∼50%. This could mean that after the He II region changed location from the white-dwarf wind to the heated part of the red-giant atmosphere more He II emission was able to reach the O^{2+} ions.

3.4. A line list for AG Peg

All emission features observed in this work are listed in Table 13. Lines longward of 1980 Å were observed with *IUE* (*LWP*), the lines between 1170 and 1980 Å with *IUE* (*SWP*) and the lines below 1170 were observed with *FUSE* (*LWRS* and *MDRS*). In order to make comparison of line strengths useful for lines within the wavelength range of each instrument all peak intensities and *FWHM* are tabulated as measured in the same spectra, LWP25995 for 1980–3350 Å, SWP47715 for 1170–1980 Å and Q1110101 for lines below 1170 Å, which we call the reference spectra. A few emission features are present in spectra other than the reference spectra. These features are marked with "oth" in the first column in the table and no information about intensity or *FWHM* are given in Table 14. The reference spectra were selected as such since they have the lowest noise level, which has the disadvantage that the strongest lines are saturated and no information about peak intensity or *FWHM* can be given in Table 13. The saturated lines are marked by "oe" in the second column. In Cols. 4–7 the identifications of the observed lines are presented. For the unidentified lines those columns are left blank. Features that are considered to be blended with unknown features are marked with the superscript "bl" on the measured intensity in the second column. In Col. 8 we have noted the subsection to which the reader can refer for our suggestion of the process responsible for the formation of the feature. For the wavelength intervals covered by the *HST* (GHRS) observations Col. 9 presents the intensities.

In Table 14 all of the emission lines absent in the reference spectra are given with the observed wavelengths (Col. 1), peak intensities (Col. 2) and widths (Col. 3). The identifications are given in Cols. 4–7 as in Table 13. Column 9 lists the spectra from which the lines were measured.

Table 15 lists all of the lines that were over-exposed in the reference spectra and is constructed in the same manner as Table 14.

Table 16 is a list of the absorption lines in AG Peg. The first column gives the observed wavelength. If the wavelength is superscripted with a; the line is measured in LWP09698, b; SWP15651 and c; SWP10454, while all other lines are measured in the reference spectra. The superscript "*" means that the line is not measured in this work but that its presence is revealed by profile fitting of the N V and C IV resonance lines (Eriksson et al. 2004). The equivalent widths of the lines are given in Col. 2 and the identifications in Cols. 3–6. In Col. 7,

IS stands for interstellar line and *bl* for line blended by unknown contributors.

4. Nature of the emission lines in symbiotic stars

4.1. White-dwarf wind lines

A question one might ask is whether the broad wind features associated with some of the lines between 1000 and 2000 Å in AG Peg (before 1986) are unique to this star or if they are common among the symbiotic stars. To answer this question the lines showing broad wind profiles in AG Peg were analyzed for the symbiotic stars listed in Table 2. It turned out that the widths of over 400 km s^{-1} observed in AG Peg before 1986 are rare but not unique among these other systems, as it was observed for four of the nineteen selected symbiotic systems (PU Vul, T CrB, CH Cyg and EG And).

PU Vul is one of the symbiotic stars classified as symbiotic novae Vogel & Nussbaumer 1992, just like AG Peg. The Si IV λ1393 line shows a P Cygni profile with terminal velocity of 750 km s^{-1}, which is similar to the white-dwarf wind velocity of AG Peg (Eriksson et al. 2004). We suggest, therefore, that the broad lines in PU Vul can be explained by a fast wind from the white dwarf triggered by the slow nova outburst. EG And is known to have a fast (~500 km s^{-1}) wind from the white dwarf (Vogel 1993), which can explain the broad profiles underlying the narrower nebular lines in its spectrum. Interestingly, in 1995 the C IV λ1548 line displayed a P Cygni profile associated with a terminal velocity of only 114 km s^{-1}. We have not been able to explain this absorption component but modeling of the same line in AG Peg has revealed an absorption component. This is the collision region of the white dwarf and red giant winds associated with a terminal velocity of half the white dwarf wind velocity. This should be noticed since EG And also has a region where the winds from the two stars collide (Tomov 1995). More surprising are the broad lines in T CrB and CH Cyg, since the white dwarf in these systems is known to be accreting matter from the red-giant wind (Iijima 1982; Kenyon & Garcia 1986), and therefore no white-dwarf wind is expected. The argument of matter falling into the disk surrounding the white dwarf is further strengthened here as inverted P Cygni profiles are observed in the lines C IV λ1548 (both systems) and He II λ1640 (only in T CrB). Even if we cannot explain how the lines are broadened to over 700 km s^{-1} the reason can be the infall of matter on the disk surrounding the white dwarf.

The 15 symbiotic systems with no trace of lines having *FWHM* greater than 400 km s^{-1} can be divided into two distinct categories with respect to the lines showing broad wind profiles in AG Peg. For eight of the stars all of those lines have *FWHM* between 40 and 70 km s^{-1}, which is normal for most of the lines observed by *IUE* in spectra of symbiotic stars. Such lines are called nebular lines and their origin being the red giant upper atmosphere irradiated by the white dwarf. For the remaining seven systems some of those emission lines have a *FWHM* between 110 and 140 km s^{-1}. Common to these latter systems is that they all have underwent outbursts which could lead to an outflow of matter from the white dwarf. In Table 9 the widths of five lines associated with the white-dwarf wind in a few of the symbiotic systems is given for 20 symbiotic systems.

4.2. Fe II fluorescence

From Sect. 3.2.1 it was clear that the Fe^{+} ions in AG Peg are subjected to radiation from both a high-temperature region and a cool region emitting H Lyα. Also, in RR Tel Fe II fluorescence lines are observed, pumped both by lines from highly-ionized ions and by H Lyα (Hartman & Johansson 2000). A study of fluorescence lines in symbiotic stars (Eriksson et al. 2004) indicated that the Fe II regions in stars associated with slow nova eruptions were pumped by both H Lyα and high-ionization lines resulting in numerous (>10) actively pumped Fe II channels. Other symbiotic stars (with no indication of slow nova eruptions) showed fewer fluorescence lines and no H Lyα pumping. A special case is those objects known to have an accreting hot component, whose spectra showed no Fe II fluorescence.

In the present study ultraviolet Fe II fluorescence lines have been searched for in the symbiotic stars listed in Table 2. The presence of the Fe II lines $\lambda\lambda$2507.55, 2509.10 in emission serves as an indication of H Lyα pumping, while lines from the C IV pumped Fe II levels (see Table 5) serve as indicators of an Fe II region subjected to radiation from a high-ionization region. Absence of fluorescence lines in *IUE* data of a symbiotic star is not a sufficient reason to conclude that there is no pumping of Fe II. The lower limit of the peak intensity, for a line to be detected with the *IUE*, is around 3×10^{-13} erg cm^{-2} s^{-1}. However, in systems where the (^{5}D)4s–(^{5}D)4p resonance transitions but still no Fe II fluorescence lines are observed fluorescence can be ruled out or assumed to play a negligible role. Therefore, a search for Fe II lines corresponding to the a^6D–z^6D and a^6D–z^6P multiplets, which normally form the strongest Fe II lines in the *IUE* wavelength domain, has been carried out. The results of this search are presented in Table 10.

Among the twenty symbiotic systems considered in this study six belong to the subgroup of symbiotic slow novae: AG Peg, HM Sge, PU Vul, RR Tel, PU Vul, V1016 Cyg and V1329 Cyg. Except for HM Sge, both H Lyα and C IV λ1548 pumping of Fe II occurs in these systems, as observed by Eriksson et al. (2004). Emission lines in HM Sge are, in general, one magnitude fainter than in other symbiotic novae and even the Fe II resonance lines cannot be observed in the *IUE* spectra. This anomaly for HM Sge could indicate that it has no significant Fe II region or that the S/N ratio of *IUE* is not high enough to see the Fe II emission.

Three of the symbiotic systems (CH Cyg, CI Cyg and T CrB) are known to have accreting disks around their hot components. As pointed out by Eriksson et al. (2004) no Fe II fluorescence can be detected in those systems. However, the Fe II resonance lines are observed in CH Cyg, which implies that there might be a Fe II region but no fluorescence in symbiotic systems involving accretion onto the hot component.

It becomes more problematic when considering the results of the 11 "normal" symbiotic stars, which do not belong to the

Table 9. The nature of lines having white dwarf wind profile in AG Peg in symbiotic stars.

Object	He II λ1640	C IV λ1548	N IV λ1486	N V λ1238	Si IV λ1393	Comment
EG And	(tcp)	52 (s, pc)	36		34	B
CH Cyg	42 (s)	730 (pc*)		321	str	B
T CrB	573 (pc*)	821 (pc*)	320	788		B
PU Vul		166			982 (pc)	B
V1329 Cyg	159	226				b
Z And	113	64	67	114	69	N*
RX Pup	68	128 (s)	118	111	112	N*
HBV475	142	130				N*
R Aqr		112			110	N*
HM Sge	137	111	130	131	110	N*
AG Dra	110	58	41	70 (pc)	56	N*
RW Hya	64	56	55			N
SY Mus	66	67	36	58	39	N
BF Cyg	38	65 (s, pc)	65		69	N
CI Cyg	68	44	53	55	50	N
V1016 Cyg	65	65	51	52	64	N
RR Tel	70	68	39	51	43	N
AX Per	64	52	46	58	58	N
KX Tra	69	50	36	58	54	N
AG Peg[a]	770	(tcp, pc)	(tcp)	800	(tcp)	B
AG Peg[b]	66	45		56	36	N

N) All five lines have *FWHM* less than 70 km s^{-1}.
N*) One, a few or all of the five lines have a *FWHM* between 120 and 150 km s^{-1}, which is significantly broader than for the majority of lines in their spectra.
b) Two of the five lines are observable in *IUE* spectra of V1329 Cyg, the widths of those lines are broader than for the stars denoted N* but narrower than 400 km s^{-1}.
B) Very broad lines (*FWHM* > 400 km s^{-1}) are observed as single lines or as narrow lines superimposed on broad sockets (str).
pc) P cygni profile.
pc*) Inverted P cygni profile.
tcp = Two component profile as the spectral line has a narrow emission component superimposed on the broad white dwarf wind profile.

subgroup symbiotic novae or show any sign of a disk. Four of those systems, BF Cyg, HBV475, AG Dra and KX Tra, have no detectable Fe II emission lines in the *IUE* spectra, and they are in a way similar to the symbiotic nova HM Sge as regards Fe II. The systems RW Hya and R Aqr show Fe II fluorescence lines from levels pumped by high-ionization lines only. However, *IUE* spectra of the systems EG And, SY Mus, Z And and RX Pup have Fe II lines from both C IV λ1548 and H Lyα pumped levels. Even if neither is designated as a symbiotic nova, recurrent outbursts have been observed for Z And (Tomov et al. 2003) and RX Pup (Mikolajewska et al. 1999). This could mean that the dynamics and structure of a symbiotic system change during the outbursts (both for recurrent and slow novae) so that emission from both highly-ionized regions and H I regions can reach the Fe^+ ions. Then the group of symbiotic stars having numerous fluorescence lines (Eriksson et al. 2004) would be expanded to include all symbiotic stars associated with outbursts and not only symbiotic novae. A complication to this simple idea is that outbursts also have been observed in the symbiotic stars CI Cyg and AG Dra (Belczynski et al. 2000), which do not have numerous fluorescence lines. Since CI Cyg is, as discussed in the previous paragraph, a disk-system for which no Fe II fluorescence has been observed and AG Dra is known to be metal deficient, the lack of Fe II emission lines in these two systems is no surprise. Two normal symbiotic stars seem to fall outside the established groups: SY Mus, which emits Fe II fluorescence from both H Lyα and C IV λ1548 pumped levels, and AX Per, which is the only symbiotic star known to emit Fe II lines only from H Lyα pumped levels.

4.3. Forbidden lines

Forbidden lines indicate low density regions in astrophysical sources. In AG Peg, this low density region must be very hot

Table 10. Fe II emission in symbiotic stars.

Object	C IV pumped	H Lyα pumped	(^{5}D)4s–(^{5}D)4p collisionally excited
AG Peg	yes	yes	yes
SY Mus	yes	yes	yes
Z And	yes	yes	yes
RX Pup	yes	yes	yes
V1016 Cyg	yes	yes	yes
RR Tel	yes	yes	yes
V1329 Cyg	yes	yes	no
PU Vul	yes	yes	no
EG And	yes	yes	no
CH Cyg	no	yes	yes
RW Hya	yes	no	no
AX Per	no	yes	no
R Aqr	no	no	yes
CI Cyg	no	no	no
HBV475	no	no	no
T CrB	no	no	no
HM Sge	no	no	no
AG Dra	no	no	no
BF Cyg	no	no	no
KX Tra	no	no	no

since the forbidden lines belong to highly ionized atoms. As a check whether such a region with high temperature and low density is common in symbiotic stars a search was conducted for forbidden lines in the *IUE* spectra of the other symbiotic stars. As indicators of lower temperature in the low density regions forbidden lines of N II, O I, O II and O III were selected. Forbidden lines of third to fifth spectra of the noble gases, as well as [Mg V] (observed in AG Peg) serve as indicators of high temperature. Also, the presence of [Mg VI] and [Mg VII] lines would imply an even higher temperature in the low density region than for AG Peg. A list of the forbidden lines searched for in the *IUE* spectra of all 20 selected symbiotic stars is given in Table 11.

Forbidden lines are detected in *IUE* spectra for 14 of the 20 selected symbiotic stars (see Table 11). [Mg V] is seen in the spectra of eight of the symbiotic stars, and is the most frequently observed among the forbidden lines. There are four systems showing forbidden lines from magnesium: EG And, RW Hya, CH Cyg and R Aqr. EG And has forbidden lines from [O II], [Ar III] and [Ne III], RW Hya from [O III] and [Ar III], CH Cyg from [O III] and [Ar III] and R Aqr from [O II] and [O III] and [Ar III]. The absence of [Ar V] and [Ne V] in these four systems indicates that the temperature in the low density region is too low for the formation of Mg^{4+}. The system AG Dra has only forbidden lines from [Mg VI] and [Mg VII]. The relative locations of the forbidden line regions within the symbiotic stars, and thereby the radiation field they are subjected to are poorly known. Therefore, a more detailed analysis of the forbidden line regions are not possible at this point. Assuming local thermal equilibrium, the forbidden lines observed can be explained by one region of one dominant temperature in 6 of the 14 systems showing forbidden lines (see Table 11).

5. Summary

The ultraviolet spectrum of AG Peg is indeed complex. In terms of number of lines the emission spectrum is dominated by nebular lines. Overall, the lines reflect a variety of physical processes and locations. A few emission lines are associated with the red-giant chromosphere such as Mg II $\lambda\lambda$2803.53, 2796.35 which are the strongest lines between 2000 and 3000 Å. They have a self-absorbed structure, which is typical for resonance lines. In large contrast to the red giant chromospheric lines, the AG Peg spectrum also contains parity-forbidden lines from highly-ionized ions like Ne^{3+} and Mg^{5+}. These forbidden lines originate in the thin outer nebula. As an indication of the complexity of the system, intercombination and allowed lines from highly ionized ions are also observed. Most of these lines, such as Si III] λ1892.03, are excited by collisions while a few lines like O V λ1506.76 are excited by recombination. These lines are formed in the heated part of the extended red-giant atmosphere. A large number of the lines in the AG Peg spectrum are fluorescence lines, for which location of formation is not well understood. Superimposed on the spectra of nebular lines are a few broad wind lines. These lines are from highly-ionized elements and those that decay to the ground level display a P Cygni profile, showing that they are formed in the white-dwarf wind. A segment of the line-list for AG Peg can be seen in Table 13.

During the 1980s the spectrum of AG Peg changed remarkably. Before 1986 six forbidden lines were observable in *IUE* spectra: [O III] λ2321.66, [Ne III] λ1814.63 and four [Ne IV] lines. After 1986 the [O III] line has disappeared while six new lines from four times ionized ions (Ar^{4+}, Ne^{4+} and Mg^{4+}) and two lines from Fe^{5+} are observed. An explanation for the change among the parity forbidden lines can be a temperature increase in the region emitting those lines. All of the 22 emission lines observed by *IUE* with $FWHM > 400$ km s^{-1} before 1986 (the white-dwarf wind lines) partially or completely disappeared after 1986 and were replaced by narrow nebular lines. The transformation of the broad wind lines occurred first for the lines of lower ionization energies and later for lines of higher ionization energies. A continuous temperature increase in the white-dwarf wind during the 1980s would explain the order in which the white-dwarf wind lines disappeared, but the temperature of the white dwarf was according to Zanstra determinations constant during the same period (Altamore & Cassatella 1997). However, a temperature increase of the wind does not mean that the temperature of the white dwarf surface increased. Eriksson et al. (2004) showed that the opacity in the white-dwarf wind for two of the wind emission lines decreased, which means that more radiation from the white dwarf reaches further into the wind. A shell in the white-dwarf wind emitting, for example, C^{3+} emission moves outward in the white-dwarf wind until all C^{3+} ions in the wind are ionized to C^{4+}.

A few of the lines which possessed wind profiles in the spectra before 1986 are shown to be pumping Fe II channels and are thereby the cause of many of the observed Fe II fluorescence lines. When the broad wind profiles disappeared in the 1980s, only the Fe II fluorescence lines corresponding to

Table 11. Forbidden lines searched for in 20 symbiotic stars.

λ_{vac} (Å)	Spectra	Config.[a]	Transition	A_{ij} (s^{-1})	No[b].
3110.08	[Ar III]	$3p^4$	$^3P_1$–$^1S_0$	4.02	3
3071.44	[N II]	$2p^2$	$^3P_2$–$^1S_0$	1.4×10^{-4}	3
3063.72	[N II]	$2p^2$	$^3P_1$–$^1S_0$	0.032	1
3006.10	[Ar III]	$3p^4$	$^3P_2$–$^1S_0$	0.043	1
2993.64	[Mg V]	$2p^4$	$^3P_0$–$^1D_2$	6.7×10^{-5}	2
2975.66	[Ne V]	$2p^2$	$^1D_2$–$^1S_0$	2.60	2
2973.15	[O I]	$2p^4$	$^3P_1$–$^1S_0$	0.075	1
2959.23	[O I]	$2p^4$	$^3P_2$–$^1S_0$	2.4×10^{-4}	1
2928.87	[Mg V]	$2p^4$	$^3P_1$–$^1D_2$	0.55	8
2868.99	[Ar IV]	$3p^3$	$^4S_{3/2}$–$^2P_{1/2}$	0.97	3
2854.48	[Ar IV]	$3p^3$	$^4S_{3/2}$–$^2P_{3/2}$	2.55	4
2786.82	[Ar V]	$3p^2$	$^3P_2$–$^1S_0$	0.081	0
2783.50	[Mg V]	$2p^4$	$^3P_2$–$^1D_2$	1.90	8
2692.02	[Ar V]	$3p^2$	$^3P_1$–$^1S_0$	6.80	4
2629.92	[Mg VII]	$2p^2$	$^3P_2$–$^1D_2$	3.39	1
2509.98	[Mg VII]	$2p^2$	$^3P_1$–$^1D_2$	1.30	1
2471.09	[O II]	$2p^3$	$^4S_{3/2}$–$^2P_{3/2}$	0.052	6
2470.97	[O II]	$2p^3$	$^4S_{3/2}$–$^2P_{1/2}$	0.021	6
2442.12	[Mg VII]	$2p^2$	$^3P_1$–$^1D_2$	1.3×10^{-4}	0
2425.15	[Ne IV]	$2p^3$	$^4S_{3/2}$–$^2D_{5/2}$	4.1×10^{-4}	3
2422.51	[Ne IV]	$2p^3$	$^4S_{3/2}$–$^2D_{3/2}$	5.3×10^{-3}	4
2418.20	[Mg V]	$2p^4$	$^1D_1$–$^1S_0$	4.20	2
2332.11	[O III]	$2p^2$	$^3P_2$–$^1S_0$	6.3×10^{-4}	1
2321.66	[O III]	$2p^2$	$^3P_1$–$^1S_0$	0.22	5
1814.63	[Ne III]	$2p^4$	$^3P_1$–$^1S_0$	2.20	3
1806.49	[Mg VI]	$2p^3$	$^4S_{3/2}$–$^2D_{5/2}$	3.2×10^{-3}	2
1805.94	[Mg VI]	$2p^3$	$^4S_{3/2}$–$^2D_{3/2}$	0.12	2
1793.70	[Ne III]	$2p^4$	$^3P_2$–$^1S_0$	5.1×10^{-3}	0
1601.67	[Ne IV]	$3p^3$	$^4S_{3/2}$–$^2P_{1/2}$	0.53	4
1601.50	[Ne IV]	$3p^3$	$^4S_{3/2}$–$^2P_{3/2}$	1.33	4
1592.27	[Ne V]	$2p^2$	$^3P_2$–$^1S_0$	6.8×10^{-3}	0
1574.77	[Ne V]	$2p^2$	$^3P_1$–$^1S_0$	4.20	2

[a] All forbidden lines in this table have the ground configuration for both upper and lower level.
[b] The number of symbiotic stars where the lines were observed.

the closest coincidances remained while the other Fe II fluorescence lines vaniched.

Observations by *FUSE* reveal that the O VI λ1031, 1037 doublet still showed a broad wind profile in 2001. The evolution of the fluorescence lines followed that of their pumping lines. As the broad wind lines vanished so did the fluorescence lines associated with channels too far apart in wavelength from the replacing nebular lines while the fluorescence lines with very close wavelength coincidences remained in the spectrum. Fe II fluorescence lines pumped by H Lyα became stronger during the 1980s, indicating growth of the H II region in the system.

Many of the emission lines in spectra of AG Peg have been and surely will continue to be used for various diagnostics. When establishing diagnostics, such as for determining temperatures or densities, it is crucial to understand the nature of the lines employed.

White-dwarf winds in symbiotic stars seem to be quite rare, since broad wind profiles only could be detected in five of the 20 symbiotic systems. In the beginning we suspected that such a wind was linked to the slow nova eruption that has occurred in some of these systems. This idea must be re-considered since only two, PU Vul and AG Peg, of the five systems having broad wind profiles belong to the subclass of symbiotic novae. For seven of the other 15 symbiotic stars the *FWHM* of the lines show wind profiles in AG Peg are between 110–140 km s^{-1}, while the *FWHM* of the same lines in the other eight symbiotic stars were 40–70 km s^{-1}.

Except for the total lack of Fe II emission lines in the *IUE* spectrum of HM Sge, Fe II fluorescence lines pumped by both H Lyα and C IV λ1548 were observed in the symbiotic novae.

Table 12. Forbidden spectra in symbiotic stars.

Object	Spectra	comm.
Z And	O I, N II, Mg V	
EG And	O II, Ne III, Ar III	*
R Aqr	O II+III, Ar III	*
T CrB		
BF Cyg		
CH Cyg	O II, Ar III	
CI Cyg		
AG Dra	Mg VI+VII	*
RW Hya	O III, Ar IV	*
SY Mus	Ar V, Mg V	
AG Peg	O III, Ne III+IV+V, Ar V, Mg V	
AX Per		
RX Pup		
HM Sge	O II, Ar IV, Ne IV, Mg V	
RR Tel	N II, O II+III, Ar III+IV+V, Ne III+IV+V, Mg V+VI	
KX Tra	Mg V+VI	*
PU Vul		
V1016 Cyg	N II, O II+III, Ar IV, Ne IV, Mg V	
V1329 Cyg		
HBV475	Mg V	*

* All forbidden lines in the system can be explaind by a low density region in local thermal equilibrium and of one dominant temperature.

Table 13. A sample of the AG Peg line list.

λ_{obs} (Å)	I^a	W^b	λ_{id} (Å)	Spec.	Lower level	Upper level	Sec^c	Exc^f
2837.13	652	43	2837.14	O III	2p3p $^3D_3$	2p3d $^3P_2$	3	fl
			7.10	O IV	2s2p(^{3}P)3s $^4P_{5/2}$	2s2p(^{3}P)3p $^4S_{3/2}$	unk	
2836.43	46	24	2836.55	Fe II	4s $b^2P_{3/2}$	4p $z^4G_{5/2}$	2.1	fl
2833.91	50	56	2834.20	Fe II	4s $a^4D_{7/2}$	4p $z^6P_{5/2}$	2.3G	col
			3.92	Fe II	4p $z^6P_{5/2}$	5s $e^6D_{5/2}$	2.1	fl
2832.28	46	26	2832.40	Fe II	4s $b^2P_{3/2}$	4p $z^2D_{5/2}$		unk
Oth			2831.76	Fe II	4s $b^2G_{7/2}$	4p $x^4G_{5/2}$	2.1	fl
2829.82	59	34	2829.91	He I	2s $^3S_1$	6p $^3P_2$	2.3A	rec

Even if Fe II fluorescence lines were observed in most symbiotic stars only four of the 14 symbiotic systems with no slow nova eruption known had Fe II pumped by both H Lyα and C IV. Three systems in our selection have suggested accretion disks around the hot component. The spectra of these three systems showed no signs of Fe II fluorescence. During slow nova eruptions the cool H I region and a region hot enough to create ions like C^{3+} simultaneously are in the line of sight with the large region with Fe^+ ions, while this rarely is the case for symbiotic systems under "normal" conditions.

Acknowledgements. All of the data presented in this paper were obtained from the Multimission Archive at the Space Telescope Science Institute (MAST). STScI is operated by the Association of Universities for Research in Astronomy, Inc., under NASA contract NAS5-26555. Support for MAST for non-HST data is provided by the NASA Office of Space Science via grant NAG-7584 and by other grants and contracts. We are grateful to the anonymous referee for a careful reading of the manuscript.

References

Allen, D. A. 1982, Nature of Symbiotic Stars, ed. M. Friedjung, & R. Viotti (Reidel: Dordrecht), IAU Coll., 70, 27
Altamore, A., & Cassatella, A. 1997, A&A, 317, 712
Belczynski, K., & Mikolajewska, J. 1998, MNRAS, 296, 77
Belczynski, K., Mikolajewska, J., Munari, U., Ivison, R. J., & Friedjung, M. 2000, A&AS, 146, 407
Bowen, I. S. 1934, PASP, 46, 146
Bowen, I. S. 1935, ApJ, 81, 1
Burgarella, D., Paresce, F., & Vogel, M. 1992, ed. L. Drissen., C. Leitherer., & A. Nota (San Francisco: Astron. Soc. Pac.), ASP Conf. Ser., 22, 298
Contini, M. 1997, ApJ, 483, 887
Contini, M. 2003, MNRAS, 339, 125

Eriksson, M., Johansson, S., & Wahlgren, G. M. 2001, ASP Conf. Ser., 242, ed. T. R. Gull, S. Johansson, & K. Davidsson (San Francisco: ASP), 325
Eriksson, M., Johansson, S., & Wahlgren, G. M. 2003, ed. R. L. M. Corradi, R. Mikolajewska, & T. J. Mahoney (San Francisco: Aston. Soc. Pac.), ASP Conf. Ser., 303, 109
Eriksson, M., Johansson, S., & Wahlgren, G. M. 2004a, A&A, 422, 987
Eriksson, M., Veenhuizen, H., Johansson, S. J., & Wahlgren, G. M. 2004b, RMxAC, 21, 132
Eriksson, M., Johansson, S. J., Wahlgren, G. M., et al. 2005, A&A, 434, 397
Iijima, T. 1982, A&A, 116, 210
Imhoff, C. L. 1984, A Progress Report: The Point-Spread Functions of the Platinum Lines with the New High Dispersion Processing Software, in Record of the International Ultraviolet Explorer NASA/ESA/SERC Three Agency Coordination Meeting, October 3–5, 1983, Computer Sciences Corporation, CSC/TM-84/6042, March 1984, pp. A139
Johansson, S. 1977, ApJ, 212, 923
Johansson, S. 1983, MNRAS, 205, 71
Johansson, S., & Jordan, C. 1984, MNRAS, 210, 239
Johansson, S., & Letokhov, V. S. 2004, A&A, 428, 497
Hartman, H., & Johansson, S. 2000, A&A, 359, 627
Kenyon, S. J., & Garcia, M. R. 1986, AJ, 91, 125
Kenyon, S. J., & Webbink, R. F. 1984, ApJ, 279, 252
Kenyon, S. J., Proga, D., & Keyes, C. D. 2001, AJ, 122, 349
Kenyon, S. J., Mikolajewska, J., Mikolajewski, M., Polidan, R. S., & Slovak, M. H. 1993, AJ, 106, 1573
Keyes, C. E., & Plavec, M. J. 1980, NASA-GSFC Symp. The Universe in Ultraviolet Wavelengths, ed. R. Chapman, (NASA CP-2717), 443
Kondo, Y., Morgan, T. H., & Modisette, J. L. 1976, ApJ, 207, 167
Mikolajewska, J., Brandi, E., Hack, W., et al. 1999, MNRAS, 305, 109
Mürset, U., & Nussbaumer, H. 1994, A&A, 282, 604
Mürset, U., Jordan, S., & Walder, R. 1995, A&A, 297, 87
Mürset, U., Wolff, B., & Jordan, S. 1997, A&A, 319, 201
Nussbaumer, H., & Schild, H. 1979, A&A, 75, 17
Nussbaumer, H., & Storey, P. J. 1979, A&A, 71, 5
Nussbaumer, H., & Schild, H. 1981, A&A, 101, 118
Nussbaumer, H., & Storey, P. J. 1982, A&A, 115, 205
Nussbaumer, H., Schmutz, W., & Vogel, M. 1995, A&A, 293, L13
Penston, M. V., & Allen, D. A. 1985, MNRAS, 212, 939
Penston, M. V., Benvenuti, P., Cassatella, A., Heck, A., et al. 1983, MNRAS, 202, 833
Schmutz, W. 1996, Science with the *HST*-II, ed. F. D. M. Piero Benvenuti, & J. S. Ethan (Baltimore: STScI), 366
Schnabel, R., Schultz-Johanning, M., & Kock, M. 2004, A&A, 414, 1169
Tomov, N. A., Taranova, O. G., & Tomova, M. T. 2003, A&A, 401, 669
Tomov, N. 1995, MNRAS, 272, 189
Vogel, M. 1993, A&A, 274, 21
Vogel, M., & Nussbaumer, H. 1992, A&A, 259, 525
Vogel, M., & Nussbaumer, H. 1994, A&A, 248, 145
Yoo, J. J., Lee, H., & Ahn, S. 2002, MNRAS, 334, 974

Online Material

Table 13. All emission lines observed in AG Peg.

λ_{obs} (Å)	I^a	w^b	λ_{id} (Å)	spec.	Lower level	Upper level	Sec^c	Exc^f	I^d_{ghrs}	w^e_{ghrs}
3341.62	996	40	3341.73	O III	2p3s $^3P_2$	2p3p $^3S_1$	3	fl		
3311.70	171	21	3311.97	Fe II	4s^2 c$^4D_{5/2}$	(^{5}D)5p $^4D_{5/2}$	2.1	fl		
Oth			3300.34	O III	2p3s $^3P_0$	2p3p $^3S_1$	3	fl		
3299.10	292	17								
3297.84	168	18	3297.72	He I	1s2s $^1S_1$	1s8p $^1P_1$	2.3A	rec		
3296.86	136	20	3296.77	Fe II	4s a$^4D_{3/2}$	4p z$^6D_{3/2}$	2.3G	col		
3255.69	205	38								
3249.08	225	39								
3245.18	126	18	3245.44	Fe II	3d^7 d$^2D_{3/2}$	4p w$^2D_{3/2}$	2.1	fl		
3244.66	121	20	3244.66	Fe II	4s c$^2G_{9/2}$	4p z$^2F_{7/2}$		fl		
3203.97	991	61	3204.02	He II	$n = 3$	$n = 5$	1	rec		
3163.86	97		3164.01	Fe II	3d^7 a$^4P_{5/2}$	4p z$^4F_{5/2}$	2.3G	col		
3162.72	91	23	3162.89	Fe II	3d^7 a$^4P_{3/2}$	4p z$^4F_{3/2}$	2.3G	col		
3157.15	71	42								
3154.96	133		3155.12	Fe II	4s b$^2G_{9/2}$	4p z$^2G_{9/2}$	2.1	fl		
3136.1	160	91								
3133.64	oe		3133.70	O III	2p3p $^3S_1$	2p3d $^3P_2$	3	fl		
3122.43	628	45	3122.54	O III	2p3p $^3S_1$	2p3d $^3P_1$	3	fl		
3117.23	112	36								
3116.47	82	38	3116.58	O III	2p3p $^3S_1$	2p3d $^3P_0$	3	fl		
3079.41	55	25	3079.57	Fe II	4p z$^4P_{5/2}$	5s e$^4D_{7/2}$	2.1	fl		
3072.44	50	21	3072.49	O IV	3s $^2S_{1/2}$	3p $^2P_{1/2}$		rec		
3072.05	44	19	3072.02	Fe II	4p z$^4P_{1/2}$	5s e$^4D_{3/2}$	2.1	fl		
3064.23	75		3064.32	O IV	3s $^2S_{1/2}$	3p $^2P_{3/2}$		rec		
3060.09	131		3060.17	O III	2p3s $^3P_2$	2p3p $^3P_1$	3	fl		
Oth			3049.88	Fe II	4p z$^4P_{3/2}$	5s e$^4D_{3/2}$	2.1	fl		
3047.98	oe		3047.99	O III	2p3s $^3P_2$	2p3p $^3P_2$	3	fl		
3043.81	90	32								
3040.62	32		3040.67	Fe II	4s^2 c$^4D_{3/2}$	4p u$^4F_{3/2}$	2.1	fl		
3036.23	53		3036.30	O III	2p3s $^3P_1$	2p3p $^3P_1$	3	fl		
3034.26	32		3034.33	Fe II	4p z$^4P_{3/2}$	5s e$^4D_{1/2}$	2.1	fl		
3030.6	35^{bl}		3030.57	Fe II	4s c$^2G_{9/2}$	4p y$^4H_{11/2}$	2.1	fl		
3025.74	78									
3025.36	94		3025.42	O III	2p3s $^3P_0$	2p3p $^3P_1$	3	fl		
3024.26	217	50	3024.31	O III	2p3s $^3P_1$	2p3p $^3P_2$	3	fl		
3003.36	128^{bl}	32	3003.52	Fe II	3d^7 a$^4P_{3/2}$	4p z$^4P_{5/2}$	2.3G	col		
2989.89	45	29	2989.94	Fe II	4p z$^4F_{5/2}$	5s e$^6D_{5/2}$	2.1	fl		
2988.36	66	35								
2986.38	66		2986.51	Fe II	4p z$^4F_{7/2}$	5s e$^6D_{7/2}$	2.1	fl		
			6.42	Fe II	3d^7 a$^4P_{1/2}$	4p z$^4P_{3/2}$	2.3G	col		
2985.63	163		2985.96	Fe II	4s^2 d$^4P_{5/2}$	(^{5}D)5p $^4P_{5/2}$	2.1	fl		
			5.70	Fe II	3d^7 a$^4P_{5/2}$	4p z$^4P_{5/2}$	2.3G	col		
2984.54	149	48	2984.65	O III	2p3s $^1P_1$	2p3p $^1D_2$	2.3F	rec		
2980.1	108		2980.22	Fe II	4s a$^4D_{1/2}$	4p z$^6F_{3/2}$	2.3G	col		
			0.19	Fe II	4s^2 d$^4P_{3/2}$	(^{5}D)5p $^4D_{3/2}$	2.1	fl		
2979.87	220		2979.95	Fe II	4s c$^2F_{5/2}$	4p w$^2D_{3/2}$	2.1	fl		
2977.23	39		2977.26	Fe II	4s a$^2I_{13/2}$	4p y$^4H_{11/2}$	2.1	fl		
2976.71	46		2976.81	Fe II	4s a$^4D_{1/2}$	4p z$^6F_{1/2}$	2.3G	col		

Table 13. continued.

λ_{obs} (Å)	I^a	w^b	λ_{id} (Å)	spec.	Lower level	Upper level	Sec^c	Exc^f	I^d_{ghrs}	w^e_{ghrs}
2974.15	103	51	2975.66	[Ne V]	$2p^2\ ^1D_2$	$2p^2\ ^1S_0$	2.2	col		
2971.23	97	30	2971.38	Fe II	4s $a^4D_{3/2}$	4p $z^6F_{5/2}$	2.3G	col		
2970.66	26		2970.80	Fe II	4s $b^2G_{7/2}$	4p $z^2F_{5/2}$		fl		
2965.6	64		2965.90	Fe II	$3d^7$ $a^4P_{3/2}$	4p $z^4P_{3/2}$	2.3G	col		
			5.53	Fe II	4s $a^4D_{3/2}$	4p $z^6F_{3/2}$	2.3G	col		
			5.49	Fe II	$3d^7$ $a^4P_{1/2}$	4p $z^4P_{1/2}$	2.3G	col		
2962.05	41		2962.14	Fe II	4s $a^4D_{3/2}$	4p $z^6F_{1/2}$	2.3G	col		
2960.47	61	38	2960.56	O III	2p3p $^1P_1$	2p3d $^1D_2$	2.3F	rec		
2954.55	130	23	2954.64	Fe II	4s $a^4D_{5/2}$	4p $z^6F_{7/2}$	2.3G	col		
2949.95	62^{bl}	32	2950.04	Fe II	4s $b^2G_{7/2}$	4p $z^2F_{7/2}$		fl		
2948.40	86	28	2948.52	Fe II	$3d^7$ $a^4P_{5/2}$	4p $z^4P_{3/2}$	2.3G	col		
2945.9	113		2946.13	Fe II	4s $a^4D_{5/2}$	4p $z^6F_{5/2}$	2.3G	col		
			5.97	He I	2s $^3S_1$	5p $^3P_2$	2.3A	rec		
2945.17	74	26	2945.26	Fe II	$3d^7$ $a^4P_{3/2}$	4p $z^4P_{1/2}$	2.3G	col		
2940.23	51^{bl}	37	2940.37	Fe II	4s $a^4D_{5/2}$	4p $z^6F_{3/2}$	2.3G	col		
2937.23	184	36	2937.37	Mg II	3p $^2P_{3/2}$	4s $^2S_{1/2}$		unk		
2935.02	43	29								
2933.70	34	29								
2931.74	99	30								
2929.33	259		2929.49	Mg II	3p $^2P_{1/2}$	4s $^2S_{1/2}$		unk		
2927.29	208		2926.44	Fe II	4s $a^4D_{7/2}$	4p $z^6F_{9/2}$	2.3G	col		
			8.0	[Mg V]	$2p^4\ ^3P_1$	$2p^4\ ^1D_2$	2.2	col		
2918.19	27		2918.32	Fe II	4s $a^4D_{5/2}$	4p $z^6P_{7/2}$	2.3G	col		
2916.91	58	16	2917.01	Fe II	4s $a^4D_{7/2}$	4p $z^6F_{7/2}$	2.3G	col		
2908.57	34		2908.71	Fe II	4s $a^4D_{7/2}$	4p $z^6F_{5/2}$	2.3G	col		
2903.17	59	33								
2895.86	51	23								
2895.52	31	13	2895.63	Fe II	4s $b^4H_{9/2}$	4p $z^4H_{11/2}$	2.1	fl		
2893.57	59	23	2893.68	Fe II	4s $a^4D_{3/2}$	4p $z^6P_{5/2}$	2.3G	col		
2892.29	30									
2891.84	50									
2890.40	48^{bl}	33	2890.53	Fe II	4p $z^4F_{3/2}$	5s $e^4D_{5/2}$	2.1	fl		
2888.81	139	24	2888.94	Fe II	4s $b^2P_{3/2}$	4p $y^4P_{5/2}$	2.1	fl		
2886.89	39	20	2887.08	Fe II	4s $b^2H_{11/2}$	4p $z^4G_{9/2}$	2.1	fl		
2885.46	78	23	2885.61	Fe II	4p $z^4D_{5/2}$	5s $e^4D_{7/2}$	2.1	fl		
2884.53	55^{bl}	36	2884.56	Fe II	4s $b^2H_{11/2}$	4p $z^4H_{13/2}$		unk		
2883.13	19^{bl}		2883.04	Fe II	4p $z^4F_{7/2}$	5s $e^4D_{7/2}$	2.1	fl		
2882.36	80	20								
2881.60	42^{bl}		2881.60	Fe II	4s $a^4D_{7/2}$	4p $z^6P_{7/2}$	2.3G	col		
2876.08	100	26	2876.19	Fe II	4s $a^2F_{7/2}$	4p $z^2G_{9/2}$	2.1	fl		
2869.66	75		2869.72	Fe II	4s $a^4D_{5/2}$	4p $z^6P_{5/2}$	2.3G	col		
2865.89	52^{bl}	69	2866.30	Fe II	4p $z^4F_{3/2}$	5s $e^4D_{3/2}$	2.1	fl		
2865.13	51	36								
2859.40	46^{bl}		2859.47	Fe II	4p $z^4D_{1/2}$	5s $e^4D_{3/2}$	2.1	fl		
2857.64	166	35	2857.75	Fe II	4p $z^4D_{7/2}$	5s $e^4D_{7/2}$	2.1	fl		
2856.92	94	43	2857.22	Fe II	4p $z^6P_{5/2}$	5s $e^6D_{7/2}$	2.1	fl		
			6.99	Fe II	4s $a^4G_{9/2}$	4p $z^4G_{9/2}$	2.1	fl		
2852.53	120		2852.56	Fe II	4p $z^4F_{3/2}$	5s $e^4D_{1/2}$	2.1	fl		
2850.45	44	22	2850.44	Fe II	4s $a^4G_{9/2}$	4p $z^4H_{11/2}$		unk		

Table 13. continued.

λ_{obs} (Å)	I^a	w^b	λ_{id} (Å)	spec.	Lower level	Upper level	Sec^c	Exc^f	I^d_{ghrs}	w^e_{ghrs}
2849.11	57		2849.16	Fe II	4p $z^4F_{5/2}$	5s $e^4D_{3/2}$	2.1	fl		
2848.81	44		2848.94	Fe II	4p $z^4D_{5/2}$	5s $e^4D_{5/2}$	2.1	fl		
			8.61	Fe II	4p $z^6P_{3/2}$	5s $e^6D_{3/2}$	2.1	fl		
2846.23	152	39	2846.43	Fe II	4p $z^4F_{7/2}$	5s $e^4D_{5/2}$	2.1	fl		
			6.26	Fe II	4p $z^4D_{3/2}$	5s $e^4D_{3/2}$	2.1	fl		
			6.22	Fe II	4s $b^4D_{5/2}$	4p $x^4F_{5/2}$	2.1	fl		
2844.21	67	44	2844.31	Fe II	4s $b^4D_{3/2}$	4p $x^4F_{5/2}$	2.1	fl		
			4.15	Fe II	4s $b^2H_{9/2}$	4p $z^4I_{9/2}$		unk		
2841.34	51^{bl}		2841.49	Fe II	4s $b^2P_{1/2}$	4p $z^2D_{3/2}$		unk		
2840.26	241	24	2840.35	Fe II	4p $z^4F_{9/2}$	5s $e^4D_{7/2}$	2.1	fl		
2838.91	49	22	2839.05	Fe II	4p $z^6P_{3/2}$	5s $e^6D_{1/2}$	2.1	fl		
2837.13	652	43	2837.14	O III	2p3p $^3D_3$	2p3d $^3P_2$	3	fl		
			7.10	O IV	2s2p(^{3}P)3s $^4P_{5/2}$	2s2p(^{3}P)3p $^4S_{3/2}$	unk			
2836.43	46	24	2836.55	Fe II	4s $b^2P_{3/2}$	4p $z^4G_{5/2}$	2.1	fl		
2833.91	50	56	2834.20	Fe II	4s $a^4D_{7/2}$	4p $z^6P_{5/2}$	2.3G	col		
			3.92	Fe II	4p $z^6P_{5/2}$	5s $e^6D_{5/2}$	2.1	fl		
2832.28	46	26	2832.40	Fe II	4s $b^2P_{3/2}$	4p $z^2D_{5/2}$		unk		
Oth			2831.76	Fe II	4s $b^2G_{7/2}$	4p $x^4G_{5/2}$	2.1	fl		
2829.82	59	34	2829.91	He I	2s $^3S_1$	6p $^3P_2$	2.3A	rec		
2829.38	57	24	2829.46	Fe II	4s $b^2H_{11/2}$	4p $z^4I_{9/2}$		unk		
2828.17	57	30	2828.26	Fe II	4s $b^2H_{11/2}$	4p $z^4I_{13/2}$		unk		
2826.53	64^{bl}	52	2826.58	Fe II	4s $a^4G_{11/2}$	4p $z^4G_{9/2}$	2.1	fl		
2824.06	30		2824.16	Fe II	4s $a^4G_{11/2}$	4p $z^4H_{13/2}$		unk		
2820.08	48	27	2820.17	Fe II	4s $a^4G_{11/2}$	4p $z^4H_{11/2}$		unk		
2819.43	62		2819.53	O III	2p3p $^3D_2$	2p3d $^3P_2$	3	fl		
2817.70	53	26	2817.92	Fe II	4p $z^6P_{5/2}$	5s $e^6D_{3/2}$	2.1	fl		
oth										
2810.49	134	46	2810.61	Fe II	4p $z^6P_{7/2}$	5s $e^6D_{7/2}$	2.1	fl		
			0.49	O III	2p3p $^3D_2$	2p3d $^3P_1$	3	fl		
2808.62	31		2808.73	O III	2p3p $^3D_1$	2p3d $^3P_2$	3	fl		
2807.94	48^{bl}		2808.00	Fe II	4s $b^4D_{5/2}$	4p $y^2D_{5/2}$	2.1	fl		
2806.04	31		2806.15	Fe II	4s $b^4D_{3/2}$	4p $y^2D_{5/2}$	2.1	fl		
2803.5	oe		2803.53	Mg II	3s $^2S_{1/2}$	3p $^2P_{1/2}$	2.3B	col		
2799.60	34^{bl}		2799.76	O III	2p3p $^3D_1$	2p3d $^3P_1$	3	fl		
2798.72	283	29	2798.82	Mg II	3p $^2P_{3/2}$	3d $^2D_{5/2}$		unk		
2796.3	oe		2796.35	Mg II	3s $^2S_{1/2}$	3p $^2P_{3/2}$	2.3B	col		
2794.88	15		2794.96	O III	2p3p $^3D_1$	2p3d $^3P_0$	3	fl		
2791.49	193	36	2791.60	Mg II	3p $^2P_{1/2}$	3d $^2D_{3/2}$		unk		
2785.98	41		2786.12	Ne III	2p^3(^{2}D)3s $^3D_2$	2p^3(^{2}D)3p $^3D_2$	3.2F	rec		
			6.01	Fe II	4p $z^6F_{11/2}$	5s $e^6D_{9/2}$	2.1	fl		
			5.85	Fe II	3d^7 $a^4F_{3/2}$	4p $z^6D_{3/2}$	2.3G	col		
2783.91	363	113	2784.51	Fe II	4s $b^2H_{11/2}$	4p $z^2G_{9/2}$	2.1	fl		
			3.50	[Mg V]	2p^4 $^3P_2$	2p^4 $^1D_2$	2.2	col		
2781.68	29		2781.83	O V	2s3s $^3S_1$	2s3p $^3P_2$	1	rec		
2780.02	44	31								
2778.80	72									
2778.45	53^{bl}		2778.47	Ne III	2p^3(^{2}D)3s $^3D_3$	2p^3(^{2}D)3p $^3D_3$	3.2F	rec		
2777.62	83	21	2777.73	Fe II	4p $z^6F_{7/2}$	5s $e^6D_{7/2}$	2.1	fl		
2776.08	96	21	2776.16	Fe II	3d^7 $a^4F_{5/2}$	4p $z^6D_{5/2}$	2.3G	col		

Table 13. continued.

λ_{obs} (Å)	I^a	w^b	λ_{id} (Å)	spec.	Lower level	Upper level	Sec^c	Exc^f	I^d_{ghrs}	w^e_{ghrs}
2775.47	88	23	2775.55	Fe II	$3d^7\ a^4F_{7/2}$	$4p\ z^6D_{9/2}$	2.3G	col		
2773.45	43	16	2773.55	Fe II	$4s\ a^4D_{5/2}$	$4p\ z^4D_{7/2}$	2.3G	col		
2771.89	631	28	2772.00	Fe II	$4s\ b^2G_{9/2}$	$4p\ y^4H_{11/2}$	2.1	fl		
2770.00	104	76	2770.17	Fe II	$4s\ a^4G_{11/2}$	$4p\ z^4I_{13/2}$		unk		
			9.97	Fe II	$4s\ a^4G_{7/2}$	$4p\ z^2G_{9/2}$	2.1	fl		
2768.21	90	30	2768.33	Fe II	$4p\ z^6F_{9/2}$	$5s\ e^6D_{7/2}$	2.1	fl		
			8.23	Fe II	$4p\ z^6F_{3/2}$	$5s\ e^6D_{5/2}$	2.1	fl		
2764.40	65	49	2764.62	He I	$2s\ ^3S_1$	$7p\ ^3P_2$	2.3A	rec		
2762.59	41		2762.63	Fe II	$4s\ a^4D_{1/2}$	$4p\ z^4D_{3/2}$	2.3G	col		
2760.01	69^{bl}	35	2760.15	Fe II	$3d^7\ a^4F_{7/2}$	$4p\ z^6D_{7/2}$	2.3G	col		
2756.44	153	29	2756.55	Fe II	$4s\ a^4D_{7/2}$	$4p\ z^4F_{9/2}$	2.3G	col		
2755.60	57	33	2755.70	Fe II	$4p\ z^6F_{7/2}$	$5s\ e^6D_{5/2}$	2.1	fl		
2753.96	56^{bl}	42	2754.10	Fe II	$4s\ b^2H_{9/2}$	$4p\ z^2I_{11/2}$		unk		
2752.66	39^{bl}	57	2752.96	Fe II	$4p\ z^6F_{3/2}$	$5s\ e^6D_{3/2}$	2.1	fl		
2751.77	29	23	2751.94	Fe II	$4s\ b^2P_{3/2}$	$4p\ z^2D_{3/2}$		unk		
2751.36	32	16								
2750.75	45	16								
2750.07	137	47	2750.30	Fe II	$4s\ a^4D_{1/2}$	$4p\ z^4D_{1/2}$	2.3G	col		
			0.13	Fe II	$4s\ a^4D_{5/2}$	$4p\ z^4F_{7/2}$	2.3G	col		
			9.99	Fe II	$4s\ a^4D_{3/2}$	$4p\ z^4D_{3/2}$	2.3G	col		
2747.74	118	24	2747.79	Fe II	$4s\ a^4D_{5/2}$	$4p\ z^4D_{5/2}$	2.3G	col		
2747.22	123	22	2747.30	Fe II	$4s\ a^4D_{3/2}$	$4p\ z^4F_{5/2}$	2.3G	col		
2745.03	39	13	2745.08	Fe II	$3d^7\ a^4F_{7/2}$	$4p\ z^6D_{5/2}$	2.3G	col		
2743.94	93	42	2794.04	Fe II	$4p\ z^6F_{3/2}$	$5s\ e^6D_{1/2}$	2.1	fl		
			4.01	Fe II	$4s\ a^4D_{1/2}$	$4p\ z^4F_{3/2}$	2.3G	col		
2742.09	100	16	2742.21	Fe II	$4s\ a^2F_{5/2}$	$4p\ y^4G_{5/2}$	2.1	fl		
2740.27	141	33	2740.36	Fe II	$4s\ a^4D_{7/2}$	$4p\ z^4D_{7/2}$	2.3G	col		
2737.71	41	21	2737.78	Fe II	$4s\ a^4D_{3/2}$	$4p\ z^4D_{1/2}$	2.3G	col		
2734.09	oe		2734.10	He II	$n = 3$	$n = 6$	1	rec		
2733.15	111	31	2733.26	Fe II	$3d^7\ a^4F_{9/2}$	$4p\ z^6D_{9/2}$	2.3G	col		
2731.45	116	33	2731.54	Fe II	$4s\ a^4D_{3/2}$	$4p\ z^4F_{3/2}$	2.3G	col		
2728.11	126	35	2728.35	Fe II	$4s\ a^4D_{5/2}$	$4p\ z^4D_{3/2}$	2.3G	col		
			8.19	Fe II	$4s\ a^4G_{11/2}$	$4p\ z^2G_{9/2}$	2.1	fl		
2725.60	103	21	2725.69	Fe II	$4s\ a^4D_{5/2}$	$4p\ z^4F_{5/2}$	2.3G	col		
2723.92	38	24	2724.00	He I	$2s\ ^3S_1$	$8p\ ^3P_2$	2.3A	rec		
2723.39	48	17	2723.43	Fe II	$4s^2\ d^4P_{3/2}$	$(^4P)4sp\ ^4P_{5/2}$	2.1	fl		
2722.77	43	17	2722.94	Fe II	$4p\ z^6P_{3/2}$	$5s\ e^4D_{1/2}$	2.1	fl		
2719.33	68	71	2719.42	Fe II	$4s\ a^2F_{7/2}$	$4p\ y^4G_{5/2}$	2.1	fl		
			9.42	Fe II	$4s^2\ b^4G_{5/2}$	$(^5D)5p\ ^4D_{3/2}$	2.1	fl		
			9.16	Fe II	$4s\ c^2P_{1/2}$	$(b^3P)4p\ ^4P_{1/2}$	2.1	fl		
2717.11	51	71	2717.34	Fe II	$4s^2\ d^4P_{5/2}$	$(^4P)4sp\ ^4P_{5/2}$	2.1	fl		
			7.02	Fe II	$4s\ a^2F_{5/2}$	$4p\ z^2F_{5/2}$		fl		
2715.13	102	24	2715.22	Fe II	$4s\ a^4D_{7/2}$	$4p\ z^4D_{5/2}$	2.3G	col		
2712.58	94	19								
2709.90	49	46	2710.18	Fe II	$4s\ a^4D_{5/2}$	$4p\ z^4F_{3/2}$	2.3G	col		
			9.86	Fe II	$4s\ b^2P_{3/2}$	$4p\ y^4D_{5/2}$		fl		
2707.36	64	48	2707.37	Fe II	$4s\ b^2D_{5/2}$	$4p\ y^2P_{3/2}$		unk		
			7.14	Fe II	$4p\ z^6P_{5/2}$	$5s\ e^4D_{3/2}$	2.1	fl		
2704.77	36	21	2704.79	Fe II	$4s\ a^2F_{7/2}$	$4p\ z^2F_{7/2}$		fl		

Table 13. continued.

λ_{obs} (Å)	I^a	w^b	λ_{id} (Å)	spec.	Lower level	Upper level	Sec^c	Exc^f	I^d_{ghrs}	w^e_{ghrs}
2698.14	48	33								
2696.77	30	39	2696.92	He I	2s $^3S_1$	9p $^3P_2$	2.3A	rec		
			6.91	N III	4s $^2S_{1/2}$	5p $^2P_{3/2}$	2.3F	rec		
2693.54	70	28	2693.63	Fe II	4s a$^4D_{7/2}$	4p z$^4F_{5/2}$	2.3G	col		
2691.65	101	40	2692.02	[Ar V]	3p^2 $^3P_1$	3p^2 $^1S_0$	2.2	col		
2689.93	54^{bl}	36	2690.01	Fe II	4s b$^2P_{3/2}$	4p y$^4D_{3/2}$		fl		
2687.18	37^{bl}		2687.27	Fe II	4s d$^2F_{7/2}$	4s4p x$^4H_{9/2}$	2.1	fl		
2686.85	26	21	2686.95	O III	2s2p^2(^{4}P)3s $^5P_3$	2s2p^2(^{4}P)3p $^5S_2$	2.3F	rec		
2683.24	86	19	2683.30	Fe II	4s d$^2F_{3/2}$	4p u$^2G_{9/2}$	2.1	fl		
2681.56	50	34								
2679.50	43	34	2679.44	Ne III	2p^3(^{4}S)3s $^3S_1$	2p^3(^{4}S)3p $^3P_1$	1	rec		
2678.67	28		2678.70	Ne III	2p^3(^{4}S)3s $^3S_1$	2p^3(^{4}S)3p $^3P_2$	1	rec		
2677.73	102	34	2677.93	He I	2s $^3S_1$	10p $^3P_2$	2.3A	rec		
2675.20	90	21	2675.38	O III	2s2p^2(^{4}P)3s $^5P_2$	2s2p^2(^{4}P)3p $^5S_2$	2.3F	rec		
2669.85	436	29	2669.95	Al II]	3s^2 $^1S_0$	3p $^3P_1$	2.3C	col		
2667.35	56	24								
2666.69	50	29								
2664.89	46^{bl}		2664.99	Fe II	4s b$^2H_{9/2}$	4p y$^4G_{11/2}$		unk		
2664.01	76^{bl}		2664.06	He I	2s $^3S_1$	11p $^3P_2$	2.3A	rec		
2650.16	76	19	2650.26	Fe II	4s d$^2F_{5/2}$	4p u$^2G_{7/2}$	2.1	fl		
Oth			2644.55	Fe II	4s^2 b$^4G_{5/2}$	4p x$^4H_{7/2}$	2.1	fl		
2639.03	85	52	2639.32	Fe II	4s^2 b$^4G_{7/2}$	4p u$^2G_{9/2}$	2.1	fl		
			9.01	Fe II	4s^2 b$^4G_{9/2}$	4p x$^4H_{11/2}$	2.1	fl		
2631.94	174	75	2632.11	Fe II	4s a$^6D_{5/2}$	4p z$^6D_{7/2}$	2.3G	col		
			1.83	Fe II	4s a$^6D_{3/2}$	4p z$^6D_{5/2}$	2.3G	col		
			1.80	Fe II	4s b$^4F_{7/2}$	4p z$^4G_{9/2}$	2.1	fl		
2630.69	43	15	2630.86	Fe II	4s b$^4F_{3/2}$	4p z$^4G_{5/2}$	2.1	fl		
2628.99	92	30	2629.08	Fe II	4s a$^6D_{1/2}$	4p z$^6D_{3/2}$	2.3G	col		
2626.35	212	29	2626.45	Fe II	4s a$^6D_{7/2}$	4p z$^6D_{9/2}$	2.3G	col		
2622.41	90	22	2622.45	Fe II	4s a$^6D_{1/2}$	4p z$^6D_{1/2}$	2.3G	col		
2621.11	125	34	2621.19	Fe II	4s a$^6D_{3/2}$	4p z$^6D_{3/2}$	2.3G	col		
2619.82	134^{bl}	56	2619.86	Fe II	4s b$^4F_{9/2}$	4p z$^4G_{9/2}$	2.1	fl		
2618.30	160^{bl}	46	2618.40	Fe II	4s a$^6D_{5/2}$	4p z$^6D_{5/2}$	2.3G	col		
2617.62	228	26								
2614.60	82^{bl}	69	2614.61	Fe II	4s a$^6D_{3/2}$	4p z$^6D_{1/2}$	2.3G	col		
2612.56	173	29	2612.65	Fe II	4s a$^6D_{7/2}$	4p z$^6D_{7/2}$	2.3G	col		
2611.83	80	34	2611.85	Fe II	4s a$^4D_{3/2}$	4p z$^4P_{5/2}$	2.3G	col		
2610.79	54	22	2610.81	Ne III	2p^3(^{2}D)3s $^3D_3$	2p^3(^{2}D)3p $^3F_4$	3.2F	rec		
2607.76	105	29	2607.87	Fe II	4s a$^6D_{5/2}$	4p z$^6D_{3/2}$	2.3G	col		
2607.13	87	20								
2605.68	208	25	2605.82	Fe II	4s c$^2F_{5/2}$	4p v$^2G_{7/2}$	2.1	fl		
2599.05	68^{bl}	50	2599.15	Fe II	4s a$^6D_{7/2}$	4p z$^6D_{5/2}$	2.3G	col		
2596.34	470	27								
2592.28	72^{bl}	35	2592.32	Fe II	4s a$^4D_{5/2}$	4p z$^4P_{5/2}$	2.3G	col		
2591.21	67^{bl}	39	2591.33	Fe II	4s b$^4P_{3/2}$	4p y$^4P_{5/2}$	2.1	fl		
2588.68	44	79	2588.95	O III]	2p3p $^1P_1$	2p3d $^3P_1$	3	fl		
			8.72	Fe II	4s c$^2G_{7/2}$	4p x$^2H_{9/2}$	2.1	fl		
Oth			2583.36	Fe II	4s a$^4D_{3/2}$	4p z$^4P_{3/2}$	2.3G	col		
Oth			2581.94	Fe II	4p z$^2D_{5/2}$	5s f$^4F_{5/2}$	2.1	fl		

Table 13. continued.

λ_{obs} (Å)	I^a	w^b	λ_{id} (Å)	spec.	Lower level	Upper level	Sec^c	Exc^f	I^d_{ghrs}	w^e_{ghrs}
2567.13	63	33	2567.26	O III]	2p3s $^3P_2$	2p3p $^1D_2$	2.3F	unk		
2564.68	105	28	2564.80	Co II	4s b$^3F_3$	4p z$^3F_4$		unk		
2564.23	42^{bl}		2564.25	Fe II	4s a$^4D_{5/2}$	4p z$^4P_{3/2}$	2.3G	col		
2563.17	90	20	2563.30	Fe II	4s a$^4D_{7/2}$	4p z$^4P_{5/2}$	2.3G	col		
2558.00	58	70	2558.27	Fe II	4s b$^4F_{9/2}$	4p y$^4D_{7/2}$		fl		
			7.92	Fe II	4s b$^4F_{3/2}$	4p z$^2D_{3/2}$		unk		
			7.85	Fe II	4s a$^4H_{7/2}$	4p z$^4G_{9/2}$	2.1	fl		
2550.49	102	20	2550.54	Fe II	4s a$^2F_{7/2}$	4p x$^4F_{5/2}$	2.1	fl		
Oth			2549.69	Fe II	4s a$^2I_{11/2}$	4p x$^2H_{9/2}$	2.1	fl		
2549.26	111	25	2549.36	Fe II	4s a$^4H_{9/2}$	4p z$^4G_{9/2}$	2.1	fl		
2542.50	126	20	2542.60	Fe II	4s a$^4H_{7/2}$	4p z$^4G_{5/2}$	2.1	fl		
			2.58	Si III	3p $^1P_1$	3p^2 $^1D_2$		unk		
2539.40	122	20	2539.56	Fe II	4s a$^4H_{11/2}$	4p z$^4G_{9/2}$	2.1	fl		
Oth			2539.35	Fe II	4s a$^2F_{5/2}$	4p y$^2D_{5/2}$	2.1	fl		
2538.03	76	31	2538.13	Fe II	3d^7 a$^4F_{5/2}$	4p z$^6F_{7/2}$	2.3G	col		
			7.90	Fe II	4p z$^6D_{9/2}$	5s e$^6D_{9/2}$	2.1	fl		
2537.43	64	30	2537.61	Fe II	4s a$^4H_{11/2}$	4p z$^4H_{13/2}$		unk		
			7.57	Fe II	4s a$^4H_{9/2}$	4p z$^4H_{9/2}$		unk		
2534.49	241	26								
2531.75	89	27	2531.85	Fe II	3d^7 a$^4F_{5/2}$	4p z$^6F_{5/2}$	2.3G	col		
2530.94	111	24								
Oth										
Oth			2527.06	Fe II	4s b$^4P_{5/2}$	4p y$^4P_{5/2}$	2.1	fl		
2526.60	133	15	2526.68	Fe II	4p z$^6D_{7/2}$	5s e$^6D_{7/2}$	2.1	fl		
2525.87	48^{bl}	38	2526.15	Fe II	4s a$^4H_{13/2}$	4p z$^4H_{13/2}$		unk		
2524.87	120	20	2524.87	Si I	3p^2 $^3P_1$	3p4s $^3P_0$	2.3E	unk		
2519.70	77	33	2519.96	Si I	3p^2 $^3P_1$	3p4s $^3P_1$	2.3E	unk		
			9.86	Fe II	3d^7 a$^4F_{7/2}$	4p z$^6F_{9/2}$	2.3G	col		
			9.81	Fe II	4s a$^2F_{7/2}$	4p y$^2D_{5/2}$	2.1	fl		
2516.79	133	38	2516.87	Si I	3p^2 $^3P_2$	3p4s $^3P_2$	2.3E	unk		
			6.75	Fe II	3d^7 a$^2D_{3/2}$	4p z$^4G_{5/2}$	2.1	fl		
2513.96	101^{bl}	36	2513.91	Fe II	4p z$^6D_{9/2}$	5s e$^6D_{7/2}$	2.1	fl		
2512.57	73^{bl}		2512.81	C II	2s2p^2 $^2P_{3/2}$	2p^3 $^2D_{5/2}$	2.3D	unk		
2511.89	529	61	2511.96	He II	n = 3	n = 7	1	rec		
2509.77	32^{bl}		2509.88	C II	2s2p^2 $^2P_{3/2}$	2p^3 $^2D_{3/2}$	2.3D	unk		
2509.02	843	23	2509.10	Fe II	4s c$^4F_{7/2}$	(^{3}F)4p $^4G_{9/2}$	2.1	fl		
2507.46	336		2507.65	Si I	3p^2 $^3P_1$	3p4s $^3P_2$	2.3E	unk		
			2507.55	Fe II	4s b$^4F_{7/2}$	(^{5}D)5p $^6F_{9/2}$	2.1	fl		
2507.13	192^{bl}		2507.19	Fe II	4s c$^4F_{9/2}$	(^{3}F)4p $^4G_{9/2}$	2.1	fl		
2506.70	62	23	2506.85	Fe II	4s a$^4G_{9/2}$	4p x$^4G_{9/2}$		unk		
2505.94	56	30	2505.97	Fe II	3d^7 a$^4F_{7/2}$	4p z$^6F_{5/2}$	2.3G	col		
2498.55	134	16	2498.57	Fe II	4s a$^4G_{5/2}$	4p x$^4G_{5/2}$		unk		
2493.94	106	49	2494.05	Fe II	3d^7 a$^4F_{9/2}$	4p z$^6F_{11/2}$	2.3G	col		
			4.02	Fe II	4s a$^4H_{13/2}$	4p z$^4I_{15/2}$		unk		
			3.98	Fe II	4s a$^4G_{7/2}$	4p x$^4G_{5/2}$		unk		
			3.94	Fe II	4s a$^4H_{11/2}$	4p z$^4I_{13/2}$		unk		
2493.02	675	34	2493.10	Fe II	4s b$^2H_{9/2}$	4p y$^4H_{11/2}$	2.1	fl		
2484.91	143^{bl}	35	2484.95	Fe II	3d^7 a$^4F_{9/2}$	4p z$^6F_{9/2}$	2.3G	col		
2484.39	80	28	2484.47	Fe II	4s c$^2G_{7/2}$	4p w$^2H_{9/2}$		unk		

Table 13. continued.

λ_{obs} (Å)	I^a	w^b	λ_{id} (Å)	spec.	Lower level	Upper level	Sec^c	Exc^f	I^d_{ghrs}	w^e_{ghrs}
2483.74	73	21								
2482.98	579	29	2483.08	Fe II	4s $c^2D_{3/2}$	4p $w^2D_{3/2}$	2.1	fl		
2481.70	628	23	2481.80	Fe II	4s $b^2H_{11/2}$	4p $y^4H_{11/2}$	2.1	fl		
2479.90	366	23	2479.98	Fe II	4s $c^2D_{5/2}$	4p $w^2D_{3/2}$	2.1	fl		
2476.96	50	25	2477.01	Fe II	4s $a^4H_{7/2}$	4p $z^2G_{9/2}$	2.1	fl		
2474.06	61^{bl}	39	2474.20	Fe II	4s $c^4P_{5/2}$	(b^3P)4p $^4S_{3/2}$	2.1	fl		
2473.53	101^{bl}	34	2473.66	Fe II	4s $c^4P_{5/2}$	(^{5}D)5p $^4D_{5/2}$	2.1	fl		
2471.06	119	16	2471.15	Fe II	3d^7 $a^2H_{11/2}$	4p $z^4G_{9/2}$	2.1	fl		
2470.23	57^{bl}	47	2470.26	Fe II	4s $b^4D_{7/2}$	(^{3}D)4p $^4P_{5/2}$		unk		
Oth			2464.76	Fe II	4s $a^4G_{9/2}$	4p $x^4F_{7/2}$	2.1	fl		
2459.65	87		2459.72	Fe II	4s $b^4D_{5/2}$	(^{3}D)4p $^4P_{3/2}$	2.1	fl		
2459.46	721	28	2459.53	Fe II	4s $a^4G_{9/2}$	4p $y^4H_{11/2}$	2.1	fl		
2458.23	121	26	2458.30	Fe II	4s $b^4D_{3/2}$	(^{3}D)4p $^4P_{3/2}$	2.1	fl		
2457.68	111	29	2457.71	Fe II	4s $c^4P_{5/2}$	(^{5}D)5p $^4P_{5/2}$	2.1	fl		
Oth			2455.71	O III	2p3s $^1P_1$	2p3p $^1S_0$	2.3F	rec		
2448.43	140	23	2448.50	Fe II	4s $a^2I_{11/2}$	4p $w^2H_{9/2}$		unk		
Oth			2437.94	Fe II	4s $a^4G_{7/2}$	4p $y^2D_{5/2}$	2.1	fl		
2436.89	582	21	2436.96	Fe II	4s $a^4G_{11/2}$	4p $y^4H_{11/2}$	2.1	fl		
Oth			2435.69	Fe II	4s $b^4F_{3/2}$	4p $y^4G_{5/2}$	2.1	fl		
			5.66	Ne III	2p^3(^{2}D)3s $^1D_2$	2p^3(^{2}D)3p $^3P_2$	2.3F	rec		
Oth			2429.98	Ne III	2p^3(^{2}D)3s $^1D_2$	2p^3(^{2}D)3p $^3P_1$	2.3F	rec		
2427.85	64^{bl}	32	2427.93	Fe II	3d^7 $a^2H_{11/2}$	4p $z^4I_{13/2}$		unk		
Oth			2426.42	Fe II	4s $b^2P_{3/2}$	4p $y^2D_{5/2}$	2.1	fl		
Oth			2425.23	[Ne IV]	2p^3 $^4S_{3/2}$	2p^3 $^2D_{5/2}$	2.2	col		
Oth			2422.60	[Ne IV]	2p^3 $^4S_{3/2}$	2p^3 $^2D_{3/2}$	2.2	col		
2417.36	159	19								
Oth			2413.67	Ne III	2p^3(^{4}S)3p $^3P_1$	2p^3(^{4}S)3d $^3D_2$	2.3F	rec		
			3.47	Ne III	2p^3(^{4}S)3p $^3P_2$	2p^3(^{4}S)3d $^3D_3$	2.3F	rec		
2411.36	84	40	2411.25	Fe II	4s $a^6D_{3/2}$	4p $z^6F_{5/2}$	2.3G	col		
2407.85	220	17	2407.96	Fe II	4s $c^4P_{1/2}$	(^{3}P)4p $^4S_{3/2}$	2.1	fl		
2399.87	166	16	2399.97	Fe II	4s $a^6D_{5/2}$	4p $z^6F_{5/2}$	2.3G	col		
			2399.96	Fe II	3d^7 $a^4F_{3/2}$	4p $z^4D_{5/2}$	2.3G	col		
2396.28	172	20	2396.36	Fe II	4s $a^6D_{7/2}$	4p $z^6F_{9/2}$	2.3G	col		
2395.47	94	38	2395.62	Fe II	3d^7 $a^2H_{11/2}$	4p $z^2G_{9/2}$	2.1	fl		
2392.19	134	28	2392.21	Fe II	3d^7 $a^4F_{7/2}$	4p $z^4F_{9/2}$	2.3G	col		
2389.34	73		2389.36	Fe II	4s $a^6D_{7/2}$	4p $z^6F_{7/2}$	2.3G	col		
2386.08	332	49	2386.13	He II	$n = 3$	$n = 8$	1	rec		
2383.96	90	24	2383.97	Fe II	3d^7 $a^4F_{5/2}$	4p $z^4D_{5/2}$	2.3G	col		
2379.91	68^{bl}	62	2380.00	Fe II	3d^7 $a^4F_{7/2}$	4p $z^4D_{7/2}$	2.3G	col		
2362.18	130	28	2362.24	Co II	4s a^5F_1	4p z^5D_2		unk		
2360.66	96	15	2360.68	Fe II	4s $b^2D_{3/2}$	4p $w^2D_{3/2}$	2.1	fl		
2359.66	131^{bl}	27	2359.83	Fe II	4s $a^6D_{3/2}$	4p $z^6P_{5/2}$	2.3G	col		
2350.86	137	29	2350.89	Si II]	3p $^2P_{3/2}$	3p^2 $^4P_{1/2}$	2.3D	col		
2348.93	116	24	2349.02	Fe II	4s $a^6D_{5/2}$	4p $z^6P_{5/2}$	2.3G	col		
2347.98	224	56	2348.12	Co II	4s a^5F_2	4p z^5D_2		unk		
			7.92	Fe II	3d^7 $d^2D1_{5/2}$	(b^3P)4p $^4S_{3/2}$	2.1	fl		
2344.94	188	24	2345.00	Fe II	4s $a^6D_{1/2}$	4p $z^6P_{3/2}$	2.3G	col		
2335.15	410	19	2335.12	Si II]	3p $^2P_{1/2}$	3p^2 $^4P_{1/2}$	2.3D	col		
2333.49	109^{bl}	33	2333.52	Fe II	4s $a^6D_{7/2}$	4p $z^6P_{5/2}$	2.3G	col		

Table 13. continued.

λ_{obs} (Å)	I^a	w^b	λ_{id} (Å)	spec.	Lower level	Upper level	Sec^c	Exc^f	I^d_{ghrs}	w^e_{ghrs}
2326.77	463	25	2326.84	Co II	4s a^5F_3	4p z^5D_2		unk		
2326.04	173	27								
Oth			2321.66	[O III]	$2p^2\ ^3P_1$	$2p^2\ ^1S_0$	2.2	col		
Oth			2316.46	Co II	4s c^3F_4	4p v^3D_3	2.1	fl		
2315.57	141	25	2315.58	Fe II	4s $c^4F_{5/2}$	4p $u^4F_{3/2}$	2.1	fl		
2311.97	282	25	2312.00	Fe II	4s $c^4F_{3/2}$	4p $u^4F_{3/2}$	2.1	fl		
2306.85	355	49	2306.91	He II	$n = 3$	$n = 9$	1	rec		
2297.49	512	25	2297.58	C III	$2s2p\ ^1P_1$	$2p^2\ ^1D_2$		unk		
2281.60	128	22	2281.73	Fe II	4s $b^4F_{9/2}$	4p $y^4H_{11/2}$	2.1	fl		
2280.55	248	22	2280.62	Fe II	4s $a^6D_{7/2}$	4p $z^4F_{9/2}$	2.3G	col		
Oth			2253.83	Fe II	4s $a^6D_{7/2}$	4p $z^4F_{7/2}$	2.3G	col		
2253.34	388	29	2253.34	He II	$n = 3$	$n = 10$	1	rec		
2228.01	270	20	2228.07	Fe II	4s $a^4H_{9/2}$	4p $y^4H_{11/2}$	2.1	fl		
2220.51	487	28	2220.59	Fe II	4s $a^4H_{11/2}$	4p $y^4H_{11/2}$	2.1	fl		
2215.31	150	39	2215.36	He II	$n = 3$	$n = 11$	1	rec		
Oth			2211.81	Fe II	4s $a^4H_{13/2}$	4p $y^4H_{11/2}$	2.1	fl		
2187.30	251	46	2187.29	He II	$n = 3$	$n = 12$	1	rec		
Oth										
2168.04	296	19	2168.11	Fe II	$3d^7\ a^2H_{11/2}$	4p $y^4H_{11/2}$	2.1	fl		
2165.93	180		2165.93	He II	$n = 3$	$n = 13$	1	rec		
Oth										
Oth			2149.28	He II	$n = 3$	$n = 14$	1	rec		
2142.43	237	25	2142.46	Fe II	4s $b^2F_{5/2}$	4p $w^2D_{3/2}$	2.1	fl		
Oth			2136.03	He II	$n = 3$	$n = 15$	1	rec		
Oth										
Oth			2125.31	He II	$n = 3$	$n = 16$	1	rec		
Oth			2122.12	Fe II	4s $b^4D_{3/2}$	4p $w^2D_{3/2}$	2.1	fl		
Oth			2038.11	Fe II	4s $c^2P_{3/2}$	$(^4P)4sp\ ^2S_{1/2}$	2.1	fl		
Oth			2003.85	Fe II	4s $c^2P_{1/2}$	$(^4P)4sp\ ^2S_{1/2}$	2.1	fl		
Oth										
1979.04	43	29								
1978.60	43	24								
1978.29	71	17	1978.51	Fe II	$4s^2\ b^4G_{9/2}$	$(^2I)4sp\ ^4H_{11/2}$	2.1	fl		
1975.36	129^{bl}	35	1975.55	Fe II	$3d^7\ a^2G_{9/2}$	4p $y^4H_{11/2}$	2.1	fl		
Oth			1975.07	Fe II	$3d^7\ a^2G_{7/2}$	4p $y^2D_{5/2}$	2.1	fl		
1974.53	29^{bl}	33	1974.83	Fe II	$4s^2\ d^4P_{3/2}$	$(^4F)4sp\ ^6D_{5/2}$	2.1	fl		
Oth			1973.78	Fe II	$4s^2\ b^4G_{9/2}$	$(^2I)4sp\ ^4H_{9/2}$	2.1	fl		
1973.32	18	20								
Oth			1972.16	Fe II	$4s^2\ b^4G_{11/2}$	$(^2I)4sp\ ^4H_{9/2}$	2.1	fl		
1971.49	25^{bl}	33	1971.63	Fe II	$4s^2\ d^4P_{5/2}$	$(^4F)4sp\ ^6D_{5/2}$	2.1	fl		
1970.83	15	20	1971.03	Fe II	$3d^7\ a^2D_{3/2}$	$(^3D)4p\ ^4P_{3/2}$	2.1	fl		
1970.58	17	17								
1970.02	24	18	1970.36	Fe II	$3d^7\ a^4P_{3/2}$	4p $z^2F_{5/2}$		fl		
1965.73	136	29	1965.92	Fe II	4s $a^2F_{5/2}$	4p $w^2D_{3/2}$	2.1	fl		
1963.99	30	20								
Oth			1957.28	[Fe VI]	$3d^3\ ^2G_{7/2}$	$3d^3\ ^2D1_{5/2}$	2.2	col		
Oth										
Oth										
Oth										

Table 13. continued.

λ_{obs} (Å)	I^a	w^b	λ_{id} (Å)	spec.	Lower level	Upper level	Sec^c	Exc^f	I^d_{ghrs}	w^e_{ghrs}
1947.41	46	14	1947.64	Fe II	4s $d^2G_{9/2}$	(^{3}H)5p $^4G_{7/2}$	2.1	fl		
1946.77	20		1947.00	Fe II	4s $c^4P_{5/2}$	(^{4}D)4sp $^4P_{3/2}$	2.1	fl		
1944.19	20	20	1944.30	[Fe VI]	$3d^3$ $^2G_{7/2}$	$3d^3$ $^2D1_{3/2}$	2.2	col		
1943.33	19	17	1943.48	Fe III	(^{4}G)4s $^5G_2$	(^{4}G)4p $^5H_3$		unk		
1941.86	26	20	1942.00	Fe II	$3d^7$ $b^2F_{5/2}$	4p $v^2G_{7/2}$	2.1	fl		
			1.90	Fe II	4s $c^2P_{3/2}$	(^{4}F)4sp $^6F_{3/2}$	2.1	fl		
1940.55	20	22	1940.70	Fe II	4s $d^2F_{5/2}$	(^{4}F)4sp $^6F_{3/2}$	2.1	fl		
1938.51	57^{bl}	46	1938.77	Fe II	4s $c^2P_{3/2}$	(^{4}D)4sp $^2P_{3/2}$		unk		
1934.30										
1928.58	63	33								
1928.01	38	26	1928.09	Fe III	(^{4}G)4s $^5G_6$	(^{4}G)4p $^5H_5$		unk		
1926.07	57	23	1926.24	Fe II	4s $a^6D_{7/2}$	4sp $z^8P_{5/2}$	2.3H	rec		
Oth										
1922.91	123	80	1923.34	C III	2s3d $^3D_1$	2s4f $^3F_2$	2.3F	rec		
			3.16	C III	2s3d $^3D_2$	2s4f $^3F_3$	2.3F	rec		
			2.96	C III	2s3d $^3D_3$	2s4f $^3F_4$	2.3F	rec		
			2.79	Fe III	(^{4}G)4s $^5G_5$	(^{4}G)4p $^5H_6$		unk		
Oth										
1919.96	19	30	1920.02	O III	2p3p $^1D_2$	2p4s $^1P_1$	2.3F	rec		
Oth										
1915.62	28	17	1915.79	Fe II	4s $a^6D_{7/2}$	4sp $z^8P_{7/2}$	2.3H	rec		
1913.89	207	33	1914.06	Fe III	(^{6}S)4s $^7S_3$	(^{6}S)4p $^7P_3$	2.1	fl		
1912.72	22	27								
1911.66	16	16	1911.72	Fe II	$4s^2$ $b^4G_{7/2}$	(^{4}F)4sp $^6F_{5/2}$	2.1	fl		
1911.37	30	16	1911.44	Fe II	$4s^2$ $b^4G_{5/2}$	(^{4}F)4sp $^6F_{5/2}$	2.1	fl		
1910.34	25^{bl}	53	1910.77	Fe II	4s $c^2P_{1/2}$	(^{4}F)4sp $^6F_{3/2}$	2.1	fl		
Oth			1909.91	Fe II	4s $b^4P_{5/2}$	4p $y^2P_{3/2}$		unk		
1908.57	oe		1908.73	C III]	$2s^2$ $^1S_0$	2s2p $^3P_1$	2.3C	col		
1907.03	41^{bl}	31	1907.24	Fe II	4s $a^4G_{5/2}$	4p $w^2D_{3/2}$	2.1	fl		
1906.67	19	30	1906.72	Mg IV	(^{3}P)3s $^4P_{3/2}$	(^{3}P)3p $^4P_{1/2}$	2.3F	rec		
			6.68	C III]	$2s^2$ $^1S_0$	2s2p $^3P_2$	2.3C	col		
1905.58	22		1905.68	Fe II	4s $c^2D_{5/2}$	(^{5}D)5p $^4D_{5/2}$	2.1	fl		
1900.15	58	27	1900.29	S I]	$3p^4$ $^3P_2$	4s $^5S_2$	2.3E	col		
1897.32	27	24	1897.55	Fe II	4s $b^2P_{3/2}$	4p $w^2D_{3/2}$	2.1	fl		
			7.48	Fe II	4s $a^4D_{5/2}$	4p $z^2D_{5/2}$		unk		
1895.31	87	35	1895.46	Fe III	(^{6}S)4s $^7S_3$	(^{6}S)4p $^7P_4$	2.1	fl		
Oth			1894.29	C III	2s3p $^1P_1$	2s4s $^1S_0$	2.3F	rec		
Oth			1893.89	Mg IV	(^{3}P)3s $^4P_{5/2}$	(^{3}P)3p $^4P_{5/2}$	2.3F	rec		
1891.90	oe		1892.03	Si III]	$3s^2$ $^1S_0$	3p $^3P_1$	2.3C	col		
1890.49	88	40	1890.66	Fe III	(^{4}G)4s $^5G_6$	(^{4}G)4p $^5F_5$		unk		
1889.34	26	25	1889.45	Fe III	(^{4}G)4s $^5G_3$	(^{4}P)4p $^5D_2$		unk		
1888.40	26	25	1888.52	P IV	3s3p $^1P_1$	$3p^2$ $^1D_2$		unk		
1887.83	29	21	1888.01	Fe II	4s $a^6D_{9/2}$	4sp $z^8P_{9/2}$	2.3H	rec		
1887.28	38^{bl}		1887.45	Fe III	(^{4}G)4s $^5G_3$	(^{4}G)4p $^5F_3$		unk		
1887.05	29^{bl}		1887.20	Fe III	(^{4}G)4s $^5G_4$	(^{4}G)4p $^5F_3$		unk		
1886.57	44	22	1886.76	Fe III	(^{4}G)4s $^5G_5$	(^{4}G)4p $^5F_4$		unk		
1884.94	110	56	1885.22	N III	3d $^2D_{5/2}$	4f $^2F_{7/2}$	2.3F	rec		
			5.09	Fe II	$3d^7$ $a^4P_{5/2}$	4p $x^4F_{5/2}$	2.1	fl		
			5.06	N III	3d $^2D_{3/2}$	4f $^2F_{5/2}$	2.3F	rec		

Table 13. continued.

λ_{obs} (Å)	I^a	w^b	λ_{id} (Å)	spec.	Lower level	Upper level	Sec^c	Exc^f	I^d_{ghrs}	w^e_{ghrs}
1883.95	60	21	1884.12	Fe II	$4s^2\ d^4P_{3/2}$	$(^3F)5p\ ^4D_{5/2}$	2.1	fl		
Oth			1883.72	Fe II	$4s\ a^4D_{7/2}$	$4p\ z^4G_{5/2}$	2.1	fl		
1882.02	35	24								
Oth			1881.89	Fe II	$4s\ a^4D_{7/2}$	$4p\ z^2D_{5/2}$		unk		
Oth			1881.25	Fe II	$3d^7\ a^2P_{1/2}$	$(^3D)4p\ ^4P_{3/2}$	2.1	fl		
1879.16	97	21								
Oth										
Oth			1877.02	Fe II	$4s\ a^4G_{5/2}$	$4sp\ x^6P_{7/2}$	2.1	fl		
1874.82	32^{bl}		1874.97	Fe II	$4s\ a^4D_{5/2}$	$4p\ y^4D_{7/2}$		fl		
1874.55	33^{bl}		1874.58	Mg IV	$(^3P)3s\ ^4P_{5/2}$	$(^3P)3p\ ^4P_{3/2}$	2.3F	rec		
1872.44	99	48	1872.64	Fe II	$4s^2\ b^4G_{9/2}$	$(^2F)4sp\ ^4G_{9/2}$	2.1	fl		
			1872.57	Fe II	$4s\ a^2S_{1/2}$	$(^3P)4p\ ^4S_{3/2}$	2.1	fl		
1870.93	19	29	1871.08	Fe II	$4s\ a^4D_{3/2}$	$4p\ z^2D_{3/2}$		unk		
1869.51	92	56	1869.82	Fe III	$(^4G)4s\ ^5G_3$	$(^4G)4p\ ^5F_2$		unk		
			9.55	Fe II	$4s^2\ b^4G_{11/2}$	$(^2F)4sp\ ^4G_{11/2}$	2.1	fl		
1862.59	248	45	1862.81	Fe II	$3d^7\ a^2P_{3/2}$	$(^3D)4p\ ^4P_{3/2}$	2.1	fl		
			2.79	Al III	$3s\ ^2S_{1/2}$	$3p\ ^2P_{1/2}$	2.3B	col		
1856.63	48	23								
1854.53	338	55	1854.72	Al III	$3s\ ^2S_{1/2}$	$3p\ ^2P_{3/2}$	2.3B	col		
Oth			1853.73	Co II	$4s^2\ a^5D_2$	$(^4F)5p\ ^5D_3$	2.1	fl		
1851.65	35	26								
1851.33	30	18	1851.53	Fe II	$4s\ a^4D_{3/2}$	$4p\ y^4D_{5/2}$		fl		
Oth										
Oth			1850.20	Fe III	$(^4F)4s\ ^5F_4$	$(^4F)4p\ ^5D_4$		unk		
Oth			1849.40	Fe III	$(^4F)4s\ ^5F_5$	$(^4F)4p\ ^5D_4$		unk		
1847.32	37	21	1847.48	Fe II	$4s\ a^4D_{7/2}$	$4p\ z^2G_{9/2}$	2.1	fl		
1843.10	47	21	1843.26	Fe II	$4s^2\ b^4G_{11/2}$	$(^4G)4sp\ ^4G_{11/2}$	2.1	fl		
1840.04	37	38	1840.25	Co II	$4s^2\ a^5D_4$	$(^4F)5p\ ^5D_4$		unk		
			0.06	Fe II	$4s^2\ b^4G_{7/2}$	$(^4G)4sp\ ^4G_{5/2}$	2.1	fl		
			0.00	Fe II	$4s^2\ b^4G_{7/2}$	$(^4G)4sp\ ^4G_{7/2}$	2.1	fl		
1839.63	54	41	1839.80	Fe II	$4s^2\ b^4G_{5/2}$	$(^4G)4sp\ ^4G_{5/2}$	2.1	fl		
			9.74	Fe II	$4s^2\ b^4G_{5/2}$	$(^4G)4sp\ ^4G_{7/2}$	2.1	fl		
1839.21	25	21	1839.27	Co II	$4s^2\ a^5D_3$	$(^4F)4p\ ^5D_3$	2.1	fl		
Oth			1836.72	N I]	$2p^3\ ^2P_{3/2}$	$3s\ ^4P_{1/2}$	2.3E	col		
			6.71	N I]	$2p^3\ ^2P_{1/2}$	$3s\ ^4P_{1/2}$	2.3E	col		
Oth			1835.57	N I]	$2p^3\ ^2P_{1/2}$	$3s\ ^4P_{3/2}$	2.3E	col		
Oth			1834.01	N I]	$2p^3\ ^2P_{1/2}$	$3s\ ^4P_{3/2}$	2.3E	col		
1831.80	171	25	1836.98	Fe II	$4s^2\ b^4G_{7/2}$	$(^4G)4sp\ ^4H_{9/2}$	2.1	fl		
1831.50	35^{bl}		1831.66	Fe II	$4s^2\ b^4G_{9/2}$	$(^4G)4sp\ ^4H_{9/2}$	2.1	fl		
1829.85	34	26	1829.95	Fe V	$(^4P)4s\ ^5P_1$	$(^4F)4p\ ^5F_2$	2.3F	rec		
1826.10	48	38	1826.25	S I	$3p^4\ g^3P_0$	$4s\ ^3S_1$	2.3E	col		
1823.39	118	18								
1820.18	28^{bl}		1820.34	S I	$3p^4\ g^3P_1$	$4s\ ^3S_1$	2.3E	col		
1817.22	191	31	1817.45	Si II	$3p\ ^2P_{3/2}$	$3p^2\ ^2D_{3/2}$	2.3D	col		
1816.75	962	31	1816.93	Si II	$3p\ ^2P_{3/2}$	$3p^2\ ^2D_{5/2}$	2.3D	col		
Oth			1814.63	[Ne III]	$2p^4\ ^3P_1$	$2p^4\ ^1S_0$	2.2	col		
Oth										
1810.15	30	20	1810.23	P II]	$2p^2\ ^1S_0$	$2s2p^3\ ^3P_1$	2.3D	col		
Oth										

Table 13. continued.

λ_{obs} (Å)	I^a	w^b	λ_{id} (Å)	spec.	Lower level	Upper level	Sec^c	Exc^f	I^d_{ghrs}	w^e_{ghrs}
1808.20	71	48								
1807.76	92	27	1808.01	Si II	3p $^2P_{1/2}$	3p^2 $^2D_{3/2}$	2.3D	col		
1807.07	26	15	1807.31	S I	3p^4 g$^3P_2$	4s $^3S_1$	2.3E	col		
1805.44	46	32	1805.67	N III	3p $^2P_{3/2}$	4s $^2S_{1/2}$	2.3F	rec		
1803.54	77	22	1803.82	S II]	3p^3 $^2P_{1/2}$	3p^4 $^4P_{1/2}$	2.3D	col		
Oth			1795.57	Fe II	4s^2 b$^4G_{7/2}$	(^{3}H)5p $^4G_{7/2}$	2.1	fl		
			5.33	Fe II	4s^2 b$^4G_{5/2}$	(^{3}H)5p $^4G_{7/2}$	2.1	fl		
			5.27	Fe II	4s^2 b$^4G_{9/2}$	(^{3}H)5p $^4G_{7/2}$	2.1	fl		
Oth			1788.00	Fe II	4s^2 a$^6S_{5/2}$	4sp x$^6P_{3/2}$	2.1	fl		
1786.58	67	40	1786.82	Si II	3d $^2D_{3/2}$	3p^3 $^2D_{3/2}$	2.3D	unk		
			6.75	Fe II	4s^2 a$^6S_{5/2}$	4sp x$^6P_{5/2}$		fl		
1785.12	108^{bl}	55	1785.27	Fe II	4s^2 a$^6S_{5/2}$	4sp x$^6P_{7/2}$	2.1	fl		
Oth			1783.98	Fe II	4s b$^4D_{7/2}$	4sp y$^6F_{7/2}$	2.1	fl		
Oth										
1781.45	47	24	1781.51	Fe II	4s a$^4D_{7/2}$	4p y$^4G_{5/2}$	2.1	fl		
1780.87	74^{bl}	45	1780.95	Fe II	4s b$^4D_{5/2}$	4sp y$^6F_{7/2}$	2.1	fl		
1779.65	51		1779.82	Fe II	4s c$^4P_{5/2}$	(^{4}F)4sp $^6F_{3/2}$	2.1	fl		
1768.15	264	17								
Oth			1760.82	C II	2s2p^2 $^2D_{3/2}$	3p $^2P_{1/2}$		col		
Oth			1760.47	C II	2s2p^2 $^2D_{3/2}$	3p $^2P_{3/2}$		col		
			0.40	C II	2s2p^2 $^2D_{5/2}$	3p $^2P_{3/2}$		col		
Oth			1757.74	Fe II	4s c$^4P_{3/2}$	(^{4}F)4sp $^6F_{3/2}$	2.1	fl		
1753.80	1482	19	1754.00	N III]	2p $^2P_{3/2}$	2s2p^2 $^4P_{1/2}$	2.3D	col		
1753.32	79	36	1753.47	Mg II	3p $^2P_{3/2}$	5s $^2S_{1/2}$		unk		
1752.03	515^{bl}	41	1752.16	N III]	2p $^2P_{3/2}$	2s2p^2 $^4P_{3/2}$	2.3D	col		
Oth			1751.66	N III	2s2p^2 $^2P_{3/2}$	2p^3 $^2D_{5/2}$	2.3D	unk		
Oth			1750.66	Mg II	3p $^2P_{1/2}$	5s $^2S_{1/2}$		unk		
1749.49	oe		1749.67	N III]	2p $^2P_{3/2}$	2s2p^2 $^4P_{5/2}$	2.3D	col		
1748.51	960	24	1748.64	N III]	2p $^2P_{1/2}$	2s2p^2 $^4P_{1/2}$	2.3D	col		
Oth			1747.85	N III	2s2p^2 $^2P_{1/2}$	2p^3 $^2D_{3/2}$	2.3D	unk		
1746.61	64^{bl}	45	1746.82	N III]	2p $^2P_{1/2}$	2s2p^2 $^4P_{3/2}$	2.3D	col		
1745.08	136	36	1745.25	N I	2p^3 $^2P_{3/2}$	3s $^2P_{1/2}$	2.3E	unk		
1742.60	39	34	1742.73	N I	2p^3 $^2P_{3/2}$	3s $^2P_{3/2}$	2.3E	unk		
1737.40	63	50	1737.62	Mg II	3p $^2P_{3/2}$	4d $^2D_{5/2}$		unk		
			7.33	Co II	4s a$^3D_3$	4sp y$^5P_3$	2.1	fl		
1728.79	157^{bl}	33	1728.85	Fe II	4s a$^4D_{3/2}$	4p x$^4F_{5/2}$	2.1	fl	37	34
1727.17	53	31	1727.38	Si IV	3d $^2D_{3/2}$	4p $^2P_{1/2}$		unk		
Oth			1725.98	Fe II	3d^7 a$^2D_{3/2}$	4sp x$^6P_{3/2}$		fl		
1725.13	86	104	1725.36	Fe II	4s b$^2D_{5/2}$	(^{4}P)4sp $^4P_{5/2}$	2.1	fl		
			5.02	Fe II	3d^7 a^{2}D2$_{5/2}$	4p w$^2D_{3/2}$	2.1	fl		
			4.96	Fe II	3d^7 a$^4F_{7/2}$	4p y$^4P_{5/2}$	2.1	fl		
1722.41	94	56	1722.56	Si IV	3d $^2D_{3/2}$	4p $^2P_{3/2}$		unk		
			2.53	Si IV	3d $^2D_{5/2}$	4p $^2P_{3/2}$		unk		
Oth			1721.68	C II	2s2p^2 $^2P_{3/2}$	2p^3 $^2P_{3/2}$	2.3D	col		
1720.96	39^{bl}	40	1721.01	C II	2s2p^2 $^2P_{1/2}$	2p^3 $^2P_{1/2}$	2.3D	col		
1720.64	33	19	1720.85	Ne V]	2p^2 $^1D_2$	2s2p^3 $^5S_2$	2.3D	col		
1718.34	214	145	1718.55	N IV	2p $^1P_1$	2p^2 $^1D_2$	1	rec	107	145
			8.10	Fe II	3d^7 a$^4F_{5/2}$	4p z$^4G_{5/2}$	2.1	fl		
Oth			1713.00	Fe II	3d^7 a$^4F_{7/2}$	4p z$^4G_{9/2}$	2.1	fl		

Table 13. continued.

λ_{obs} (Å)	I^a	w^b	λ_{id} (Å)	spec.	Lower level	Upper level	Sec^c	Exc^f	I^d_{ghrs}	w^e_{ghrs}
Oth			1706.83	Fe II	4s $c^2G_{7/2}$	4sp $x^4H_{7/2}$	2.1	fl		
1698.63	50	12	1698.78	Mg IV	$(^3P)3s\ ^4P_{3/2}$	$(^3P)3p\ ^4D_{5/2}$	2.3F	rec		
1696.47	153^{bl}	34	1696.79	Fe II	$3d^7\ a^4F_{9/2}$	4p $z^4G_{9/2}$	2.1	fl		
1682.79	45	32	1683.00	Mg IV	$(^3P)3s\ ^4P_{5/2}$	$(^3P)3p\ ^4D_{7/2}$	2.3F	rec		
1682.30	114	27	1682.37	Fe II	4p $z^4P_{1/2}$	$(^3F)4d\ ^4P_{3/2}$	2.1	fl		
1679.95	42	30	1679.96	Mg IV	$(^3P)3s\ ^4P_{3/2}$	$(^3P)3p\ ^4D_{3/2}$	2.3F	rec		
1677.67	115	18	1677.84	Fe II	$3d^7\ a^2P_{1/2}$	4p $w^2D_{3/2}$	2.1	fl		
1675.48	63	29	1675.71	Fe II	4p $z^4P_{3/2}$	$(^3F)4d\ ^4P_{3/2}$	2.1	fl		
1671.35	53	25	1671.42	Fe II	4p $z^4P_{5/2}$	$(^3F)4d\ ^4P_{5/2}$	2.1	fl		
1669.47	68	23	1669.57	Mg IV	$(^3P)3s\ ^4P_{3/2}$	$(^3P)3p\ ^4D_{1/2}$	2.3F	rec		
1666.81	158	18	1666.69	S I	$3p^4\ ^1D_2$	$(^2D)4s\ ^1D_2$	2.3E	unk		
1666.01	oe		1666.15	O III]	$2p^2\ ^3P_2$	$2s2p^3\ ^5S_2$	2.3D	col		
1665.14	131	31								
1660.61	oe		1660.81	O III]	$2p^2\ ^3P_1$	$2s2p^3\ ^5S_2$	2.3D	col		
1640.07	oe		1640.35	He II	$n = 2$	$n = 3$	1	rec	8700	82
1625.45	97^{bl}	35	1625.58	Fe II	4s $b^2F_{5/2}$	4p $u^4F_{3/2}$	2.1	fl		
1613.83	63	39	1613.94	Fe II	4s $b^4D_{1/2}$	4p $u^4F_{3/2}$	2.1	fl		
			3.84	Fe II	4s $b^4D_{3/2}$	4p $u^4F_{3/2}$	2.1	fl		
1601.51	60	45	1601.67	[Ne IV]	$2p^3\ ^4S_{3/2}$	$2p^3\ ^2P_{1/2}$	2.2	col		
			1.50	[Ne IV]	$2p^3\ ^4S_{3/2}$	$2p^3\ ^2P_{3/2}$	2.2	col		
1601.18	71									
1599.85	55	23	1600.01	Fe II	$3d^7\ a^2H_{9/2}$	4p $v^2G_{7/2}$	2.1	fl		
1589.91	79	26								
Oth			1588.29	Fe II	$3d^7\ a^4F_{3/2}$	4p $x^4G_{5/2}$	2.1	fl		
1579.06	90	36								
1577.84	125^{bl}	49	1577.88	C III	$2s3d\ ^3D_1$	$2p3d\ ^3F_2$	2.3F	rec		
1577.13	129	23	1577.30	C III	$2s3d\ ^3D_2$	$2p3d\ ^3F_3$	2.3F	rec		
1576.37	153^{bl}	48	1576.48	C III	$2s3d\ ^3D_3$	$2p3d\ ^3F_4$	2.3F	rec		
1574.53	258	84	1575.18	[Ne V]	$2p^2\ ^3P_1$	$2p^2\ ^1S_0$	2.2	col		
1565.72	118	35								
1560.02	242	27	1560.25	Fe II	$3d^7\ a^4F_{7/2}$	4p $x^4F_{5/2}$	2.1	fl		
1553.32	225	33							137	21
1550.65	oe		1550.77	C IV	2s $^2S_{1/2}$	2p $^2P_{1/2}$	1	col	7570	48
1548.11	oe		1548.19	C IV	2s $^2S_{1/2}$	2p $^2P_{3/2}$	1	col	11650	46
Oth			1538.63	Fe II	4s $a^4G_{5/2}$	$(^5D)5p\ ^4D_{3/2}$	2.1	fl		
1538.13	98	27	1538.16	Fe II	$3d^7\ a^4P_{5/2}$	4p $w^2D_{3/2}$	2.1	fl		
1537.10	324	37	1537.37	Fe II	4s $c^2F_{5/2}$	$(^3H)5p\ ^4G_{7/2}$	2.1	fl	129	25
			7.03	Fe II	4s $c^2F_{7/2}$	$(^3H)5p\ ^4G_{7/2}$	2.1	fl		
Oth			1534.05	O V	$2p3p\ ^1P_1$	$2s4p\ ^1P_1$	2.3F	rec		
1533.25	390	35	1533.43	Si II	3p $^2P_{3/2}$	4s $^2S_{1/2}$		unk		
Oth										
1515.01	44	30	1515.23	Fe II	4s $b^2H_{11/2}$	4sp $x^4H_{11/2}$	2.1	fl		
1514.20	135	30	1514.38	Fe II	4s $a^4G_{5/2}$	4sp $x^4H_{7/2}$	2.1	fl		
1512.55	235	32	1512.69	Fe II	4s $a^4G_{7/2}$	4sp $x^4H_{7/2}$	2.1	fl		
1506.75	144	52	1506.76	O V	$2s4d\ ^3D_3$	$2s5f\ ^3F_4$	2.3F	rec		
1502.55	79	26	1502.69	Fe II	4s $a^4G_{5/2}$	4p $u^2G_{7/2}$	2.1	fl		
Oth			1501.76	S V	$3s3p\ ^1P_1$	$3p^2\ ^1D_2$	1	unk		
1492.10	144^{bl}	32	1492.26	Co II	4s a^5P_2	4sp y^5P_3	2.1	fl	125	24
1488.36	139	32	1438.38	Si I	$3p^2\ ^1S_0$	$3s3p^3\ ^1P_1$	2.3E	unk		

Table 13. continued.

λ_{obs} (Å)	I^a	w^b	λ_{id} (Å)	spec.	Lower level	Upper level	Sec^c	Exc^f	I^d_{ghrs}	w^e_{ghrs}
1486.42	oe		1486.50	N IV]	$2s^2\ ^1S_0$	$2p\ ^3P_1$	1	col	8290	38
1483.26	139	160	1483.32	[N IV]	$2s^2\ ^1S_0$	$2p\ ^3P_2$	2.3C	col	73	301
1471.93	95	26	1471.94	Fe II	$4p\ z^6D_{5/2}$	$(^3F)4d\ ^4P_{5/2}$	2.1	fl		
Oth										
1467.25	134	33	1467.43	P IV]	$3s^2\ ^1S_0$	$3p\ ^3P_1$	2.3C	col		
1464.68	84	29								
1459.73	98	31								
Oth			1457.76	Fe II	$4s^2\ a^6S_{5/2}$	$(^4D)4sp\ ^6F_{3/2}$	2.1	fl		
1445.59	82^{bl}	62	1445.69	Fe II	$4s\ a^2S_{1/2}$	$(^4F)4sp\ ^6F_{3/2}$	2.1	fl		
1423.71	433	32	1423.79	S IV]	$3p\ ^2P_{3/2}$	$3p^2\ ^4P_{1/2}$	2.3D	col		
1422.37	137	25	1422.53	Fe II	$4s\ b^4D_{3/2}$	$4p\ u^4F_{3/2}$	2.1	fl		
1416.77	582	40	1416.98	S IV]	$3p\ ^2P_{3/2}$	$3p^2\ ^4P_{3/2}$	2.3D	col	235	36
1413.57	130	23	1413.70	Fe II	$4s\ a^4H_{11/2}$	$4sp\ x^4H_{11/2}$	2.1	fl	61	23
1411.77	1182	36	1411.94	N I	$2p^3\ ^2P_{3/2}$	$3s\ ^2D_{5/2}$	2.1	fl	301	49
1409.15	106	92	1409.34	S I	$3p^4\ ^3P_1$	$(^4S)5s\ ^3S_1$	2.1	fl	60	51
			9.33	Co II	$3d^8\ a^3P_2$	$4p\ v^3D_3$		unk		
1407.24	1630	51	1407.38	O IV]	$2p\ ^2P_{3/2}$	$2s2p^2\ ^4P_{1/2}$	2.3D	col	854	42
1406.54	67	41								
1405.90	1214	36	1406.08	S IV]	$3p\ ^2P_{3/2}$	$3p^2\ ^4P_{5/2}$	2.3D	col	384	38
1404.65	oe		1404.80	O IV]	$2p\ ^2P_{3/2}$	$2s2p^2\ ^4P_{3/2}$	2.3D	col	1350	41
			4.77	S IV]	$3p\ ^2P_{1/2}$	$3p^2\ ^4P_{1/2}$	2.3D	col		
1402.65	oe		1402.77	Si IV	$3s\ ^2S_{1/2}$	$3p\ ^2P_{1/2}$	1	col	579	49
1401.04	oe		1401.16	O IV]	$2p\ ^2P_{3/2}$	$2s2p^2\ ^4P_{5/2}$	2.3D	col	3870	41
1399.61	1723	47	1399.78	O IV]	$2p\ ^2P_{1/2}$	$2s2p^2\ ^4P_{1/2}$	2.3D	col	1030	41
1397.96	58		1398.13	S IV]	$3p\ ^2P_{1/2}$	$3p^2\ ^4P_{3/2}$	2.3D	col		
1397.08	385	34	1397.23	O IV]	$2p\ ^2P_{1/2}$	$2s2p^2\ ^4P_{3/2}$	2.3D	col	185	56
1393.67	oe		1393.76	Si IV	$3s\ ^2S_{1/2}$	$3p\ ^2P_{3/2}$	1	col	1080	54
Oth			1393.21	Fe II	$3d^7\ a^2H_{11/2}$	$4sp\ x^4H_{9/2}$	2.1	fl		
1387.10	214	80	1387.38	N III	$3p\ ^2P_{3/2}$	$4d\ ^2D_{5/2}$	2.3F	rec		
			7.26	N III	$2s2p^2\ ^2S_{1/2}$	$2p^3\ ^2D_{3/2}$	2.3D	unk		
1385.64	129	35	1385.78	Fe II	$3d^7\ a^2P_{1/2}$	$(^5D)5p\ ^4D_{3/2}$	2.1	fl		
1383.41	117	22	1383.54	Fe II	$3d^7\ a^2P_{3/2}$	$(^5D)5p\ ^4D_{5/2}$	2.1	fl		
1381.08	193	30	1381.22	Fe II	$4s\ b^4P_{3/2}$	$(^4P)4sp\ ^4P_{5/2}$	2.1	fl		
1376.26	67		1376.34	Fe V	$(^4F)4s\ ^5F_5$	$(^4F)4p\ ^5F_5$	2.3F	rec		
1375.56	164	33	1375.75	Fe II	$3d^7\ a^2P_{3/2}$	$(^5D)5p\ ^4D_{3/2}$	2.1	fl	110	24
1373.44	69	22	1373.59	Fe V	$(^4F)4s\ ^5F_4$	$(^4F)4p\ ^5F_4$	2.3F	rec		
1372.93	209	28								
1371.18	473	83	1371.30	O V	$2s2p\ ^1P_1$	$2p^2\ ^1D_2$	1	unk	214	126
			0.94	Fe V	$(^4F)4s\ ^5F_1$	$(^4F)4p\ ^5F_2$	2.3F	rec		
1367.80	89	22								
1362.60	161	22	1362.78	Fe II	$4s\ b^4P_{5/2}$	$(^4P)4sp\ ^4P_{5/2}$	2.1	fl		
1360.05	184	40	1360.30	O III]	$2s2p^3\ ^1P_1$	$2p^4\ ^3P_1$	2.3D	unk		
1358.35	298	31	1358.51	O III]	$2s2p^3\ ^1P_1$	$2p^4\ ^3P_0$	2.3D	unk	107	24
			1358.51	O I]	$2p^4\ ^3P_1$	$3s\ ^5S_2$	2.3E	unk		
1355.43	406	31	1355.60	O I]	$2p^4\ ^3P_2$	$3s\ ^5S_2$	2.3E	unk	121	24
1345.54	99	31								
1344.80	115	45	1344.85	P III	$3p\ ^2P_{3/2}$	$3p^2\ ^2D_{3/2}$	2.3D	col		
1344.29	85		1344.33	P III	$3p\ ^2P_{3/2}$	$3p^2\ ^2D_{5/2}$	2.3D	col		
1343.41	253	34	1343.51	O IV	$2s2p^2\ ^2P_{3/2}$	$2p^3\ ^2D_{5/2}$	2.3D	unk		

Table 13. continued.

λ_{obs} (Å)	I^a	w^b	λ_{id} (Å)	spec.	Lower level	Upper level	Sec^c	Exc^f	I^d_{ghrs}	w^e_{ghrs}
1338.47	85	38	1338.62	O IV	$2s2p^2\ ^2P_{1/2}$	$2p^3\ ^2D_{3/2}$	2.3D	unk		
1336.71	119	63								
1335.55	315	25	1335.71	C II	$2p\ ^2P_{3/2}$	$2s2p^2\ ^2D_{5/2}$	2.3D	col		
1324.25	115	20	1324.45	[Mg V]	$2p^4\ ^3P_1$	$2p^4\ ^1S_0$	2.2	col		
1323.15	63	20								
Oth			1312.49	Fe II	4s $b^4D_{7/2}$	$(^2F)4sp\ ^4G_{9/2}$	2.1	fl		
1310.92	58	27	1310.95	N I	$2p^3\ ^2P_{1/2}$	$3d\ ^2D_{3/2}$	2.3E	unk		
1310.47	60	46	1310.70	P II	$3p^2\ ^3P_2$	$3p^3\ ^3P_2$	2.3D	col		
			0.54	N I	$2p^3\ ^2P_{3/2}$	$3d\ ^2D_{5/2}$	2.3E	unk		
Oth			1310.15	Fe II	$3d^7\ a^2G_{9/2}$	$4p\ u^2G_{9/2}$	2.1	fl		
1309.69	74^{bl}		1309.87	P II	$3p^2\ ^3P_2$	$3p^3\ ^3P_1$	2.3D	col		
1308.63	41		1308.71	C III	$2p^2\ ^1S_0$	$2s3p\ ^1P_1$	2.3F	rec		
1305.90	2566	46	1306.03	O I	$2p^4\ ^3P_0$	$3s\ ^3S_1$	2.3E	col		
1304.73	2345	46	1304.86	O I	$2p^4\ ^3P_1$	$3s\ ^3S_1$	2.3E	col		
1301.86	83	16	1301.87	P II	$3p^2\ ^3P_0$	$3p^3\ ^3P_1$	2.3D	col		
1301.03	96^{bl}		1301.15	Si III	$3p\ ^3P_1$	$3p^2\ ^3P_0$	2.3D	unk		
Oth			1300.86	O III]	$2p^2\ ^1S_0$	$2s2p^3\ ^3D_1$	2.3D	col		
Oth			1298.89	Si III	$3p\ ^3P_1$	$3p^2\ ^3P_1$	2.3D	unk		
Oth			1296.73	Si III	$3p\ ^3P_0$	$3p^2\ ^3P_1$	2.3D	unk		
Oth							1			
Oth							1			
Oth							1			
1252.48	149	26								
1250.01	197	108	1250.43	Si II	$3p^2\ ^2D_{5/2}$	$3p^3\ ^2D_{5/2}$	2.3D	unk		
			0.09	Si II	$3p^2\ ^2D_{3/2}$	$3p^3\ ^2D_{3/2}$	2.3D	unk		
1248.20	130^{bl}	50	1248.43	Si II	$3p^2\ ^4P_{3/2}$	$3p^3\ ^4S_{3/2}$	2.3D	unk		
1247.25	236	29	1247.38	C III	$2s2p\ ^1P_1$	$2p^2\ ^1S_0$		unk		
1242.73	oe		1242.78	N V	$2s\ ^2S_{1/2}$	$2p\ ^2P_{1/2}$	1	col	6080	67
1238.74	oe		1238.80	N V	$2s\ ^2S_{1/2}$	$2p\ ^2P_{3/2}$	1	col	9990	67
1227.70	283	73								
1218.26	2237	71	1218.34	O V]	$2s^2\ ^1S_0$	$2p\ ^3P_1$	2.3F	unk		
1215.65	936	106	1215.67	H I	$n = 1$	$n = 2$		rec		
1199.04	1066	40	1199.13	S V]	$3s^2\ ^1S_0$	$3p\ ^3P_1$	1	unk		
1184.43	180	28	1184.51	N III	$2s2p^2\ ^2P_{3/2}$	$2p^3\ ^2P_{3/2}$	2.3D	unk		
Oth			1174.93	C III	$2s2p\ ^3P_1$	$2p^2\ ^3P_2$		unk		
1151.04	65		1151.15	Fe II	4s $a^6D_{5/2}$	4s4p $y^6F_{7/2}$	2.1	fl		
1147.27	71		1147.41	Fe II	4s $a^6D_{7/2}$	4s4p $y^6F_{7/2}$	2.1	fl		
1145.38	1014	58	1145.58	Ne V]	$2p^2\ ^3P_2$	$2s2p^3\ ^5S_2$	2.3D	col		
1141.22	94									
1136.38	492	60	1136.49	Ne V]	$2p^2\ ^3P_1$	$2s2p^3\ ^5S_2$	2.3D	col		
1128.21	96	90	1128.35	Si IV	$3p\ ^2P_{3/2}$	$3d\ ^2D_{5/2}$		unk		
			8.33	Si IV	$3p\ ^2P_{3/2}$	$3d\ ^2D_{3/2}$		unk		
1124	115^{pc}	700								
1084.7	1940	63	1084.9	He II	$n = 2$	$n = 5$	2.3F	rec		
1067.62	227									
1037.62	4140	116	1037.61	O VI	$2s\ ^2S_{1/2}$	$2p\ ^2P_{1/2}$	1	col		
1031.92	7970	120	1031.92	O VI	$2s\ ^2S_{1/2}$	$2p\ ^2P_{3/2}$	1	col		
974	359^{pc}	700								
967	212^{pc}	700								

Table 13. continued.

λ_{obs} (Å)	I^a	w^b	λ_{id} (Å)	spec.	Lower level	Upper level	Sec^c	Exc^f	I^d_{ghrs}	w^e_{ghrs}
958.51	351									

[a] Peak intensity measured in 10^{13} erg cm^{-2} s^{-1} Å^{-1}.
[b] Gaussian widths measured in km s^{-1}.
[c] Reference to the section in the paper the mechanism responsible for the line is discussed.
[d] Intensity measured with GHRS.
[e] width measured with GHRS.
[f] Excitation mechanism, fl=fluorescence, rec=recombination, col=collision and unk=unknown excitation mechanism

Table 14. Intensities of emission lines not detectable with LWP25995 or SWP47715.

λ_{obs}	I^a	w^b	λ_{id}	spec.	Lower level	Upper level	spectra
3300.29	234	45	3300.34	O III	2p3s $^3P_0$	2p3p $^3S_1$	LWP19253
3049.78	58	18	3049.88	Fe II	4p $z^4P_{3/2}$	5s $e^4D_{3/2}$	LWP25565
2831.45	57	22	2831.76	Fe II	4s $b^2G_{7/2}$	4p $x^4G_{5/2}$	LWR06398
2817.11	52	20					LWP19253
2644.61	76	32	2644.55	Fe II	4s^2 $b^4G_{5/2}$	4p $x^4H_{7/2}$	LWP09698
2583.28	144	17	2583.36	Fe II	4s $a^4D_{3/2}$	4p $z^4P_{3/2}$	LWP09698
2581.81	79	20	2581.94	Fe II	4p $z^2D_{5/2}$	5s $f^4F_{5/2}$	LWP25565
2549.69	61		2549.69	Fe II	4s $a^2I_{11/2}$	4p $x^2H_{9/2}$	LWP09698
2539.19	91		2539.35	Fe II	4s $a^2F_{5/2}$	4p $y^2D_{5/2}$	LWR06389
2528.28	89	23					LWR09130
2527.02	32		2527.06	Fe II	4s $b^4P_{5/2}$	4p $y^4P_{5/2}$	LWR09130
2464.62	62	30	2464.76	Fe II	4s $a^4G_{9/2}$	4p $x^4F_{7/2}$	LWR06398
2455.53	47		2455.71	O III	2p3s $^1P_1$	2p3p $^1S_0$	LWP09698
2437.89	142	28	2437.94	Fe II	4s $a^4G_{7/2}$	4p $y^2D_{5/2}$	LWP09698
2435.70	159	47	2435.69	Fe II	4s $b^4F_{3/2}$	4p $y^4G_{5/2}$	LWP09698
			5.66	Ne III]	2p^3(^{2}D)3s $^1D_2$	2p^3(^{2}D)3p $^3P_2$	
2429.94	61	16	2429.98	Ne III]	2p^3(^{2}D)3s $^1D_2$	2p^3(^{2}D)3p $^3P_1$	LWP09698
2426.32	79	16	2426.42	Fe II	4s $b^2P_{3/2}$	4p $y^2D_{5/2}$	LWR09130
2425.28	64	19	2425.23	[Ne IV]	2p^3 $^4S_{3/2}$	2p^3 $^2D_{5/2}$	LWP09698
2422.66	108	16	2422.60	[Ne IV]	2p^3 $^4S_{3/2}$	2p^3 $^2D_{3/2}$	LWP09698
2413.64	85		2413.67	Ne III	2p^3(^{4}S)3p $^3P_1$	2p^3(^{4}S)3d $^3D_2$	LWP09698
			3.47	Ne III	2p^3(^{4}S)3p $^3P_2$	2p^3(^{4}S)3d $^3D_3$	
2321.28	48	25	2321.66	[O III]	2p^2 $^3P_1$	2p^2 $^1S_0$	LWR09130
2316.42	53	26	2316.46	Co II	4s c^3F_4	4p v^3D_3	LWR09130
2253.78	187	37	2253.83	Fe II	4s $a^6D_{7/2}$	4p $z^4F_{7/2}$	LWR09130
2211.72	221	23	2211.81	Fe II	4s $a^4H_{13/2}$	4p $y^4H_{11/2}$	LWP25565
2179.99	619	29					LWP25565
2152.70	230	29					LWR06389
2149.26	195	45	2149.28	He II	n = 3	n = 13	LWP09698
2136.06	158	35	2136.03	He II	n = 3	n = 14	LWP09698
2127.87	241	24					LWR06389
2125.30	113		2125.31	He II	n = 3	n = 15	LWR06389
2121.96	62		2122.12	Fe II	4s $b^4D_{3/2}$	4p $w^2D_{3/2}$	LWR09130
2092.38	235	19					LWR06389
2037.98	299	19	2038.11	Fe II	4s $c^2P_{3/2}$	(^{4}P)4sp $^2S_{1/2}$	LWR06389
2003.72	242	39	2003.85	Fe II	4s $c^2P_{1/2}$	(^{4}P)4sp $^2S_{1/2}$	LWR06389
2001.77	195	28					LWR06389
1974.85	32	15	1975.07	Fe II	3d^7 $a^2G_{7/2}$	4p $y^2D_{5/2}$	SWP15651
1973.58	25	20	1973.78	Fe II	4s^2 $b^4G_{9/2}$	(^{2}I)4sp $^4H_{9/2}$	SWP37477
1971.98	45	21	1972.16	Fe II	4s^2 $b^4G_{11/2}$	(^{2}I)4sp $^4H_{9/2}$	SWP15651
1957.05	36	44	1957.28	[Fe VI]	3d^3 $^2G_{7/2}$	3d^3 ^{2}D1$_{5/2}$	SWP43007
1956.35	77	28					SWP43007
1951.69	34	23					SWP43007
1950.85	65	28					SWP43007
1925.70	137	25					SWP02334
1921.14	58	20					SWP15651
1919.00	30	30					SWP15651
1909.74	89	17	1909.91	Fe II	4s $b^4P_{5/2}$	4p $y^2P_{3/2}$	SWP15651
1894.16	40	17	1894.29	C III	2s3p $^1P_1$	2s4s $^1S_0$	SWP15651
1893.83	61	36	1893.89	Mg IV	(^{3}P)3s $^4P_{5/2}$	(^{3}P)3p $^4P_{5/2}$	SWP15651
1883.71	31	19	1883.72	Fe II	4s $a^4D_{7/2}$	4p $z^4G_{5/2}$	SWP37477
1881.75	24		1881.89	Fe II	4s $a^4D_{7/2}$	4p $z^2D_{5/2}$	SWP29862
1880.99	28	19	1881.25	Fe II	3d^7 $a^2P_{1/2}$	(^{3}D)4p $^4P_{3/2}$	SWP15651

Table 14. continued.

λ_{obs}	I^a	w^b	λ_{id}	spec.	Lower level	Upper level	spectra
1877.66	146	53					SWP15651
1876.94	93	16	1877.02	Fe II	4s $a^4G_{5/2}$	4sp $x^6P_{7/2}$	SWP02334
1853.52	53	31	1853.73	Co II	$4s^2$ a^5D_2	$(^4F)4p$ $^5D_3$	SWP15651
1850.50	136	26					SWP43007
1850.06	53	91	1850.20	Fe III	$(^4F)4s$ $^5F_4$	$(^4F)4p$ $^5D_4$	SWP43007
1849.15	38	24	1849.40	Fe III	$(^4F)4s$ $^5F_5$	$(^4F)4p$ $^5D_4$	SWP43007
1836.52	22	34	1836.72	N I	$2p^3$ $^2P_{3/2}$	3s $^4P_{1/2}$	SWP40149
			6.71	N I	$2p^3$ $^2P_{1/2}$	3s $^4P_{1/2}$	
1835.37	27	21	1835.57	N I	$2p^3$ $^2P_{3/2}$	3s $^4P_{3/2}$	SWP40149
1833.83	29	20	1834.01	N I	$2p^3$ $^2P_{1/2}$	3s $^4P_{3/2}$	SWP40149
1814.50	51	40	1814.63	[Ne III]	$2p^4$ $^3P_1$	$2p^4$ $^1S_0$	SWP15651
1813.85	41	18					SWP43007
1809.84	101	22					SWP43007
1795.30	94	52	1795.57	Fe II	$4s^2$ $b^4G_{7/2}$	$(^3H)5p$ $^4G_{7/2}$	SWP15651
			5.33	Fe II	$4s^2$ $b^4G_{5/2}$	$(^3H)5p$ $^4G_{7/2}$	
			5.27	Fe II	$4s^2$ $b^4G_{9/2}$	$(^3H)5p$ $^4G_{7/2}$	
1787.79	49	22	1788.00	Fe II	$4s^2$ $a^6S_{5/2}$	4sp $x^6P_{3/2}$	SWP37477
1783.88	99	44	1783.98	Fe II	4s $b^4D_{7/2}$	4sp $y^6F_{7/2}$	SWP10454
1782.64	42	49					SWP43007
1760.78	40	32	1760.82	C II	$2s2p^2$ $^2D_{3/2}$	3p $^2P_{1/2}$	SWP29862
1760.26	103	49	1760.47	C II	$2s2p^2$ $^2D_{3/2}$	3p $^2P_{3/2}$	SWP29862
			0.40	C II	$2s2p^2$ $^2D_{5/2}$	3p $^2P_{3/2}$	
1757.61	46	22	1757.74	Fe II	4s $c^4P_{3/2}$	$(^4F)4sp$ $^6F_{3/2}$	SWP43007
1751.45	47	33	1751.66	N III	$2s2p^2$ $^2P_{3/2}$	$2p^3$ $^2D_{5/2}$	SWP15651
1750.46	65	41	1750.66	Mg II	3p $^2P_{1/2}$	5s $^2S_{1/2}$	SWP40149
1747.64	36		1747.85	N III	$2s2p^2$ $^2P_{1/2}$	$2p^3$ $^2D_{3/2}$	SWP15651
1725.78	141	17	1725.98	Fe II	$3d^7$ $a^2D_{3/2}$	4sp $x^6P_{3/2}$	SWP15651
1721.46	102	23	1721.68	C II	$2s2p^2$ $^2P_{3/2}$	$2p^3$ $^2P_{3/2}$	SWP10454
1712.99	56	18	1713.00	Fe II	$3d^7$ $a^4F_{7/2}$	4p $z^4G_{9/2}$	SWP43007
1706.78	164	19	1706.83	Fe II	4s $c^2G_{7/2}$	4sp $x^4H_{7/2}$	SWP15651
1588.07	167	21	1588.29	Fe II	$3d^7$ $a^4F_{3/2}$	4p $x^4G_{5/2}$	SWP06355
1538.59	152	18	1538.63	Fe II	4s $a^4G_{5/2}$	$(^5D)5p$ $^4D_{3/2}$	SWP29862
1533.8	170		1534.05	O V	2p3p $^1P_1$	2s4p $^1P_1$	SWP29862
1531.0	232	127					SWP29862
1502.0	429	937	1501.76	S V	3s3p $^1P_1$	$3p^2$ $^1D_2$	SWP02334
1468.88	103	49					SWP29862
1457.53	163	23	1457.76	Fe II	$4s^2$ $a^6S_{5/2}$	$(^4D)4sp$ $^6F_{3/2}$	SWP15651
1392.99	195	24	1393.21	Fe II	$3d^7$ $a^2H_{11/2}$	4sp $x^4H_{9/2}$	SWP02334
1312.41	94	16	1312.49	Fe II	4s $b^4D_{7/2}$	$(^2F)4sp$ $^4G_{9/2}$	SWP29862
1310.01	184	27	1310.15	Fe II	$3d^7$ $a^2G_{9/2}$	4p $u^2G_{9/2}$	SWP06355
1300.75	145	16	1300.86	O III]	$2p^2$ $^1S_0$	$2s2p^3$ $^3D_1$	SWP15651
1298.78	120	30	1298.89	Si III	3p $^3P_1$	$3p^2$ $^3P_1$	SWP29862
1296.58	90	19	1296.73	Si III	3p $^3P_0$	$3p^2$ $^3P_1$	SWP29862
1265.98	858	554					SWP02334
1260.40	1556	699					SWP02334
1253.26	1469	789					SWP02334
1174.86	399	41	1174.93	C III	2s2p $^3P_1$	$2p^2$ $^3P_2$	SWP15651

[a] Peak intensity measured in 10^{13} erg cm^{-2} s^{-1} Å^{-1}.
[b] Gaussian widths measured in km s^{-1}.

Table 15. Emission lines saturated in LWP25995 or SWP47715.

λ_{obs}	I^a	w^b	λ_{id}	spec.	Lower level	Upper level	spectra
3133.62	3204	49	3133.70	O III	2p3p $^3S_1$	2p3d $^3P_2$	LWP21635
3047.86	805	34	3047.99	O III	2p3s $^3P_2$	2p3p $^3P_2$	LWP30936
2803.5	717		2803.53	Mg II	3s $^2S_{1/2}$	3p $^2P_{1/2}$	LWP21635
2796.3	828		2796.35	Mg II	3s $^2S_{1/2}$	3p $^2P_{3/2}$	LWP21635
2734.00	596	54	2734.10	He II	$n = 3$	$n = 5$	LWP19253
1908.65	3389	36	1908.73	C III	2s^2 $^1S_0$	2s2p $^3P_1$	SWP55055
1891.96	5239	29	1892.03	Si III	3s^2 $^1S_0$	3p $^3P_1$	SWP55055
1749.55	2077	36	1749.67	N III	2p $^2P_{3/2}$	2s2p^2 $^4P_{5/2}$	SWP55055
1666.06	8540	38	1666.15	O III]	2p^2 $^3P_2$	2s2p^3 $^5S_2$	SWP55055
1660.70	3540	34	1660.81	O III]	2p^2 $^3P_1$	2s2p^3 $^5S_2$	SWP55055
1640.28	22040	60	1640.35	He II	$n = 2$	$n = 3$	SWP55055
1550.79	24420	45	1550.77	C IV	2s $^2S_{1/2}$	2p $^2P_{1/2}$	SWP55055
1548.21	44470	37	1548.19	C IV	2s $^2S_{1/2}$	2p $^2P_{3/2}$	SWP55055
1486.42	14200	32	1486.50	N IV	2s^2 $^1S_0$	2p $^3P_1$	SWP55055
1404.74	2389	26	1404.80	O IV]	2p $^2P_{3/2}$	2s2p^2 $^4P_{3/2}$	SWP55055
			4.77	S IV	3p $^2P_{1/2}$	3p^2 $^4P_{1/2}$	
1402.78	2439	36	1402.77	Si IV	3s $^2S_{1/2}$	3p $^2P_{1/2}$	SWP55055
1401.07	7500	43	1401.16	O IV]	2p $^2P_{3/2}$	2s2p^2 $^4P_{5/2}$	SWP55055
1393.75	3796	37	1393.76	Si IV	3s $^2S_{1/2}$	3p $^2P_{3/2}$	SWP55055
1242.78	12570	56	1242.78	N V	2s $^2S_{1/2}$	2p $^2P_{1/2}$	SWP55055
1238.79	19560	70	1238.80	N V	2s $^2S_{1/2}$	2p $^2P_{3/2}$	SWP55055

[a] Peak intensity measured in 10^{13} erg cm^{-2} s^{-1} Å^{-1}.
[b] Gaussian widths measured in km s^{-1}.

Table 16. Aborption lines in AG Peg.

λ_{obs}	ekv[i]	λ_{id}	spec.	Lower level	Upper level	shift	rem
2852.92	0.21	2852.96	Mg I	$3s^2\ ^1S_0$	$3s3p\ ^1P_1$	IS	
2606.49[a]	0.26	2606.46	Mn II	$4s\ a^7S_3$	$4p\ z^7P_2$		
2600.13	0.20	2600.17	Fe II	$4s\ a^6D_{9/2}$	$4p\ z^6D_{9/2}$		
2594.51	0.17	2594.50	Mn II	$4s\ a^7S_3$	$4p\ z^7P_3$		
2586.68	0.37	2585.65	Fe II	$4s\ a^6D_{9/2}$	$4p\ z^6D_{7/2}$		
2576.88	0.14	2576.87	Mn II	$4s\ a^7S_3$	$4p\ z^7P_4$		
2514.83	0.21	2515.07	Si I	$2p^2\ ^3P_0$	$2p3s\ ^3P_1$		
2382.75	0.26	2382.77	Fe II	$4s\ a^6D_{9/2}$	$4p\ z^6F_{11/2}$		
2374.55	0.20	2374.46	Fe II	$4s\ a^6D_{9/2}$	$4p\ z^6F_{9/2}$		
1969.90[b]	0.15	1970.36	Fe II	$3d^7\ a^4P_{3/2}$	$4p\ z^2F_{5/2}$		
1913.26	0.15	1913.25	Fe I	$4s^2\ a^5D_3$	$(^2D)4p\ ^3D_2$		
1859.44	0.18						
1838.34[b]	0.21						
1801.49	0.15						
1788.61	0.21						
1737.82	0.13						
1719.41[b]	0.23	1720.03	Fe II	$3d^7\ a^4P_{1/2}$	$(^3D)4p\ ^4P_{3/2}$		
1670.76	0.37	1670.99	Fe II	$3d^7\ a^4F_{3/2}$	$4p\ y^4D_{3/2}$		
		0.79	Al II	$2s^2\ ^1S_0$	$3p\ ^1P_1$		
		0.79	Fe II	$3d^7\ a^4F_{5/2}$	$4p\ y^4D_{5/2}$		
		0.75	Fe II	$3d^7\ a^4F_{9/2}$	$4p\ y^4D_{7/2}$		
1658.97	0.12	1659.48	Fe II	$3d^7\ a^4F_{7/2}$	$4p\ y^4D_{5/2}$		
1656.82	0.21	1657.07	Fe II	$3d^7\ a^4F_{3/2}$	$4p\ x^4D_{3/2}$		
		6.93	C I	$2p^2\ ^3P_0$	$2p3s\ ^3P_1$	IS	
1642.33	0.11	1642.37	Fe II	$4s\ a^6D_{9/2}$	$4p\ z^4H_{11/2}$		
1608.34	0.31	1608.45	Fe II	$4s\ a^6D_{9/2}$	$4sp\ y^6P_{7/2}$		
1558.97	0.23	1559.09	Fe II	$3d^7\ a^4F_{9/2}$	$4p\ x^4F_{9/2}$		
1558.51	0.14	1558.54	Fe II	$3d^7\ a^4F_{5/2}$	$4p\ y^2D_{5/2}$		
1548.56*	0.04	1548.70	Fe II	$3d^7\ a^4F_{7/2}$	$4p\ y^2D_{5/2}$		
1548.27*	0.02	1548.41	Fe II	$3d^7\ a^4P_{1/2}$	$4p\ w^2D_{3/2}$		
1548.06*	0.02	1548.20	Fe II	$3d^7\ a^4F_{9/2}$	$4p\ y^4H_{11/2}$		
1526.64	0.16	1526.71	Si II	$3p\ ^2P_{1/2}$	$4s\ ^2S_{1/2}$		
1470.35[c]	0.10						
1470.08[c]	0.15						
1401.50	0.06	1401.51	S I	$3p^4\ ^3P_2$	$(^4S)5s\ ^3S_1$		
1334.40	0.22	1334.53	C II	$2p\ ^2P_{1/2}$	$2s2p^2\ ^2D_{3/2}$	IS	
1328.71	0.15	1328.83	C I	$2p^2\ ^3P_0$	$2s2p^3\ ^3P_1$	IS	
1304.35	0.07	1304.49	P II	$3p^2\ ^3P_1$	$3p^3\ ^3P_0$		
1304.19	0.09	1304.37	Si II	$3p\ ^2P_{1/2}$	$3p^2\ ^2S_{1/2}$		
1302.12	0.10	1302.12	O I	$2p^4\ ^3P_2$	$3s\ ^3S_1$	IS	
1277.14	0.21	1277.28	C I	$2p^2\ ^3P_1$	$2p3d\ ^3D_2$	IS	
		7.25	C I	$2p^2\ ^3P_0$	$2p3d\ ^3D_1$	IS	
1260.35	0.16	1260.53	Fe II	$4s\ a^6D_{9/2}$	$4sp\ x^6P_{7/2}$		
		1260.42	Si II	$3p\ ^2P_{1/2}$	$3d\ ^2D_{3/2}$		
1259.41	0.23	1259.52	S II	$3p^3\ ^4S_{3/2}$	$3p^4\ ^4P_{5/2}$		
1253.70	0.21	1253.81	S II	$3p^3\ ^4S_{3/2}$	$3p^4\ ^4P_{3/2}$		
1250.47	0.24	1250.58	S II	$3p^3\ ^4S_{3/2}$	$3p^4\ ^4P_{1/2}$		
1242.63*	0.03	1242.74	Fe II	$3d^7\ a^4F_{5/2}$	$4p\ v^2G_{7/2}$		
1206.39	0.10	1206.50	Si III	$3s^2\ ^1S_0$	$3p\ ^1P_1$		
1200.64[b]	0.14	1200.71	N I	$2p^3\ ^4S_{3/2}$	$3s\ ^4P_{5/2}$	IS	
1200.16[b]	0.18	1200.23	N I	$2p^3\ ^4S_{3/2}$	$3s\ ^4P_{3/2}$	IS	
1199.48[b]	0.13	1199.55	N I	$2p^3\ ^4S_{3/2}$	$3s\ ^4P_{1/2}$	IS	
1193.19	0.11	1193.29	Si II	$3p\ ^2P_{1/2}$	$3p^2\ ^2P_{1/2}$		

Table 16. continued.

λ_{obs}	ekv[i]	λ_{id}	spec.	Lower level	Upper level	shift	rem
1190.29[b]	0.14	1190.42	Si II	$3p\ ^2P_{1/2}$	$3p^2\ ^2P_{3/2}$		
1187.42	0.05	1187.42	Co II	$3d^8\ a^3F_4$	$4p\ v^3D_3$		
1134.96	0.18	1134.97	N I	$2p^3\ ^4S_{3/2}$	$2p^4\ ^4P_{5/2}$	IS	
1134.28	0.45	1134.42	N I	$2p^3\ ^4S_{3/2}$	$2p^4\ ^4P_{3/2}$	IS	
		4.17	N I	$2p^3\ ^4S_{3/2}$	$2p^4\ ^4P_{1/2}$	IS	
1122.42	0.98						
1110.10	0.19	1110.28	Fe II	$4s\ a^6D_{9/2}$	$(^5D)5p\ ^6F_{9/2}$		
1108.45	0.66	1108.51	Fe II	$3d^7\ a^4F_{3/2}$	$4p\ u^4F_{3/2}$	bl	
1094.06	0.28	1094.08	Fe II	$3d^7\ a^4F_{7/2}$	$(^4D)4s4p\ ^6D_{5/2}$		
1092.37	0.44						
1078.97	0.31						
1077.34	0.58						
1064.63	0.25						
1063.11	0.59	1063.18	Fe II	$4s\ a^6D_{9/2}$	$(^4D)4s4p\ ^6D_{9/2}$	bl	
1051.15	0.38						
1049.50	0.59						
1040.31	0.13						
1039.17	0.15	1039.23	O I	$2p^4\ ^3P_2$	$2p^3\ (^4S)4s\ ^3S_1$	IS	
1038.62	0.11						
1038.09	0.15						
1014.33	0.14						
1012.90	0.40						
1009.76	0.15						
1008.53	0.28						
974.06	0.10	974.07	O I	$2p^4\ ^3P_2$	$(^2D)3s\ ^1D_2$	IS	
973.22	0.10	973.23	O I	$2p^4\ ^3P_1$	$(^4S)4d\ ^3D_2$		

[i] Equivalent width measured in Å.